EVALUATION OF NITROGEN-FOAM FLOODING IN MULTILAYERED HETEROGENEOUS RESERVOIR

Mrs. Seema Tarannum Shaikh

จุฬาลงกรณ์มหาวิทยาลัย
Chulalongkorn University

บทคัดย่อและแฟ้มข้อมูลฉบับเต็มของวิทยานิพนธ์ตั้งแต่ปีการศึกษา 2554 ที่ให้บริการในคลังปัญญาจุฬาฯ (CUIR)
เป็นแฟ้มข้อมูลของนิสิตเจ้าของวิทยานิพนธ์ ที่ส่งผ่านทางบัณฑิตวิทยาลัย
The abstract and full text of theses from the academic year 2011 in Chulalongkorn University Intellectual Repository (CUIR)
are the thesis authors' files submitted through the University Graduate School.

A Thesis Submitted in Partial Fulfillment of the Requirements
for the Degree of Master of Engineering Program in Petroleum Engineering
Department of Mining and Petroleum Engineering
Faculty of Engineering
Chulalongkorn University
Academic Year 2014

Copyright of Chulalongkorn University

การประเมินผลการฉีดอัดโฟมไนโตรเจนในแหล่งกักเก็บน้ำมันวิวิธพันธุ์หลายชั้น

นางซีม่า ทารานนัม เชคห์

จุฬาลงกรณ์มหาวิทยาลัย
Chulalongkorn University

วิทยานิพนธ์นี้เป็นส่วนหนึ่งของการศึกษาตามหลักสูตรปริญญาวิศวกรรมศาสตรมหาบัณฑิต
สาขาวิชาวิศวกรรมปิโตรเลียม ภาควิชาวิศวกรรมเหมืองแร่และปิโตรเลียม
คณะวิศวกรรมศาสตร์ จุฬาลงกรณ์มหาวิทยาลัย
ปีการศึกษา 2557
ลิขสิทธิ์ของจุฬาลงกรณ์มหาวิทยาลัย

Thesis Title	EVALUATION OF NITROGEN-FOAM FLOODING IN MULTILAYERED HETEROGENEOUS RESERVOIR
By	Mrs. Seema Tarannum Shaikh
Field of Study	Petroleum Engineering
Thesis Advisor	Falan Srisuriyachai, Ph.D.

Accepted by the Faculty of Engineering, Chulalongkorn University in Partial Fulfillment of the Requirements for the Master's Degree

.....Dean of the Faculty of Engineering

(Professor Bundhit Eua-arporn, Ph.D.)

THESIS COMMITTEE

.....Chairman

(Assistant Professor Jirawat Chewaroungroaj, Ph.D.)

.....Thesis Advisor

(Falan Srisuriyachai, Ph.D.)

.....Examiner

(Assistant Professor Suwat Athichanagorn, Ph.D.)

.....External Examiner

(Monrawee Pancharoen, Ph.D.)

จุฬาลงกรณ์มหาวิทยาลัย
Chulalongkorn University

ซีม่า ทารานนัม เชคห์ : การประเมินผลการฉีดอัดโฟมไนโตรเจนในแหล่งกักเก็บน้ำมันวิวิธพันธุ์หลายชั้น (EVALUATION OF NITROGEN-FOAM FLOODING IN MULTILAYERED HETEROGENEOUS RESERVOIR) อ.ที่ปรึกษาวิทยานิพนธ์หลัก: อ. ดร.ฟ้าลั่น ศรีสุริยชัย, 174 หน้า.

แหล่งกักเก็บน้ำมันแบบวิวิธพันธ์ส่วนใหญ่จะผลิตน้ำในปริมาณมากอย่างรวดเร็ว ส่งผลให้การกวาดน้ำมันมีประสิทธิภาพต่ำซึ่งรวมไปถึงให้ผลผลิตน้ำมันต่ำด้วยเช่นกัน การเลือกวิธีการเพิ่มผลผลิตน้ำมันถือเป็นความสำคัญสูงสุดและสิ่งที่ควรคำนึงถึงคือการควบคุมความสามารถในการไหลของน้ำและก๊าซ การฉีดอัดด้วยโฟมเป็นหนึ่งในวิธีที่สามารถเพิ่มประสิทธิภาพการกวาดน้ำมันในเชิงมหรรพภาคในแหล่งกักเก็บน้ำมันแบบวิวิธพันธ์ ในการศึกษานี้ การฉีดอัดโฟมไนโตรเจนถูกเลือกทำในแหล่งกักเก็บแบบวิวิธพันธ์หลายชั้น แบบจำลองแหล่งกักเก็บถูกสร้างโดยอาศัยโปรแกรมสร้างแบบจำลองแหล่งกักเก็บน้ำมันดิบ และค่าความเป็นวิวิธพันธ์ของแหล่งกักเก็บถูกคำนวณและแสดงโดยค่าสัมประสิทธิ์ลอเรนซ์โฟมไนโตรเจนถูกสร้างโดยการฉีดอัดร่วมกันระหว่างสารละลายสารลดแรงตึงผิวขั้วลบและก๊าซไนโตรเจน

ผลจากการทดสอบแบบจำลองแหล่งกักเก็บแสดงให้เห็นว่าการฉีดอัดร่วมของสารละลายสารลดแรงตึงผิวและก๊าซไนโตรเจนโดยทำการปรับตัวแปรเชิงปฏิบัติการอย่างเหมาะสมช่วยทำให้เกิดผลเชิงบวกเมื่อเปรียบเทียบกับการฉีดอัดน้ำแบบปกติ การฉีดอัดโฟมไนโตรเจนด้วยการปรับตัวแปรเชิงปฏิบัติการอย่างเหมาะสมสามารถให้ค่าประสิทธิภาพการผลิตได้สูงถึง 0.59 กรณีศึกษาพื้นฐานที่ได้รับเลือกเกิดจากการฉีดอัดของของผสมที่อัตราการไหล 1000 บาร์เรลของแหล่งกักเก็บต่อวัน อัตราส่วนการผลิตต่อการฉีดอัด 1.5 อัตราส่วนก๊าซต่อของเหลวในการผลิตโฟม 2.0 และขนาดมวลโฟม 0.25 เท่าของขนาดช่องว่างในแหล่งกักเก็บ โฟมที่เกิดจากการสร้างจากค่าตัวแปรดังกล่าวสามารถผลิตน้ำมันมวลเบาด้วยการแทนที่อย่างมีประสิทธิภาพในแหล่งกักเก็บแบบวิวิธพันธ์ จากการศึกษาตัวแปรอื่น ๆ ที่สนใจพบว่า ค่าความสามารถในการซึมผ่านแนวตั้งมีแนวโน้มลดค่าประสิทธิภาพการผลิตเนื่องมาจากการปลดปล่อยก๊าซที่ละลายอยู่ในน้ำมันเกิดขึ้นรวดเร็ว และยังก่อให้เกิดการแซงของมวลน้ำฉีดไล่ แหล่งกักเก็บที่มีหินที่เปียกด้วยน้ำมันได้รับผลประโยชน์จากการฉีดอัดด้วยโฟมไนโตรเจนเนื่องจากสารลดแรงตึงผิวสามารถเพิ่มช่วงของน้ำมันที่ผลิตได้ในระหว่างการฉีดอัด อย่างไรก็ตามหินที่มีความเปียกด้วยน้ำมันอาศัยเวลานานในการผลิตน้ำมันดังนั้นน้ำในปริมาณมากจึงถูกผลิตอย่างไม่สามารถหลีกเลี่ยงได้ การเคลื่อนที่ของโฟมได้รับผลประโยชน์จากความหนาของชั้นหินเนื่องจากความดันของแหล่งกักเก็บด้านบนที่ต่ำกว่า การฉีดอัดโฟมหลายมวลแบบสลับไม่ให้ผลประโยชน์ใดเนื่องจากมวลโฟมที่บางลงส่งผลให้น้ำฉีดไล่สามารถแซงโฟมได้ ค่าสัมประสิทธิ์วิวิธพันธ์สูงกว่า 0.35 อาจส่งผลให้ผลิตน้ำมันได้ต่ำเนื่องจากโฟมไม่สามารถควบคุมความสามารถการไหลได้อย่างมีประสิทธิภาพ

ภาควิชา วิศวกรรมเหมืองแร่และปิโตรเลียม ลายมือชื่อนิสิต .....

สาขาวิชา วิศวกรรมปิโตรเลียม ลายมือชื่อ อ.ที่ปรึกษาหลัก .....

ปีการศึกษา 2557

5571203621 : MAJOR PETROLEUM ENGINEERING
KEYWORDS: NITROGEN-FOAM FLOODING / HETEROGENITY

SEEMA TARANNUM SHAIKH: EVALUATION OF NITROGEN-FOAM FLOODING IN MULTILAYERED HETEROGENEOUS RESERVOIR. ADVISOR: FALAN SRISURIYACHAI, Ph.D., 174 pp.

Most oil reservoirs yield early high water cut due to heterogeneity, resulting in poor sweep efficiency and consecutively inefficient oil recovery. Selection of proper Enhanced Oil Recovery (EOR) technique is therefore top priority and prime concern is to control mobility of water and gas. Foam flooding is one of the techniques that can increase macroscopic sweep efficiency in heterogeneous reservoir. In this study, injection of nitrogen-foam is performed in multi-layered heterogonous reservoir. Reservoir model is built using black oil reservoir simulator and reservoir heterogeneity is quantified by Lorenz coefficient. Nitrogen-foam is created by co-injecting of anionic surfactant solution and nitrogen gas.

Simulation results show that co-injection of surfactant solution and nitrogen gas with proper adjustment of operational parameters yields positive results compared to conventional waterflooding. Nitrogen-foam flooding with proper adjustment of operational parameters yields recovery efficiency up to 0.59. Finalized base case is performed at fluid injection rate 1,000 rb/day, production-injection ratio 1.5, gas-liquid ratio 2.0 and slug size 0.25 PV. Foam generated under these parameters helps displacing light oil efficiently in multilayered heterogeneous reservoir. Study of interest parameters shows that high vertical permeability tends to reduce oil recovery factor due to solution gas liberation and also bypassing of chasing water. Formation with oil-wet condition gains benefit from nitrogen-foam flooding since surfactant can increase a gap of recoverable oil during flooding mechanism. However, time required to recover oil is higher in oil-wet rock and hence, high water production cannot be avoided. Foam advancement obtains benefit from higher thickness due to smaller formation pressure in top layers. Injecting foam in multi-slug does not yield great benefit since thinner slug could result in bypassing of chasing water. Lorenz coefficient higher than 0.35 might yield low oil recovery since foam cannot control mobility effectively.

Department:	Mining and Petroleum Engineering	Student's Signature	.....
		Advisor's Signature	.....
Field of Study:	Petroleum Engineering		
Academic Year:	2014		

ACKNOWLEDGEMENTS

First of all, I would like to express my heartfelt gratitude to Dr.Falan Srisuriyachai, my thesis advisor, for his true advices, supports and sincere guidance during my study in petroleum engineering program.

I would like to pay sincere respect and thank to Asst. Prof. Dr.Jirawat Chewaroungroaj and Asst. Prof. Dr.Suwat Athichanagorn for their valuable suggestions for my thesis. I would like to thank other program members for providing knowledge during my study. My thanks also go to Mrs. Siriluck Saenglaor for helping me in administrative work.

I appreciate and would like to thank my classmates Warat Tongbunsing, Charat Thamcharoen and Rawin Pitakwatchara for giving sincere friendships and valuable supports, both personally and professionally. I would also like to thank Kunwadee Teerakijpaiboon for her valuable technical guidance on foam flooding.

I sincerely thank Chevron Thailand Exploration and Production, Ltd. for providing financial support for this study.

I would like to dedicate this thesis to my parents and last but not least, I would like to thank very much to my husband Mr.Javeed Shaikh, for his sacrifices, supports and encouragement. Without him, this thesis would not be completed.

CONTENTS

Page

จุฬาลงกรณ์มหาวิทยาลัย
Chulalongkorn University

Page

Page

จุฬาลงกรณ์มหาวิทยาลัย
Chulalongkorn University

List of Tables

Page

Chulalongkorn University

List of Figures

Page

จุฬาลงกรณ์มหาวิทยาลัย
Chulalongkorn University

จุฬาลงกรณ์มหาวิทยาลัย
Chulalongkorn University

จุฬาลงกรณ์มหาวิทยาลัย
Chulalongkorn University

จุฬาลงกรณ์มหาวิทยาลัย
CHULALONGKORN UNIVERSITY

จุฬาลงกรณ์มหาวิทยาลัย
Chulalongkorn University

จุฬาลงกรณ์มหาวิทยาลัย
Chulalongkorn University

List of Abbreviations

°API	American Petroleum Institute
STB	Stock Tank Barrel
STB/D	Stock Tank Barrel per day
cP	Centipoise
CMC	Critical Micelle Concentration
N_2	Nitrogen
EOR	Enhanced oil recovery
°F	Degree Fahrenheit
GOR	Gas-Oil ratio
IFT	Interfacial tension
IWS	Irreducible water saturation
mD	Millidarcy
MMSTB	Million Stock Tank Barrel
MSTB	Thousand Stock Tank Barrel
MMSCF	Million standard cubic foot
MMSCF/D	Million standard cubic foot per day
PV	Pore volume
PVT	Pressure-volume-temperature
Psi	Pounds per square inch
SAG	Surfactant Alternating Gas
SCF	Standard cubic foot
w/v	Weight per volume
BHP	Bottomhole pressure

จุฬาลงกรณ์มหาวิทยาลัย
Chulalongkorn University

CMG	Computer Modeling Group
ft^3/bbl	Cubic feet per barrel
OOIP	Original oil in place
psi/ft	Pound per square inch per feet
RF	Recovery factor
ROS	Residual oil saturation
SCAL	Special core analysis
scf/stb	Standard cubic feet per stock-tank barrel
STB/D	Stock-tank barrel per day
STO	Stock-tank oil
STW	Stock-tank water
STF	Total Surface phase rate
Fmmob	Reference mobility reduction factor
Lc	Lorenz Coefficient
BCF	Billion cubic feet
ft	feet
psia	Pound per square inch absolute
psi/ft	Pound per square inch per foot
psig	Pound per square inch gauge
rb/day	Reservoir barrel per day
STL	Total Surface Liquid rate
WCUT	Water Cut

จุฬาลงกรณ์มหาวิทยาลัย
Chulalongkorn University

List of Nomenclatures

Φ	Porosity
μ_o	Oil viscosity
μ_w	Water viscosity
B_g	Formation volume factor of gas
B_o	Formation volume factor of oil
C_o	Corey-oil exponent
C_m	Cumulative storage capacity
F_n	Fraction of storage capacity
C_w	Corey-water exponent
Epsurf	Exponent for composition contribution to dimensionless foam interpolation calculation
Epoil	Exponent for oil saturation contribution
F_1	Surfactant concentration
F_2	Oil saturation
F_3	Capillary number
F_4	Critical capillary number
F_5	Critical oil mole fraction for component numx and
F_6	Salt mole fraction.
FM	Dimensionless interpolation factor for relative permeability to gas in the presence of foam
fmmob	Reference mobility reduction factor
fmsurf	Critical concentration of surfactant which normally is the injected fluid concentration

จุฬาลงกรณ์มหาวิทยาลัย
Chulalongkorn University

fmoil	Critical oil saturation value
K^{f}_{rg}	Relative permeability to gas in presence of foam
K^{nf}_{rg}	Relative permeability to gas in the absence of foam
Ws	Concentration of surfactant in the grid block
h	Thickness
k	Absolute permeability
k_h	Horizontal permeability
k_{rg}	Relative permeability to gas
k_{ro}	Relative permeability to oil (Oil/Water function)
k_{rog}	Relative permeability to oil (Gas/Liquid function)
k_{rw}	Relative permeability to water
k_v	Vertical permeability
L_c	Lorenz coefficient
R_s	Solution gas-oil ratio
S_l	Liquid saturation
S_w	Water saturation
S_{wc}	Connate water saturation
S_{wcr}	Critical water saturation
S_{wi}	Irreducible water saturation (connate water saturation)
S_{wmin}	Minimum water saturation (irreducible water saturation)
S_{wmax}	Maximum water saturation
S_{or}	Residual oil saturation

จุฬาลงกรณ์มหาวิทยาลัย
Chulalongkorn University

CHAPTER I
INTRODUCTION

1.1 Background

Nowadays, life cycle of petroleum reservoir involves major three phases of production which are primary, secondary and tertiary recoveries. Most studies and literature reviews point out that approximately 30 percent of original oil in place can be recovered by means of primary and secondary recoveries. Due to an increment in demand for hydrocarbon, this leads to focusing of the remaining 70 percent hydrocarbon which is normally called residual oil. This phase of production generally refers to tertiary recovery.

Tertiary recovery or so-called Enhanced Oil Recovery (EOR) refers to processes to produce remaining oil by injecting additional energy other than conventional reservoir energy and reservoir re-pressurizing techniques by gas or water injection. Different types of EOR methods are gas-solvent injection, chemical injection, microbial injection and thermal recovery. The recovery of oil is enhanced truly by means of interactions between the injected fluid and rock-oil-formation brine system, generating more favorable conditions [1]. EOR techniques are performed either after primary recovery or secondary recovery and there is no specific rule that these steps should be carried out in order [1]. Different techniques have proven to be successful in indifferent field properties, reaching their maximum limits.

Several methods of both secondary and EOR involve with gas as injectant (e.g., natural gas, CO_2, N_2, steam, air) which normally encounters a major drawback of low sweep efficiency and consecutively results in low yield of oil recovery. This drawback is due to gas density that is much lower than that of oil which is displaced phase. This big difference of density causes gas overriding which is unfavorable flow regime. Moreover, mobility of gas which is relatively high than that of oil also causes unfavorable mobility ratio that results in a viscous fingering phenomenon. In

heterogeneous reservoirs, unfavorable mobility problem leads to even a severe channeling flow regime. So, large area of reservoir is untouched by the displacing fluids and this yields very low volumetric sweep efficiency.

In 1958, Bond and Helbrook [2] enlightened the utilization of foam to increase oil recovery. A large interface area and large volume of foam is generated when gas disperses in liquid, thereby improving flow resistance. If this flow resistance is in the least resistant areas of the reservoir, displacing fluid is forced to flow through areas of higher resistance, sweeping non-swept zone of reservoir and recovering larger quantity of residual oil. Thus, by using foam, sweep efficiency can be improved. As gaseous part of foam is dispersed, gas-phase flow mobility is greatly decreased which leads to reduction of gravity override and viscous fingering through high permeability zones. So, foam can be used to control gas mobility by increasing effective viscosity and also relative permeability to gas is reduced. Applying of nitrogen to create foam leads to an evolution of nitrogen-foam injection, providing a low price technique as nitrogen is abundant and mobility control function of foam is achieved at the same time. Nitrogen-foam has an ability to decrease relative permeability of injectant, high permeability contrast is reduced, improving sweep efficiency, and increasing residual oil recovery.

In heterogeneous reservoir, physical properties of reservoir rock including permeability, porosity, thickness, presence of faults and fractures can affect effectiveness of foam flooding. Besides, effectiveness of nitrogen-foam injection is also dependent on properties of oil, foam quality, foam stability, formation type, etc.

As previously mentioned, effects of various interest parameters are investigated with an aid of reservoir simulation. Reservoir model is built up by using black oil simulator called **STARS®** commercialized by **Computer Modeling Group Ltd. (CMG).** An attempt is made to analyze effects of various parameters in both operational and reservoir aspects. A selected base case model is identified for first heterogeneous model by adjusting operational parameters including nitrogen-foam injection rate, production-injection ratio, gas-liquid ratio and foam slug size. Later, selected parameters are applied with other range of heterogeneity values to observe

effects of heterogeneity. Heterogeneous reservoir models are created by varying reservoir permeability in ten layers to represent multi-layered sandstone reservoir. Lorenz coefficient is calculated for every model in order to quantify heterogeneity. Effect of heterogeneity is observed and pre-screening for nitrogen-foam flooding is obtained for implementation of this technique in heterogeneous reservoir. Sensitivity analysis study is performed to evaluate effects of uncertain parameters such as wettability, ratio of vertical permeability to horizontal permeability ratio, and also thickness of reservoir. Alternating foam slug by water is also performed in this study. Simulation outcomes which are oil recovery factor, cumulative water production, cumulative oil production, oil, gas and water production rates, injection well bottomhole pressure and cumulative injected pore volume of injectant are used for discussions and judgment of flooding performance. At the end of study, conclusion and new observations are summarized.

1.2 Objectives

1. To evaluate effects of operational parameters which are Fluid injection rate (nitrogen rate + liquid rate), production-injection ratio, gas liquid ratio and foam slug size on effectiveness of nitrogen-foam flooding in reservoir containing heterogeneity.
2. To investigate effect of heterogeneity on effectiveness of nitrogen-foam flooding in reservoir containing heterogeneity.
3. To study co-effects of reservoir parameters together with heterogeneity which are vertical permeability to horizontal permeability ratio, presence of alternating foam slugs, wetting condition of rock and thickness of reservoir on effectiveness of nitrogen-foam flooding.

1.3 Outline of methodology

This study is performed through the following steps of methodology. At the end of this section summarized flow charts are illustrated in Figures 1.1 and 1.2, describing selection steps of base case and effect of interest parameters, respectively. Methodology of this study is described as follow:

1. Review literature to obtain more information related to keywords of this study which are nitrogen-foam flooding and reservoir heterogeneity.
2. Construct physical heterogeneous models using Schmalz and Rahme method (Lorenz coefficient) with desired range of heterogeneity.
3. Perform initialized nitrogen-foam flooding on constructed heterogeneous reservoir model prior to selection of operational properties. Water flooding is performed for comparing results of nitrogen-foam flooding.
4. Simulate foam model with different operating parameters to observe their effects on performance of production and select best value for each parameter. Operating parameters in this study are:
   - Fluid Injection rate (nitrogen rate + liquid rate)
   - Production-injection ratio
   - Gas-liquid ratio
   - Foam slug size
5. Selected operating parameters are applied to reservoir models to study effects of interest parameters which are:
   - Heterogeneities values (Lorenz coefficient)
   - Ratio of vertical to horizontal permeability
   - Multi-slug foam
   - Wetting condition of rock
   - Thickness of formation
6. Analyze and summarize effects of parameters on performance of nitrogen foam flooding for each parameter which yields the optimum production.

จุฬาลงกรณ์มหาวิทยาลัย
Chulalongkorn University

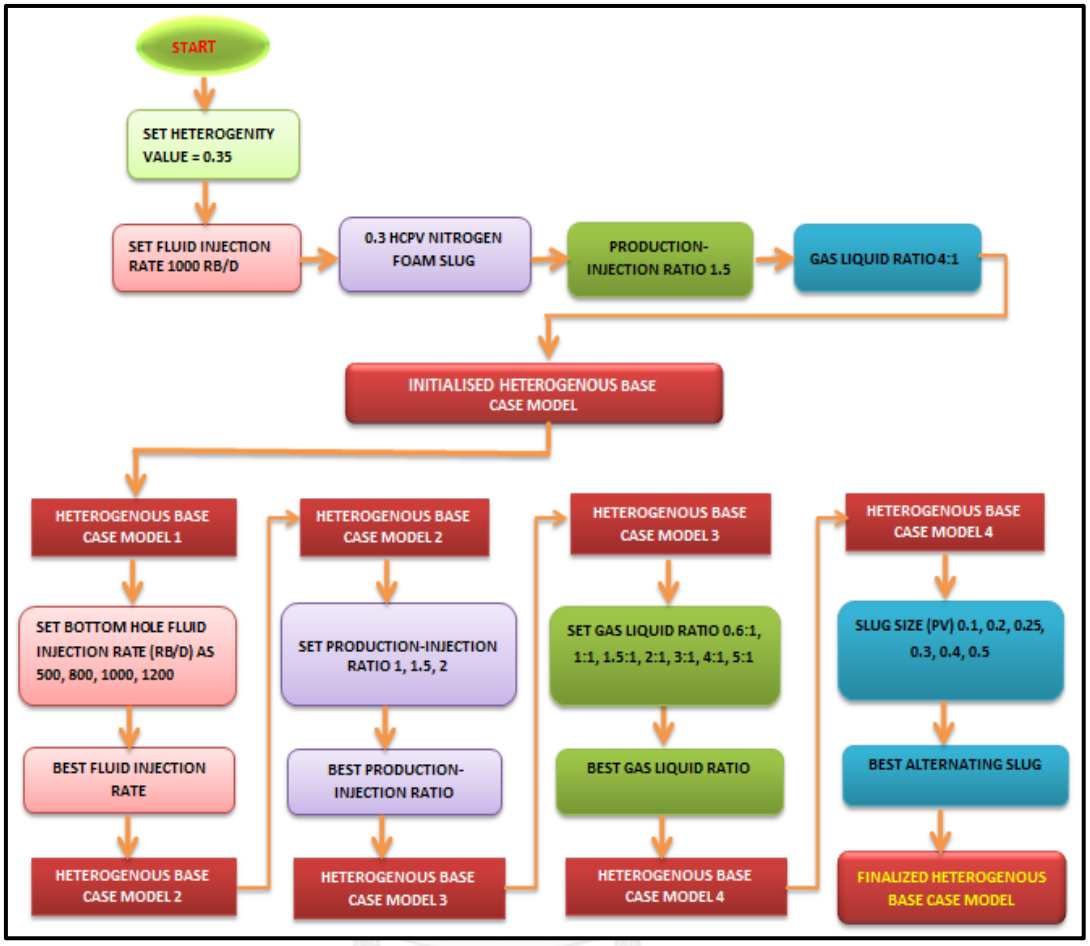

Figure 1.1 Flow chart illustrating selection of foam base case and study of effects of heterogeneity

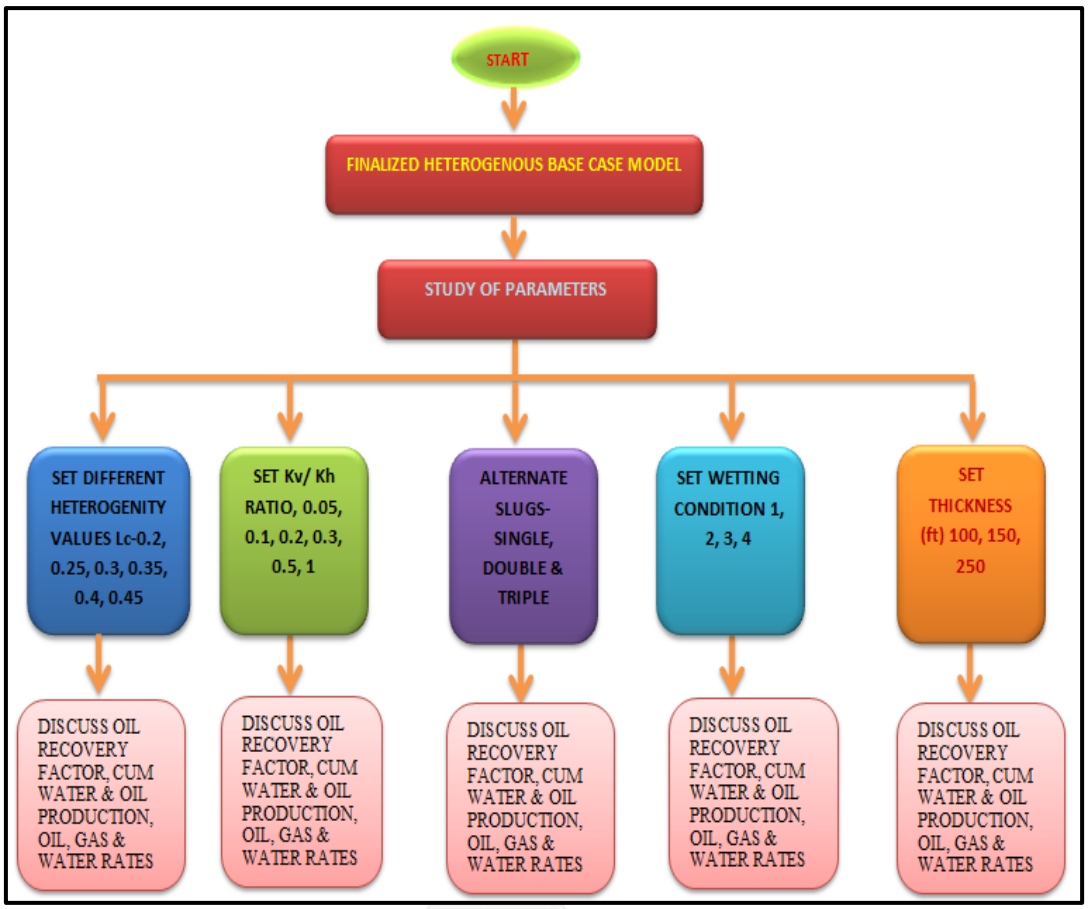

Figure 1. 2 Flow chart illustrating study of reservoir parameters and interest parameters and study of parameters

จุฬาลงกรณ์มหาวิทยาลัย
Chulalongkorn University

1.4 Outline of thesis

This thesis consists of six chapters as mentioned below:

Chapter I introduces background of nitrogen-foam flooding and reveals objectives and outline methodology of this study.

Chapter II summarizes literature reviews related to keywords of this study which are foam flooding and nitrogen-foam flooding.

Chapter III provides technical concepts of nitrogen-foam flooding and petrophysical properties involved with this technique.

Chapter IV describes in detail about selection of reservoir physical properties, Pressure-Volume-Temperature (PVT) properties, petrophysical properties, construction of heterogeneous reservoir model and nitrogen-foam flooding. Detail of methodology is discussed.

Chapter V represents simulation outcomes together with discussion prior to conclusion.

Chapter VI summarizes final conclusions and recommendations for further studies.

จุฬาลงกรณ์มหาวิทยาลัย
Chulalongkorn University

CHAPTER II
LITERATURE REVIEW

This chapter summarizes previous studies related to nitrogen-foam-flooding. These literatures provide valuable information concerning evolution, properties, parameters and applications of general foam as well as nitrogen-foam in enhanced oil recovery.

2.1 Generality of Foam Flooding, Concerning Parameters and Applications

Effect of various parameters of foam flooding and properties of foam have been investigated in many studies during past decades. Foam flooding was firstly used in enhanced oil recovery as foam flooding yields better performance compared to injection of gas.

Mixing of gas, water and a foamer leads to formation of foam. It consists of thin liquid film called lamella. Three lamellae meet at a point with an angle of 120° that is called plateau border. Gas velocity is much higher than liquid one. So, if both gas and liquid flow at almost the same velocity, oil recovery can be improved .This improvement in oil recovery is accomplished when lamellae trap gas phase and move together, leading to stable foam flow.

Farajzadeh et al. [3] studied effects of foam flooding mainly using two gases which are carbon dioxide and nitrogen for oil recovery. Gas purity of 99.88% was used to conduct experiments. They sub-divided their experiments into two parts. The first part was carried out at atmospheric pressures and at room temperature (20°C). For the second part, experiment was performed above critical point under both miscible and immiscible conditions (temperature is 50°C). Conclusions were highlighted by comparing effectiveness of carbon dioxide- and nitrogen-foam flooding. Stability of foam varied with different types of surfactant. Generated foam might collapse, decayed and ruptured, depending upon characteristics of each surfactant. Additional conclusion was made that nitrogen-foam flooding yields better oil recovery compared to solely nitrogen injection for improving oil recovery.

Kovscek et al. [4] performed a study on displacement mechanism by foam in porous media as well as foam texture. Extent of this study was also performed by reservoir simulator, using population balance method under transient and steady state conditions to analyze foam texture as it controls foam mobility. The study was performed by displacing foam in a 1.3-μm^2 Boise sandstone sample with porosity of 0.25 at backpressure 700 psi and at superficial velocities between 0.40 and 2.1 m/day. At different injection modes, path of foam fronts were analyzed. Both theoretical and experimental results matched. Finally, they concluded that foam texture controls path of foam. In the transient and steady-state conditions, fine foam textures were responsible for large pressure gradients and low liquid saturations, whereas coarse textures were responsible to lesser gradients and higher liquid saturations. The net foam i.e. fine and coarse foam was generated in linear area close to the inlet face of core and un-foamed surfactant solution and gas (nitrogen) are transformed to fine texture foam.

Vikingstad [5] researched on effect of foam generation and foam stability on oil displacement mechanism. Bulk foam methods, micro visual cell observation experiments, core flooding test and reservoir simulation were performed to study foam stability. Stability of foam film depends on capillary pressure and this capillary pressure varies with surfactant, velocity and permeability. Static foam test indicated that foam stability was reduced by interacting with oil, leading to adsorption of surfactant molecules. Foam stability was also affected by wettability of rock as well as pore structure. Core flooding test did not affect foam strength. Residual oil saturation affected foam propagation rate as it affected stability of generated foam. During gravity segregation study, reservoir parameters and foam properties were varied to analyze different injection methods. Segregation length is almost the same for different injection methods. Simulations of production well treatment showed a decrease in gas-oil ratio for foam and resulted in an increment of oil recovery when compared to different levels of injection periods.

Al-Mossawy et al. [6] researched on foam dynamics in porous media and its application in EOR. Foam generation, stability and flow regimes in porous media were

studied. Factors affecting foam dynamics such as surfactant, injection parameters, permeability and heterogeneity were also investigated. They observed that all field trials based on simulation data were not always successful. Sometimes the estimated value of injectant was wrong. So, proper foam injection method should be selected. Foam was generated during drainage process but not by imbibition process. So, target reservoir should be thoroughly understood to apply foam flooding for successful field application.

2.2 Application of Nitrogen-foam Flooding

EOR methods are indeed advantageous in the area possessing specific characteristics. While selecting one of these methods, it is very important to keep eyes on availability of injectant sources, and relative cost. Usually for gas injection process, either hydrocarbon or carbon dioxide is used to inject into reservoirs. In several projects source of gas is not fully available or there might be limitation due to environmental problems. When compared to nitrogen-foam flooding, this method is found to be very useful as cost is much less and availability of injectant is abundance. Therefore, many companies worldwide have switched their interest to nitrogen-foam injection process.

Dong et al. [7] published a paper concerning air-foam injection for highly heterogeneous reservoirs. The effects of Low Temperature Oxidization (LTO) reaction was analyzed for different type of oil. During LTO reaction process, oxygen consumption, carbon dioxide and other factors were observed to check oil sample quality for air injection flooding process. Isothermal-combustion experiments were performed to study the effects of factors such as foam, oil type, minerals that effect LTO reaction process. Later, dynamic foam displacement experiments were conducted to evaluate oxidation consumption, retention time of air and displacement of air-foam injection. Dual-tube EOR experiment was performed to simulate process of flow and displacement of air-foam in heterogeneous reservoir. This experiment was conducted to observe pressure drop and production liquid. At initial stage of displacement process, oil in both high permeability and low permeability tubes was displaced at high pressure drops. Air-foam slug of 0.1PV was

injected when water cut ratio reaches 98% and foam slug was followed by chasing water. Similarly, other two slugs were injected and pressure drop during each stage was observed. Plugging of gas–water channeling path leads to a rise in pressure drop and sweep efficiency was also improved. Total recovery of oil enhanced was 10.9%.

Yu et al. [8] described performance of air-foam injection in Middle SaSan 8 unit of HU-12 block, in Zhong Yuan oilfield, China. In this study, the field consisted of many highly heterogeneous reservoirs. Permeability of mixed oil- and water-bearing formations varied from 100 to 1000 mD. Reservoir temperature was 90°C and initial reservoir pressure of 25MPa was reduced to less than 20MPa. Formation water contained high salinity. Present water cut was approximately 95% and porosity of this sandstone formation was 21%. Secondary recovery resulted in oil recovery factor around 20-25% within 20 years. A try was made to improve oil recovery by using nitrogen injection but it was not possible to achieve as firstly desired due to gas early breakthrough. Therefore, high pressure air-foam injection had been planned and effectively applied to this reservoir. Laboratory experiments included regarding LTO, sand pack flooding and displacements studies. After conducting several experiments, 15% increment of oil recovery was obtained. Through reservoir simulation model, over 13% original oil in place increment in oil recovery was obtained within operation period of1 5years.

Wang et al. [9] studied oxidation process of air/air-foam with oil and air-foam displacement efficiency in the Xi11-72 Block, in Hailaer Oilfield, China. Reservoir rock possessed low permeability as well as porosity. Natural fractures were present. Initial reservoir pressure and temperature were 22.5 MPa and 82°C, respectively. Primary and secondary recoveries yielded quite low recovery due to insufficient reservoir energy. The block consisted of 20 wells of four test well groups and formations contained oil density of 0.8234 g/cm^3, average oil viscosity of about 5.875 MPa, and original gas oil ratio 11.61 m^3/m^3. Isothermal flooding experiments were performed using core and samples of oil from the well at the same temperature and pressure. Displacement efficiency of air flooding obtained was 45.88 %, whereas waterflooding technique yielded only 33.08 %. Results reflected that mixed gases solubility was

larger than by solely nitrogen. This decreased oil viscosity and density, leading to oil expansion and increase in formation volume factor. Air-foam injection was planned as a small cyclic injection plug by creating in-situ foam. Injection rate was increased gradually. Injection pattern was 30 m^3 of foam liquid, 5 m^3 of water and 10,000 m^3 of air at standard conditions. Air injection rate was 5,000 m^3/day and foam liquid injection was more than 2.0 m^3/day. Concentration of foaming agent was about 1.33% w/w. lastly, it was highlighted in study that all experiments carried out were effective in low permeability reservoirs and oil recovery was obtained by blocking channeling of air-foam. Nevertheless, only problem occurred was corrosion of pipeline which was considered as very severe problem.

Liu et al. [10] studied effectiveness of nitrogen-foam flooding in highly heterogeneous reservoir of Shengli oil field. Foam depends on many factors to deliver best performance which include, foam stability at reservoir temperature and pressure, fluid compatibility, less adsorption on rock surfaces, high viscosity and less cost. Optimum surfactant concentration was found to yield maximum foaming ability and stability with less cost of surfactant. Gas-liquid ratio (GLR) was very important on foam. Foam flooding was performed by co-injecting of nitrogen and water at fixed gas liquid ratio until reduction in pressure was observed. An optimum GLR was considered. Oil recovery improved from 21.7% to 47.6%. Investigators also stated that foam in high permeability zone was more stable, showing better blocking ability compared to cases of lower permeability zones. Field simulation model consisting of 3-D and 3-phase was performed at reservoir pressure 12.3 MPa, porosity 31%, depth 1200 ft, and average permeability to air 2000 md, oil viscosity 100 mPa-s, oil density 0.92 g/cm^3 and temperature 60°C. Reservoir was initially waterflooded and later nitrogen-foam flooding was performed when water cut reached 90%. Chosen values of average permeability were 500 md, 1,000 md and 4,000 md; whereas three slug sizes were selected include 0.1PV, 0.2PV, and 0.3PV. Concentration of surfactant agent selected was 0.5% by weight. Various models were studied and finally optimum ratio of gas to liquid was at 1.5:1 and optimum foam slug of 0.2 PV. Ultimate oil recovery was substantially enhanced. Result from this study was

implemented in field test on four reservoirs and oil recovery achieved was higher and water cut was obviously declined. In summary, nitrogen-foam flooding was considered as a good technique for heterogeneous reservoir with cost effective.

Xu et al. [11] studied effects of air-foam flooding for Longdong Jurassic reservoir. This Jurassic reservoir was highly heterogeneous with average to low permeability values. After primary recovery, secondary recovery process was carried out to improve oil recovery. Unfortunately, waterflooding technique failed due to early water breakthrough. Therefore, air-foam flooding technique was proposed after analyzing behavior of reservoir and benefit could be obtained from this technique. The research was started with obtaining proper air-foaming agent formula by analyzing foam parameters such as Foamability and foam stability. Interfacial tension was also considered and analyzed. Final formulation was 0.5wt% HD-6 mixed with 0.15wt% HD-Y. Core flooding test were carried out to view process parameters. Gas-liquid ratio of 3:1 was selected for this process. Slug size was fixed at 0.9PV.The test turned to be very advantageous as displacement efficiency of was improved higher than the use of surfactant flooding. After achieving expected results, the same air-foam flooding technique was implemented in Maling Block. This technique helped in increasing injection pressure. Water cut was outstandingly decreased. Finally, oil recovery factor was increased as expected. This technique proved to be an effective method for highly heterogeneous reservoir containing low permeability and high water cut ratio. Oil recovery mechanism was mainly obtained by controlling mobility of injected fluid that consecutively resulted in improving sweep efficiency.

Kuehne et al. [12] performed laboratory and simulation studies on nitrogen-foam flooding and later applied for the Painter reservoir. This reservoir is located in the over thrust belt of south western Wyoming. For the field trial, 60% quality and 20,400 bbl of foam was injected. The surfactant concentration used was 0.5 wt% to 1.5 wt%. In the discussion, they mentioned that a thorough understating of respective reservoir was needed and also low injectivity of foam close to fracture pressure might open existing channels instead of diverting the flow. So the well

should not be over pressured and this could be done by using high quality foam of around 80% or by increasing surfactant concentration.

Zhu et al. [13] researched on recent progress and analysis of foam flooding field test in China. The application of foam flooding can be clearly observed in different test. This study concluded performance of pilot test and also effects of foam on oil recovery. Totally 18 pilot tests were executed and 16 tests were successful executed. Table 2.1 summarizes pilot tests in China including types of injected gas, reservoir permeability and also results obtained and Table 2.2 summarizes applications of nitrogen-foam flooding at different reservoir conditions.

Table 2.1 Summary of pilot test in china [13]

Time	**Name of Oil filed**	**gas**	**Permeability ($\times 10^{-}um^{2}$)**	**Injected foamer**	**Increase oil production (tons)**	**Effectiveness portion of wells**
1994	Shengli	N_2	1,300	9.7 tons foamer	≥6,000	50%
1995	Shengli	N_2	1,300	18	≥5,000	
1996	Baise	Air	13.41-450	1,747 m^3 solution	≥2,454	43.57%
1996	Liaohe	N_2	1065	691.45 tons foamer	≥10,800	
1996	Baise	N_2	24-150	2,266 m^3 solution	883	57%
1997	Daqing	H.C.gas	314	0.552PV ASP foam	≥78,501	70%
1999	Liaohe	N_2	1,065	5,373.6 tons foamer	174,100	

Time	Name of Oil filed	gas	Permeability ($\times 10^{-}um^{2}$)	Injected foamer	Increase oil production (tons)	Effectiveness portion of wells
2003	Shengli	N_2	1,500	34.75 tons foamer	≥12,072	100%
2003	Shengli	N_2	1,300-1,800	274.3 tons foamer	11,000	50%
2004	Baise	N_2	24-150	600 m^3 solution	509.6	75%
2005	Yanchang	Air	140-900	4,477 m^3 solution	3,486	66%
2005	Changqing	Air	0.3-0.5	1,128 m^3 solution	5,157	54.5%
2006	Changqing	Air	30	3,606 m^3 solution	≥118	33.33%
2006	Changqing	Air	30	2022 m^3 solution	≥440	83%
2007	Zhongyuan	Air	235.5	2,001 m^3 solution	768.2	
2007	Yanchang	Air	0.82	1,091.8 m^3 solution	573.5	100%(#54) 62.5%(#55)
2007	Daqing	N_2	600-1,000	11,000 m^3 solution		Gas fingering
2009	Daqing	CH_4	520-1,000	0.6PV Solution		Gas fingering

จุฬาลงกรณ์มหาวิทยาลัย
CHULALONGKORN UNIVERSITY

Table 2.2 Performance of nitrogen-foam flooding under different reservoir conditions

	Shengli Tuo 11	**Shengli Gudao 28-8**	**Daqing Bei 2-6-33**
Gas	N_2	N_2	N_2
Permeability ($x10^{-}um^2$)	1,500	1,300-1,800	600-1,000
Oil Viscosity(mPa.s)	178 ~198	74	8 ~10
Foam formula	Foamer:DP-4, Cs:0.5%-1%,Cp:0.2%-0.18%	Foamer:DP-4,Pre-slug:0.18%P+1.5%S, Main-slug:0.18%P+0.75%S	Foamer 0.3%SW Pre-slug: Gel
Injected foamer	34.75 tons	274.3 tons	11,000 m^3
Increase oil production (tons)	12,100	11,000	
Effectiveness portion of wells	100%	50%	Gas fingering
Development stage	After waterflooding	After polymer flooding	After polymer flooding

จุฬาลงกรณ์มหาวิทยาลัย
Chulalongkorn University

Authors suggested that if foam injection methods like co-Injection or Surfactant solution Alternating Gas (SAG) is to be performed, a thorough understanding of target reservoir, reservoir temperature, salinity of formation, foam slug size and gas liquid ratio are required as these parameters affect performance of foam flooding.

CHAPTER III
THEORY AND CONCEPT

3.1 Introduction

This chapter aims to present fundamental concepts of foam used in enhancing oil recovery. Also a brief discussion is made on some basic petrophysical concepts and reservoir properties that are involved in foam flooding.

3.2 Fundamentals of Foam and Applications

3.2.1 Foam and Oil Recovery Mechanics

Foam is a mixture of gas, water and a surfactant where gas volume is scattered as bubbles in a liquid medium or in other words foam is made up of liquid (solution of surfactant) and gas (N_2, CO_2 etc.). So, foam properties fall between liquid and gas properties, depending on foam quality[14]. Foam usually contains very small bubbles or can be large bubbles but all are separated by liquid films. Texture of foam is usually arranged in hexagonal structure and diameter of bubble is usually in a range of 10 to 1,000 μm. Sometimes bubble size can be as large as several centimeters, depending on characteristic of foaming agent. Component of foam is illustrated in Figure 3.1, whereas Figures 3.2 shows hexagonal structure of foam and details of foam system in two dimensions. Foam consists of thin liquid films so-called lamella. Three lamellae meeting at a point at an angle of 120° is called plateau border. Pseudo-emulsion film is an asymmetrical oil water gas film in a presence of oil between oil drops and bubbles of gas phase and it is a lean liquid film bounded by gas on one side and oil on other side[15]. If foam consists of spherical shaped bubbles separated by thick layers of liquid is called as wet foam (kugelschaum) and if foam consists of polyhedral bubbles separated by thin films is called as dry foam (polyederschaum)[15]. Thin or thick liquid is usually water.

Sometimes it can be hydrocarbon-based fluids or acids, creating foam which is usually called non-aqueous foam.

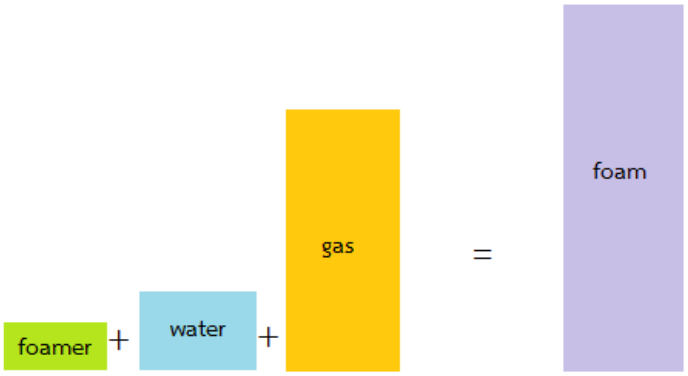

Figure 3.1 Foam components

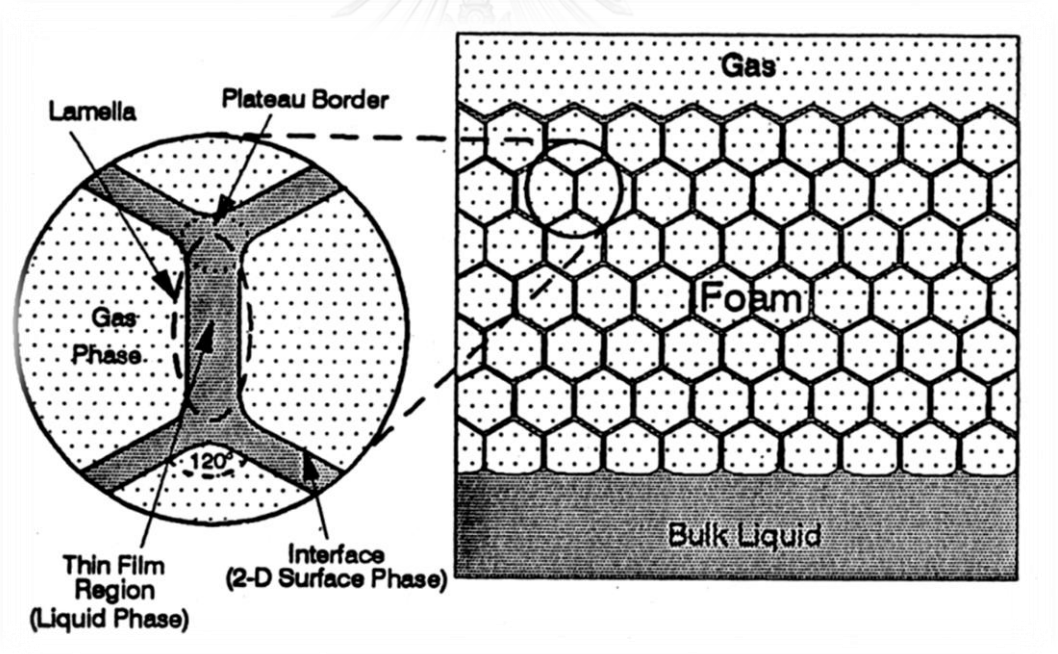

Figure 3.2 Hexagonal foam structure and foam system in two dimensions [16]

Foam is injected into formations to enhance oil recovery and also to divert acid solution in matrix acidizing which is one of well stimulation techniques. Foam can be injected continuously or in alternating slugs of gas and liquid. For EOR, foam

is used 1) as a stimulant to improve production of gas, 2) to decrease water cut, and 3) to reduce the mobility of gas.

3.2.2 General Foam Terminologies

There are several general foam related terminologies and even though some concepts are not applied during this research, they are still discussed to give specific knowledge.

Gravity Drainage

Thin layer of liquid separates foam bubbles from each other. Therefore, liquid gravity causes liquid to drain in liquid layers [15].This effect makes films thinner and causes gas bubbles to coalesce.

Laplace Capillary Suction

As shown in Figure 3.2, the interface (gas–liquid) at the plateau borders is slightly curvaceous with smaller radii, whereas the interface at thin liquid film regions are mostly flat with larger radii and this is because of capillary pressure. There is always difference of pressure between these two styles of region and this causes the movement of liquid towards the plateau borders, letting films to be thin [15].

Effect of Marangoni

Due to surface tension gradient, fluid mass transfer takes place along an interface between two regions is called Marangoni effect. In a foam system whenever a liquid film (surfactant solution) undergoes expansion, local concentration of surfactant gets lowered by increasing surface area and thus, causing film to become thinner. As surfactant concentration gets lowered, surface tension is higher, causing contraction of surface in order to maintain low energy and this surface contraction makes liquid to flow from low to high tension region in the film. This kind of liquid movement provides resistance against liquid film to get thinner. In other words, the Marangoni effect with an aid of surface tension gradient helps stabilizing foam system. Surface elasticity is also referred as Marangoni effect [15].

Interfacial Tension

In any system, two immiscible fluids are separated by an interface. The interaction that takes place due to their co-existence is called Interfacial tension (IFT) [17]. IFT facilitates the process of forming bubbles. However, there is no guarantee that stable foams will be achieved [15].

Gas diffusion

Many theories describes that size of bubble are different. Small bubbles possess larger pressure compared to large bubbles. Difference in pressure causes diffusion of gas through liquid layer from small bubbles to larger bubbles and eventually this leads to coalesce of foam bubble [15].

Liquid Viscosity

The higher the liquid viscosity, the more stable are foams. Liquid drainage process reactions takes place at slower rate which helps to achieve stable foams. Several viscous fluids are nowadays added into solution to generate highly stable foam such as high molecular weight alcohol or polymer.

Static and Dynamic

Static and dynamic properties of foam are different. Rate of foam formation is zero in static foam and the previously formed foam collapses without foam regeneration. Such type of foam experiments are carried out by mixing foam with presence of oil. Oil will be forced into lamellae during mixing process. After foam formation, oil may drain out from lamellae. In dynamic foam experiments, foam is formed continuously. Dynamic foam situation is completely different from static foam in porous media. If foam is injected into oil-bearing core, foam will be in contact with residual oil at certain locations in porous media. Stability of foam in presence of oil is very important [5].

3.2.3 Foam Stability, Foam Texture, and Foam Quality

Foam stability is defined as an ability of foam to withstand spontaneous collapse or breakdown from external causes [18]. It depends mainly on surfactant used to generate and stabilize foam [15]. Selecting a right surfactant is one big step for successful foam flooding operation. This step however, is performed in laboratory to carry out tests for a specific application [15]. Stability of foam is observed by counting number of days in which foam volume is reduced to half. Foam stability can be increased by increasing number of surfactant at air-liquid surface, resulting in an increment of surface viscosity. Foam instability can be caused by drain of liquid from foam. Moreover, when foam is in contact with oil, foam stability can be reduced. Stabilization of foam is caused by Van der Waals forces between each foam particle where electrical double layers created by di-polar surfactants are located on its surface. Moreover, Marangoni effect, which behaves like a restoring force to lamellae, is also taken place in foam stability. Foam stability is strongly affected by temperature. As temperature increases foam stability decreases due to higher rate of coalescence of foam bubbles. Salinity decreases foam stability by obstructing forming of surfactant layer at surface. At high pressure, surface viscosity obtains higher strength and this helps maintaining foam stability. Nevertheless, foam stability can be varied in different technique. During immiscible flooding, foam stability should be kept as high as possible, whereas in miscible flooding foam stability should be kept at appropriate value in order to obtain both effects from miscibility by liberating gas and at the same time, mobility control has to be maintained. Ultimately, liquid drainage rate and foam strength controls foam stability. But in practical, no foam is thermodynamically stable for all the times [15].

Foam texture is a distribution of bubble size in foam matrix or number of lamellae per unit volume. Foam texture is an important parameter that affects rheology of foam fluid [16]. Foam texture is classified according to size and shape of bubble and also distribution within the matrix of foam. Foam texture is affected from quality of foam, pressure, foam generating method, and chemical composition [16]. Equilibrium is achieved at a typical shear rate. At high shear rate, high pressure, and

high surfactant concentration, fine texture of foam with high dynamic stability is produced. Bubble size reduces with an increase of surface viscosity by increasing surfactant concentration and hence, foam stability is maintained.

Foam quality or Foamability or foaminess is defined as ratio of gas volume per total foam volume and is generally expressed in fraction or percentage [19]. Foam quality is interrelated to bubble size [15]. As foam bubbles are formed, the new foam will be at the bottom and aged foams i.e. are old foams at the top. The aged foams film contains less liquid and so quality of foam is high than the new formed foams. Foam quality plays a major role in displacement mechanism as mobility of foam and foam resistance factors directly depend on it. Foams with qualities less than 55% are Newtonian fluids and above 55% foams exhibit shear thinning properties and a major factor that affects foam quality is the shear rate that is imposed on foam [4]. Foaming quality reaches its maximum at or above the Critical Micelles Concentration (CMC) of surfactant. Typical range of foam quality is from 75% to 90%. Bubble size varies for each foam and average size of varies from 0.01-0.1 μm to tenths of millimeters. Larger size bubble tends to be unstable and it is very poor in foam flooding performance.

Increase of pressure reduces foam bubble size. As foam bubble becomes smaller, liquid films become larger and thinner which in turn, reduces liquid drainage effect by lowering drainage process. In general higher pressure always leads to more stable foam. But one application should identify the right pressure as too high pressure might leads to breakage of foams [15].

Higher temperature always increases solubilizing effect that is surfactant easily gets solubilize in liquid phase leading to less surfactant in gas/liquid interface. Liquid drainage effect is also increased due to foam breaking from coalescence. Temperature effect should be investigated thoroughly before selecting a perfect surfactant that can withstand thermal effects.

จุฬาลงกรณ์มหาวิทยาลัย
CHULALONGKORN UNIVERSITY

3.2.4 Nitrogen -Foam Flooding

Carbon dioxide (CO_2), nitrogen (N_2), steam and air flooding techniques generally result in very low sweep efficiency and consecutively low oil recovery due to viscous fingering and gas overriding as shown in Figure 3.4. Gas overriding emerges due to density of gas that is much smaller than displaced oil and formation water. This causes a preferential flow on top of formation and eventually gas early breakthroughs. Viscous fingering instead is a result of lower viscosity of gas compared to displaced oil and formation water. Unfavorable mobility ratios cause even extreme channeling in heterogeneous reservoirs. Generally Water Alternating Gas (WAG) is implemented to achieve favorable mobility ratio to improve sweep efficiency. However, WAG can encounter several problems such as trapped oil by water that results in difficulty to be in contact with injected gas. Therefore, WAG seems not to be totally successful method to control gas mobility.

By adding surfactant into water, a process called Surfactant Alternating Gas (SAG) was developed where alternating slugs of surfactant solution and gas were injected. This generates a foam concept and it is nowadays widely used to overcome adverse effects when performing solely gas injection. As shown in Figure 3.3, foam can smoothen flood front compared to the use of just solely gas injection. Generally, foam flooding is performed after waterflood process. Foam is usually created at in-situ conditions, resulting in foam that is very delicate to handle. When foam is created at surface and injected to reservoir, foam bubble might collapse, rupture or decay. Air-foam flooding is typically performed in a broad range of reservoir characteristics such as light oil reservoir, heavy oil reservoir, high water cut reservoir, high heterogeneity, or reservoir with fractures.

จุฬาลงกรณ์มหาวิทยาลัย
Chulalongkorn University

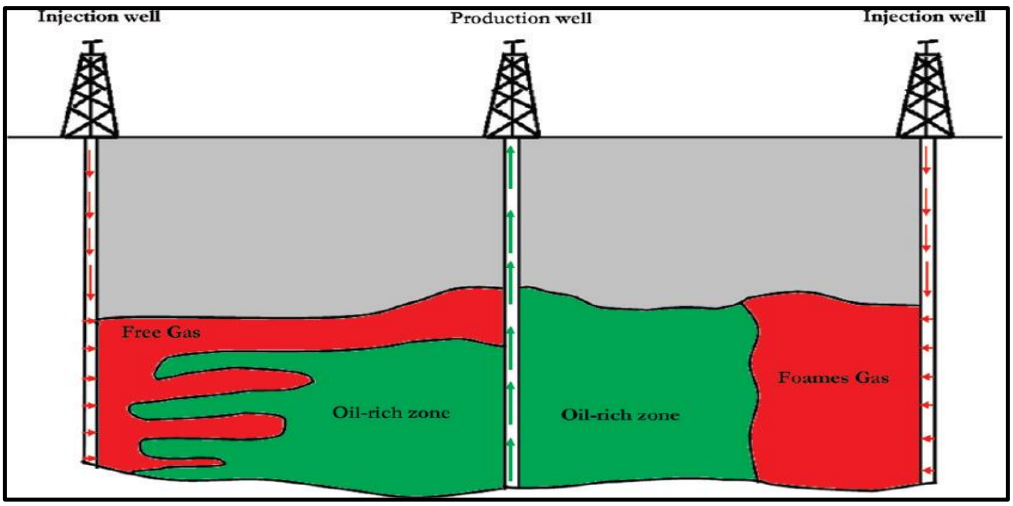

Figure 3.3 Flow regimes obtained from solely gas flooding compared to foam flooding [3]

3.2.5 Effects of Surfactant in Foam

A single molecule of surfactant so-called monomer composes of a hydrophobic alkyl chain and a hydrophilic head group and formation of micelle is also shown in Figure 3.4.

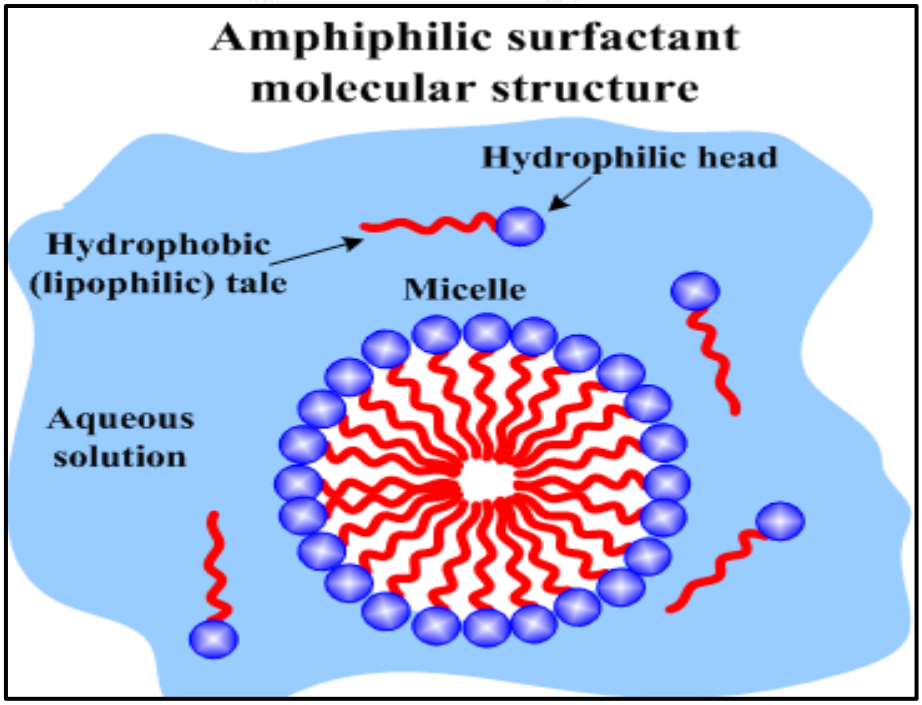

Figure 3.4 Structures of surfactant monomer and micelles [20]

There are different types of surfactant such as anionic surfactant, cationic surfactant, nonionic surfactant and zwitterionic surfactant. Concentration of surfactant is very important to identify CMC. Actually, when surfactant concentration is raised, monomers are formed up to CMC. Beyond that concentration monomers start to aggregate to reduce dispersion of charge, forming a structure called micelle. There are several structures of micelle such as spherical, cylindrical, lamellar, inverse, bicontinous, and vesicle. Figure 3.5 illustrates possible structures of micelle.

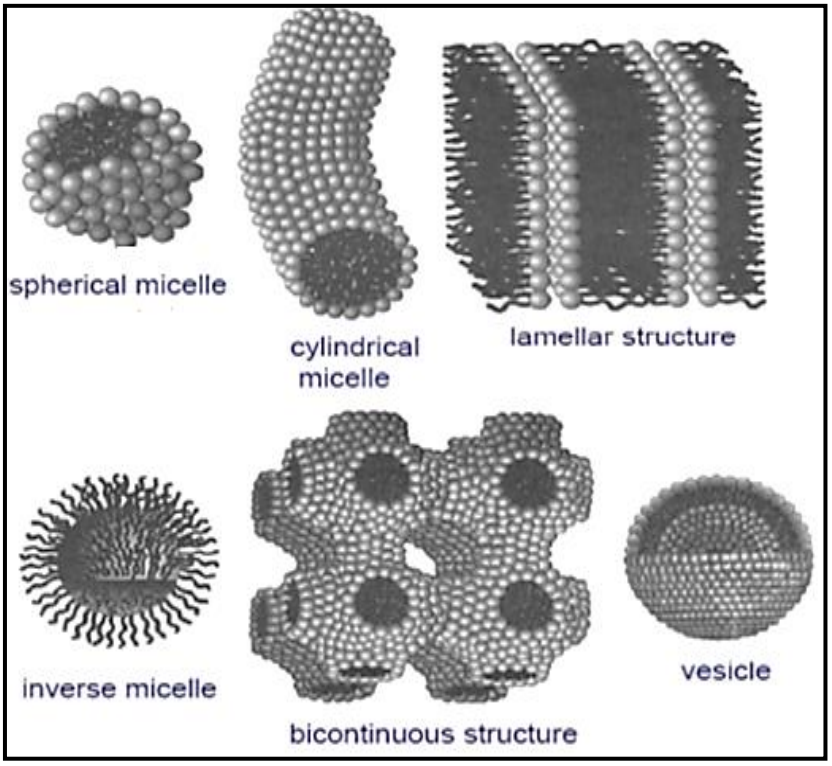

Figure 3.5 Possible structures of micelle [21]

Surfactant lowers interfacial tension (IFT) as well as surface tension (ST) up to CMC point. Identifying proper surfactant concentration to achieve optimum condition also depends on adsorption mechanism. Therefore, surfactant concentration should be slightly kept higher than CMC to prevent loss of surfactant due to adsorption that could drastically reduce IFT and ST. It was reported that foams was generated from several foaming agents such as alpha olefin sulfonate and modified ammonium lauryl sulfate. Nevertheless, most foam is generated from anionic surfactant to form foam in order to reduce adsorption onto reservoir rocks. Foam selection for certain

reservoir conditions is also based on foaming ability and foam stability. Properties of foam are mainly affected from temperature, pressure and salinity.

3.2.6 Foam-Oil Interactions in Porous Media

Interaction between oil and foam greatly affects efficiency of foam flooding. When foam is in direct contact with oil, surface tension between foam and air is raised and foam gets destabilized. Surface active agents forming foam may be adsorbed by porous media or might partition in oil phase. Pore structure and wettability might also affect stability of foam. Foam efficiency is reduced when it comes in contact with oil. The phenomena of spreading, entering and emulsifying in flowing foam lamellae are as shown in Figure 3.6.

During spreading mechanism, as oil spreads over interface of gas and water, both gas-oil and water-oil interface are created. Oil that spreads over lamella lowers surface tension, increasing radius of curvature of bubbles and consecutively altering original surface elasticity and surface viscosity. Therefore, interfacial film loses its foam stabilizing strength. Next type of rupture mechanism is entering (pseudo-emulsion film rupture) in which water - gas interface penetrates within lamellae liquid by oil. Pseudo-emulsion films are films of aqueous solution separating oil from gas. Thus, interfacial film can lose its foam stabilizing strength and thin to the point of rupture. In emulsifying mechanism, when oil contacts foam, oil phase becomes emulsified and imbibes into foam lamellae through a simplified balance of forces by lamella number, *L* [16].

$$L=\Delta P_C \times \Delta P_R \tag{3.1}$$

where ΔP_C and ΔP_R are difference in pressure between inside border of plateau and inside laminar part of lamella and difference of pressure across the oil-water

interface respectively. As lamella of foam travels in porous media and when $L > 1$, oil will move inside foam lamella and pinched off to produce emulsified drops.

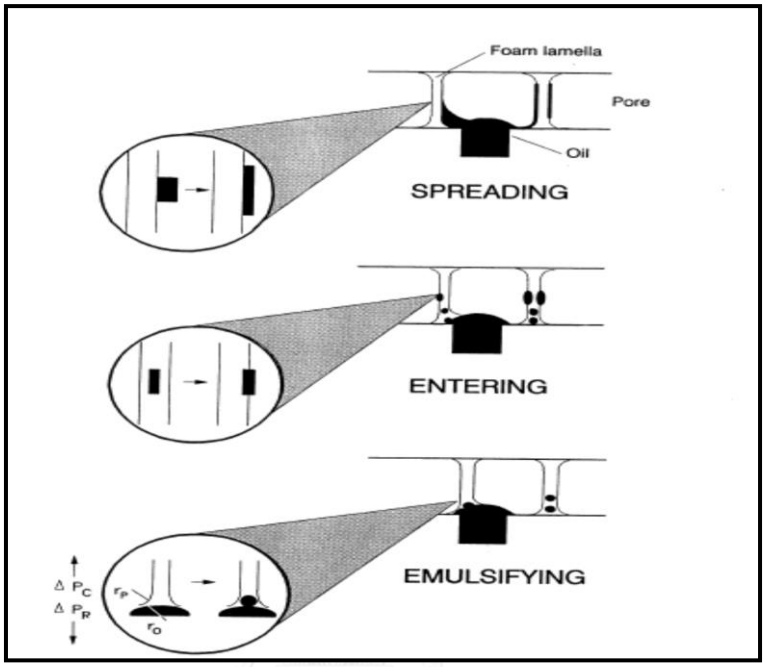

Figure 3.6 Interaction between foam and oil interaction [5]

Past literatures mentioned that foam efficiency is less at high oil saturation. Hence, foam flooding should be performed after waterflooding. Nowadays, foam is generated to be tolerant with high oil saturation i.e. oil resistant foams. This newly invented foam is valid for all range of oil. This oil resistant foam may be formed with pure foaming agents, generally high cost method, or with special formulation which can be cost effective and insensitive with oil.

3.2.7 Foam Formation and Foam Decay

The three basic mechanisms with respect to foam formation and foam decay are snap-off, lamella division, and leave-behind.

Snap-off Mechanism

This phenomenon occurs when bubble enters through pore restriction and due to this, entering formation of new bubble takes place as shown in Figure 3.7. A

repeating process can occur at the same location. This mechanism dominates the foam generation process as it helps to increase discontinuity of gas phase forming new lamella. This lamella then, finds a place for it somewhere in porous medium, blocking some pathways for gas flow and leading to reduction of gas permeability.

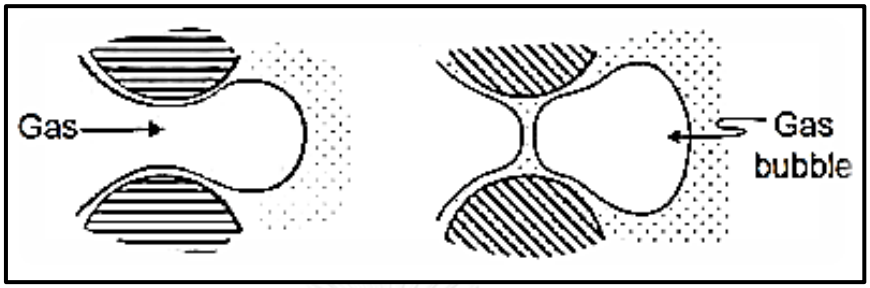

(a) (b)

Figure 3.7 Snap-off mechanism showing a) gas penetrating through pore restriction b) formation of new gas bubble [15]

Lamella Division Mechanism

The mechanism occurs when lamella is divided into two or more lamellae after arriving to a branch point as shown in Figure 3.8. This mechanism is more or less identical to snap-off mechanism and it is more pronounced at high flow velocities.

จุฬาลงกรณ์มหาวิทยาลัย
Chulalongkorn University

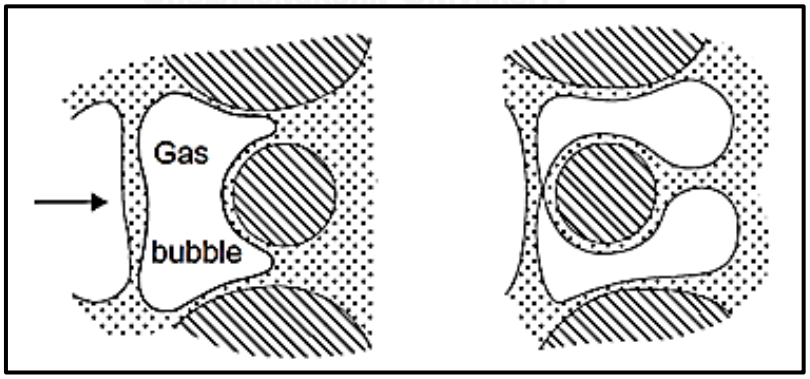

(a) (b)

Figure 3.8 Lamella division mechanism showing a) lamella approaching to branch point location b) formation of divided gas bubbles [15]

Leave-behind Mechanism

This mechanism begins as two gas menisci from different directions invade adjacent liquid-filled pore bodies as shown in Figure 3.9 and as the two menisci converge downstream, a lens is left behind [16]. Lens depends on capillary pressure of medium and pressure gradient. This mechanism occurs due to low flow velocities and at continuous gas phase. Foam generated by leave-behind mechanism gives approximately a five-fold reduction in steady-state gas permeability and discontinuous-gas foams created by snap-off mechanism led in a several hundred-fold reduction in gas permeability [15] [16].

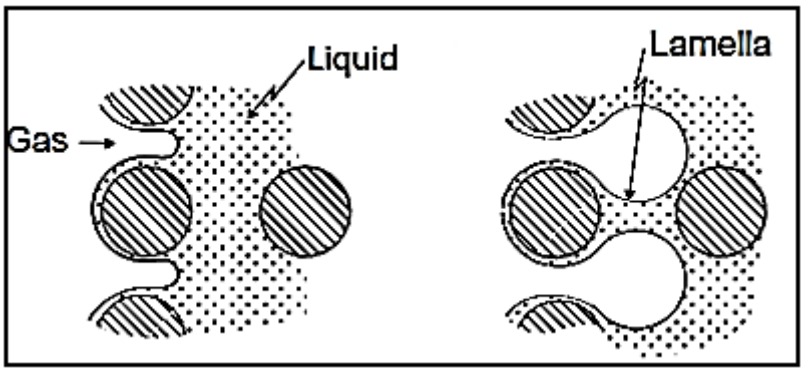

(a) (b)

Figure 3.9 Leave behind mechanism showing a) Invasion of gas
b) Lens formation [15]

3.2.8 Foam Modeling Concepts

General concepts in foam modelling are discussed in this section. The topics covered are mainly on modelling issues, foam flow, foam reactions and slight knowledge of screening criteria.

Foam Modelling Issues

The foam model as to be designed considering many factors and such complicated factors are discussed below:

Foam quality

Foam quality or Foamability or foaminess is defined as ratio of gas volume per total foam volume and is generally expressed in fraction or percentage [19] . Foam is made up of liquid and gas and so its flow behavior is between liquid and gas properties. The correct foam model is one in which the foam flows need to change as a function of quality [22].

Foam density

This is another important issue as it affects to gravity. Foam density is a function of foam quality and should be calculated properly to achieve correct gravity model. Foam density falls between properties of surfactant solution and gas that used to make up foam.

Foam degradation

Foam degradation is a function of time, oil saturation and capillary pressure for a particular foaming agent [22]. It is reported that when oil saturation is high, foam degradation is faster. But nowadays, high resistant foaming agents are available to withstand high oil saturations. But at one stage foam lamella collapses at certain capillary pressure.

จุฬาลงกรณ์มหาวิทยาลัย
Chulalongkorn University

Foam regeneration

At formation surface when liquid and gas are injected together, in-situ foam is formed with an aid of snap off and lamella division mechanisms and hence, pre-generation of foam is not required at the surface. This technique also helps to recover more oil.

Mobility control/ foam blocking/ foam trapping

Lamellae created propagate into pores and are trapped at pore throat, resulting blocking of gas flow. Mobility control is important parameter of foam to recover more oil.

IFT reduction

After foam collapse and turn back to water, surfactant and gas. Surfactant solution therefore can reduce IFT between oil and water, resulting in wettability alteration and reduction of residual oil saturation. Low values of IFT increases capillary number, leading to reduction of residual oil saturation.

Surfactant adsorption

Consumption of surfactant is responsible by the reservoir rock. This option is available in every numerical simulator. The adsorption models are based on Langmuir Isotherm and empirical Freundlich model. To utilize this function, laboratory data is required. Anionic surfactants are widely used in EOR process because they exhibit low adsorption property on sandstone rocks since sandstone surface is negatively charged [15].

Non-Newtonian flow

Foam flow behavior can be both shear thinning and shear thickening as a function of overall flow rate [22]. Shear thinning leads to increase of injectivity.

จุฬาลงกรณ์มหาวิทยาลัย
Chulalongkorn University

$$FM = \frac{1}{1 + F_{mmob} \times F_1 \times F_2 \times F_3 \times F_4 \times F_5 \times F_6} \quad (3.2)$$

where,

Fmmob is reference gas mobility reduction factor,

F_1 is surfactant concentration,

F_2 is oil saturation,

F_3 is capillary number,

F_4 is critical capillary number,

F_5 is critical oil mole fraction for component numx and

F_6 is salt mole fraction

An .Each function captures respective physical effects.

And

$$F_1 = \left[\frac{\text{Mole fraction of surfactant}}{\text{FMSURF}}\right]^{\text{EPSURF}} \tag{3.3}$$

$$F_2 = \left[\frac{(\text{FMOIL-Oil saturtion})}{(\text{FMOIL-FLOIL})}\right]^{\text{EPOIL}} \tag{3.4}$$

$$F_3 = \left[\frac{\text{FMCAP}}{\text{Capillary Number}}\right]^{\text{EPCAP}} \tag{3.5}$$

$$F_4 = \left[\frac{(\text{FMGCP-Capillary Number})}{\text{FMGCP}}\right]^{\text{EPGCP}} \tag{3.6}$$

$$F_5 = \left[\frac{(\text{FMOMF-Oil Mole Fr.}(\text{NUMX}))}{\text{FMOMF}}\right]^{\text{EPOMF}} \tag{3.7}$$

$$F_6 = \left[\frac{(\text{Mole Fraction }(\text{NUMW})\text{-FLSALT})}{(\text{FMSALT-FLSALT}}\right]^{\text{EPSALT}} \tag{3.8}$$

จุฬาลงกรณ์มหาวิทยาลัย
Chulalongkorn University

where *Fmsurf* is critical component mole fraction value and allowed range is 0 to 1, *Fmcap* is reference rheology capillary number value and allowed range is 0 to 1, *Fmoil* is critical oil saturation value and allowed range is 0 to 1, *Fmgcp* is critical generation capillary number value and allowed range is 0 to 1, *Fmomf* is critical oil mole fraction for component *numx* and allowed range is 0 to 1, *Fmsalt* is critical salt mole fraction value (component *numw*) and allowed range is 0 to 1, *Fmmob* is reference foam mobility reduction factor and minimum allowed value is 0, and the suggested maximum is 100,000, *Epsurf* is exponent for composition contribution and allowed range is -4 to 4 with default value 0, which makes foam interpolation independent of composition, *Epcap is* exponent for capillary number contribution and allowed range is -10 to 10 with default value 0, which makes foam interpolation

independent of capillary number, *Epoil* is exponent for oil saturation contribution and allowed range is 0 to 5 with default value 0, which makes foam interpolation independent of oil saturation, *Epgcp* is exponent for generation capillary number contribution and allowed range is -10 to 10 with default value 0, which makes foam interpolation independent of capillary number, *Epomf* is exponent for oil mole fraction contribution and allowed range is 0 to 5 with default value 0, which makes foam interpolation independent of oil mole fraction of component *numx*, *Epsalt* is exponent for salt contribution and allowed range is -4 to 4 with default value 0, which makes foam interpolation independent of composition of component *numw*, *Floil* is lower oil saturation value and allowed range is 0 to 1, *Flsalt is* lower salt mole fraction value (component *numw*) and allowed range is 0 to 1 [23].

The simplest application of using foam interpolation option is to rescale relative permeability to gas, that is, from $K_{rg}(f)$ to FM $K_{rg}(f)$ that is [23]

$$K_{rg}(f) = K_{rg}(nf) \times FM \tag{3.9}$$

where

$K_{rg}(f)$ is relative permeability to gas in the presence of foam, and

$K_{rg}(nf)$ is relative permeability to gas without foam.

Chulalongkorn University

Foam Reactions

Foam reactions discussed in this section represent foam regeneration and foam degradation models.

Table 3.1 Reactions in foam model [22]

Reactions		
1.Lamella	→	Water + Surfactant
2.Foam Gas	→	Nitrogen
3.Lamella+ oil	→	Water + Surfactant +Oil
4.Foam Gas + Oil	→	Oil + Nitrogen
5.Water + Surfactant + Nitrogen	→	Lamella + Nitrogen
6.Lamella + Nitrogen	→	Lamella +Foam Gas
7. Lamella	→	Trapped Lamella
8. Lamella + Trapped Lamella	→	Lamella
9.Trapped Lamella	→	Water + surfactant
10 Trapped lamella + oil	→	water +surfactant +oil

Gas and liquid are injected separately from surface and foam is created in-situ when it enters rock formation. In STARS, this mechanistic creation of foam is performed by foam regeneration model and reactions No. 5 and 6 are used. Reactions No. 1, 2, 3, 4, 9, and 10 represent foam degradation models. Reactions No. 7 and 8 are used to create trapped lamella where reaction No. 7 is used for blockage purpose and reaction No. 8 is used for flow diversion to limit the creation of trapped lamella. The selection of reactions depends on the desired research of foam model [22].

Important Factors in Designing Foam Flooding Applications

Important factors like screening criteria, surfactants and injection modes are discussed here.

Screening criteria – In literatures, screening criteria for foam flooding in field applications were rarely discussed. One of the most important concerns is the use of surfactant. Temperature of reservoir should not exceed 200°F as it can degrade properties of surfactant. Permeability of reservoir should be high enough to allow injection process of foreign fluids. Low quantity of divalent ion is desirable. Waterflooded zone would maintain foam stability better than virgin reservoir with high initial oil saturation. Several literatures stated that the most important factors of foam in EOR projects are 1) foam injection methods in the reservoir such as preformed foam, co-injection foam, or surfactant alternating gas foam, 2) reservoir pressure, and 3) permeability.

Selection of surfactant – Selection of good surfactant is the most important step for foam flooding. Selection of surfactant can be based on considering foaming ability, foam stability, thermal stability, salinity and divalent ion resistance, compatibility with formation fluids, performance in presence of high oil saturation, IFT reduction, and adsorption [15]. Several surfactants that are efficiently used in field application worldwide are shown in Figure 3.10

Injection modes – Co-injection method and Surfactant Alternating Gas (SAG) method are globally used methods. It depends on field application demand to choose the right method. High gas-liquid ratio causes high resistance factor in co-injection method compared to surfactant-alternating gas. Laboratory study reveals that oil recovery obtained is higher for co-injection method compared to surfactant alternating gas for the same amount of chemicals used. Some projects selected SAG because of simulation results reporting that injection pressure was higher than fracture pressure. If SAG is considered, many small slugs are better than just one single large slug as foam forming becomes more difficult.

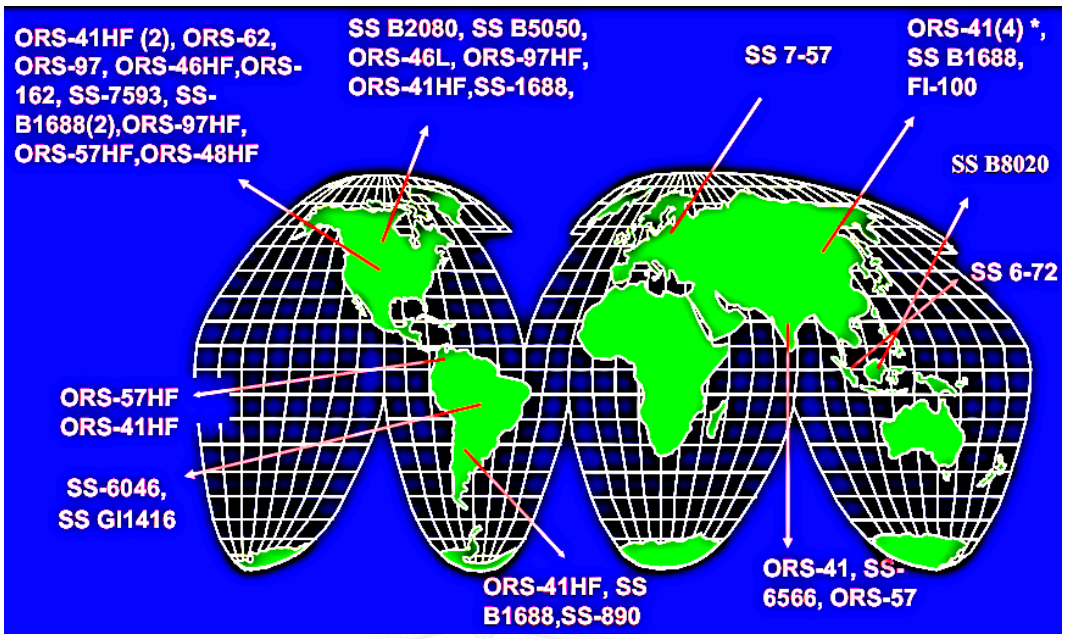

Figure 3.10 Ongoing chemical and approved projects with different surfactants [21]

3.3 Reservoir Heterogeneity

Variation in erosion, deposition, lithification, faulting etc. causes reservoir rocks to be heterogeneous and non-uniform [24]. This term is considered as an important factor to control performance of any operation in reservoir. Reservoir rocks are rarely found homogenous in physical properties. Reservoir heterogeneity is defined as a difference in reservoir properties as a function of space. These properties may include permeability, porosity, thickness, saturation, faults and fractures, rock facies and rock characteristic. Reservoir heterogeneity usually results in early breakthrough and reduction of sweep efficiency, resulting in large pockets of by-passed oil. Generally, heterogeneity is represented by permeability since it reflects flow ability of fluid enclosed in pore space. From years to years, solutions to the questions related to heterogeneity can be answered by several numerical methods and computer modeling. Even though well logging, geo-statistic etc. sometimes cannot solve problems of heterogeneity, all porous media is microscopically heterogeneous and only macroscopic variations in rock properties need to be considered [24].

Heterogeneous reservoir can be classified into three major types: (1) vertical variations, (2) areal variations, and (3) non-pattern heterogeneity [24]. Vertical

permeability variations or vertical heterogeneity is a formation composing layers and fluids flow in horizontal direction. Areal variations are those permeability varies in lateral direction and these might be caused by presence of vugs or salt dome. Last type is non-patterned permeability such as reservoir containing fractures which could result in tremendous thief zones.

3.3.1 Calculation of Heterogeneity Coefficients

Reservoir heterogeneity can be represented by a quantitative number. This number shows how reservoirs are deviated from uniformity or homogeneity. Homogeneous reservoir is generally represented by zero degree of heterogeneity. The highest heterogeneity index is represented by unity. Common methods to identify heterogeneity are Schmalz and Rahme, Dykstra and Parson, and Warren and Price.

In most reservoirs, permeabilities have a log-normal distribution. Geological processes and conditions that leads to permeability in reservoir rocks appear to leave permeabilities distributed around the geometric mean. If an assumption is made that there are enough samples of core to create the true shape of the distribution curve, reservoir subdivision into layers using the distribution curve should lend a good representation of the reservoir stratification. The permeability dataset is sorted from minimum to maximum to obtain permeability variation value and displayed on a graph of log probability scale, as shown in Figure 3.11. Equation 3.10 describes calculation of permeability variation. If rock is fully uniform then all samples will have the same permeability and the line will be parallel to the base line. As heterogeneity increases, slope of distribution line also increases. Dykstra and Parsons introduced theory of permeability variation (*V*), which is obtained to describe degree of heterogeneity in reservoir

$$V = \frac{\text{stdev}(\text{Log}(k))}{\text{avg}(\text{Log}(k))} = \frac{\text{Log}(k)_{P50} - \text{Log}(k)_{P84.1}}{\text{Log}(k)_{P50}}, \qquad (3.10)$$

where, *stdev* and *avg* are standard deviation and mean value of permeability. $Log(k)P_{50}$ is the permeability value at probability of 50%, whereas $Log(k)P_{84.1}$ is the permeability at 84.1% of cumulative sample

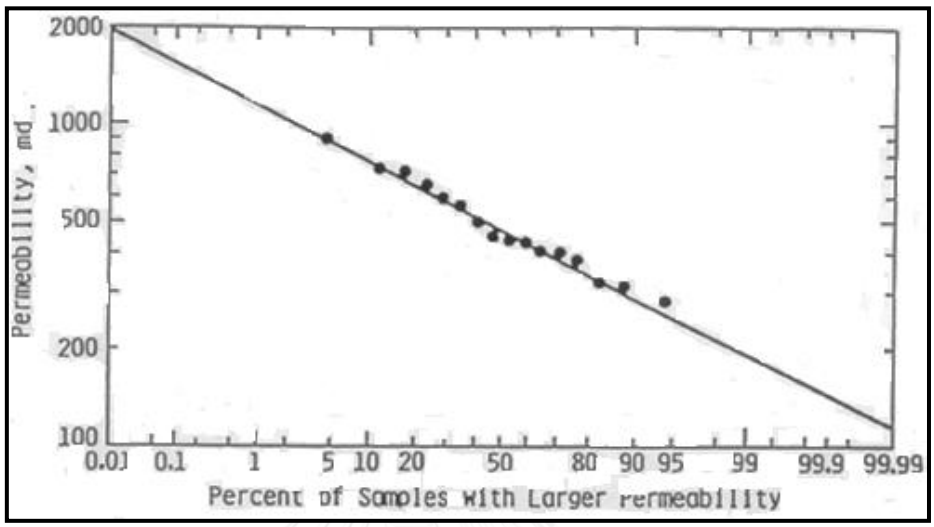

Figure 3.11 Illustration of Dykstra and Parsons Permeability distribution [25]

In 1950, Schmalz and Rahme proposed a single term for characterizing permeability distribution within a single pay zone. To estimate the Lorenz coefficient, the area above straight line or area under the curve is required. This area calculation can be done by using Trapezoidal rule or Simson's rule. Using Figure 3.12, they defined the Lorenz coefficient of heterogeneity as

$$\text{Lorenz Coefficient} = \frac{\text{Area ABCA}}{\text{Area ADCA}} \tag{3.11}$$

The Lorenz coefficient is a static measure of heterogeneity considering static porosity and permeability of a stratified reservoir consisting of N sub layers of hj -net pay thickness, Kj - absolute permeability and Φj - absolute porosity. To construct this graph, properties of reservoir layer are arranged in tabular form in order of constantly decrementing values of permeability. The next step is to calculate cumulative fraction of total volume and cumulative fraction of total flow capacity in

each layer. Fractional flow capacity F_n can be calculated from equation (3.12) and fractional storage capacity C_n can be calculated from equation (3.13).

$$F_n = \sum_{j=1}^{n} k_j h_j / \sum_{j=1}^{N} k_j h_j \tag{3.12}$$

$$C_n = \sum_{j=1}^{n} \varphi_j h_j / \sum_{j=1}^{N} \varphi_j h_j \tag{3.13}$$

A plot of F_n versus C_n on linear scale is shown in Figure 3.12, illustrating connecting points to form Lorenz curve. The curve passes coordinates (0, 0) and (1, 1). Trapezoidal rule is used to calculate areas between Lorenz curve and area under diagonal line for the curve segment corresponding to each layer and total area is obtained by adding all areas together. Lorenz coefficient is zero for homogeneous reservoirs and equals to one for highly heterogeneous reservoir. Lorenz coefficient can be evaluated with a good accuracy for any oil field depending on precisions of data including thickness, porosity and permeability.

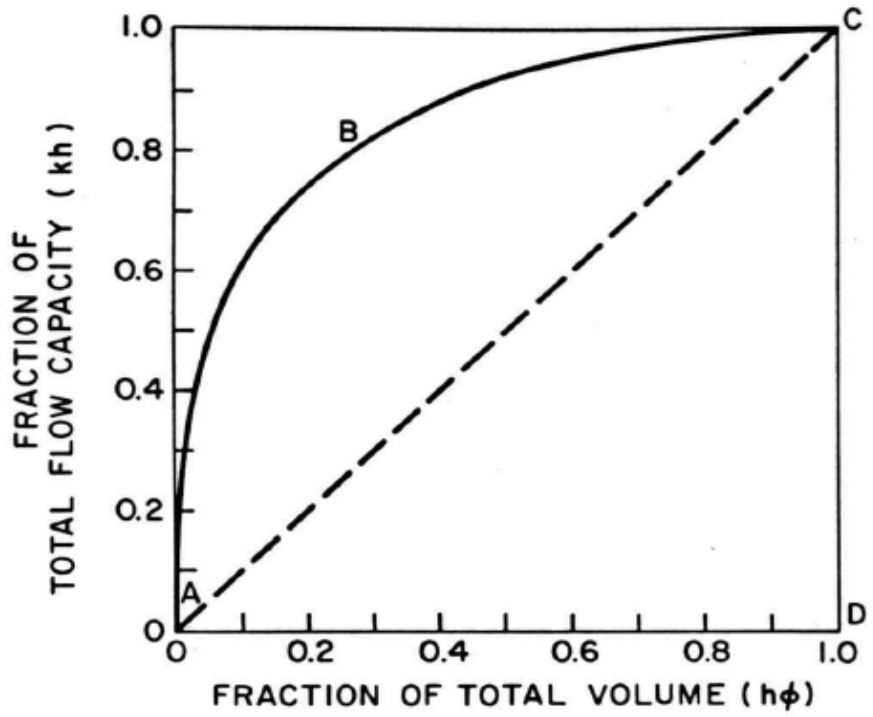

Figure 3.12 Plot of F_n against C_n, illustrating Lorenz curve [26]

CHAPTER IV

RESERVOIR SIMULATION MODEL

This chapter describes construction of reservoir model, regarding selection of reservoir parameters and calculation of heterogeneity. Cartesian grid reservoir model is constructed using STARS commercialized by Computer Modeling Group Ltd. (CMG). Fundamental component of STARS simulation including reservoir, components, rock fluid, initial conditions and well- recurrent are discussed in the Chapter. Part of reservoir simulation detail is shown in Appendix section.

4.1 Reservoir Parameter Selection

Parameters should be determined from laboratory studies which are designed to duplicate conditions of reservoir. There are a few technical papers published on screening criteria to duplicate conditions of reservoir. This study is based on screening criteria as shown in Tables 4.1 and 4.2 for general foam and nitrogen gas, respectively to select formation lithology, approximate depth, porosity, permeability, and viscosity, ° API gravity of oil, permeability and formation thickness. Pressure-volume-temperature (PVT) properties must be determined by analogy or with the aid of empirically derived correlations.

Table 4.1 Range of reservoir parameters from the surveyed field projects implemented by foam flooding [15]

Parameters	Value	Unit
Thickness	3-350	m
Permeability	1-1,500	mD
Temperature	<101	℃
Pressure	< 500	MPa
Oil viscosity	< 10000	cP
Well spacing	30-1,500	m
Salinity of formation water	< 180000	ppm
Surfactant concentration	< 1	%

Table 4.2 Screening criteria of reservoir parameters for immiscible nitrogen injection [15]

Parameters	Value	Unit
Porosity	0.11-0.28 (avg 0.19)	fraction
Oil saturation	0.47-0.98 (avg 0.71)	PV
Formation	Sandstone	
Permeability	3-2,800 (avg 1042)	mD
Net thickness	-	-
Depth	1,700-18,500 (avg 7914)	ft
Temperature	82-325 (avg 173)	°F
Oil gravity	16-54 (avg 34.6)	°API
Oil viscosity	0-18,000 (avg 2,257)	cP

Regarding Table 4.1 and 4.2, sandstone formation is selected at formation depth of 5000 ft and formation thickness is 100 ft. Porosity of 0.25 is considered possible for sandstone with previously mentioned formation depth. Selected average permeability is 150 mD which is still in proper range corresponded to porosity of 0.25 [26]. Vertical permeability is 10% of horizontal permeability based on compaction in vertical direction. Reservoir temperature is set at 145°F, whereas reservoir pressure is fixed at 2,500 psia. based on relationship of depth against temperature and pressure [27, 28].

Fracture pressure is considered as very important as undesired fracture can occur if bottomhole pressure exceeds this value during injection process, resulting in thief zone and loss of injected fluids. In this study, fracture pressure is calculated based on Hubbert & Willis equation [29]. Minimum value is 3,333 psi and maximum value is 3,750 psi. Hence, fracture pressure is set to 3,500 psi.

In foam flooding, oil gravity affects foaming agents and its concentration. For heavy oil reservoir, large amount of surfactant concentration is required while a few percent is adequate in case of light oil. As nitrogen gas is usually implanted in light

oil reservoir, this study therefore uses light oil to represent type of oil. Regarding Table 4.2 and Table 4.3 selected oil °API gravity is therefore at value of 35. Solution gas-oil ratio is selected around 500 scf/stb for black oil based on summary data in Table 4.3.

Table 4.3 Pressure Volume Temperature for Black oil [30]

PVT property	Maximum	Minimum	Average
Reservoir pressure (Psi)	10,280	1106	4016.8
Reservoir Temperature (°F)	290	120	222.3
Specific Gravity of gas	1.2720	0.6777	0.9941
Specific gravity of oil	0.9499	0.7908	0.8433
GOR, scf/STB	1662.1	45.2	633.5
Gravity (°API)	47.4	17.5	36.6

Bubble point pressure is calculated and input manually into the STARS simulator. The simulator calculates solution gas ratio or bubble point pressure using Standing Correlation. So in this study bubble point pressure is calculated empirically by Standing Correlation as well as verified by graphically using Figure 4.1. The calculated value and graphical value are mostly equal at 1,025 psi.

จุฬาลงกรณ์มหาวิทยาลัย
CHULALONGKORN UNIVERSITY

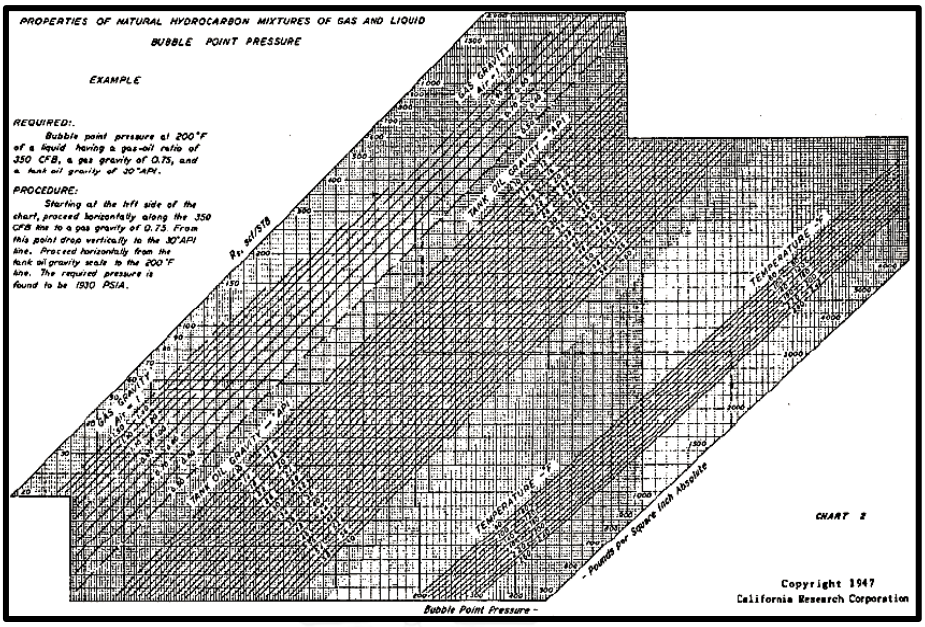

Figure 4.1 Relationship between bubble point pressure and other PVT properties [31]

4.2 Physical Model of Reservoir

In this study, units selected are based on field units. Porosity of reservoir is maintained constant for all layers at 0.25. The grid type used is Cartesian and size of reservoir is 1,100 ft × 1,100 ft × 100 ft in x, y and z directions, respectively. The total number of grids blocks is 20, 20, and 10 in x, y and z directions. Heterogeneous reservoir models are created by varying reservoir permeability in ten layers to represent multi-layered sandstone reservoir. Reservoir parameters used for construction with reservoir properties are summarized in Table 4.4.

Table 4.4 Reservoir parameters for physical reservoir model

Parameter	Value	Unit
Number of blocks in x, y, and z	30 × 30 × 10	Grid
Grid size in x, y, and z	20 × 20 × 10	Ft
Porosity	0.25	Fraction
Average permeability	150	mD
Maximum permeability	300	mD
Median value of permeability	150	mD
Minimum permeability	10	mD
Horizontal permeability (k_h)	Varied	mD
Vertical permeability (k_v)	$k_v = 0.1 \times k_h$	mD
Datum depth	5,000	Ft
Initial pressure @ datum depth	2,500	Psia
Fracture pressure	3,500	Psia
Reservoir temperature	145	°F
Oil gravity	35	°API
Gas gravity	0.8	s.g. air
Gas oil ratio (R_s)	500	scf/ stb
Well spacing	849	Ft
Water mole fraction	1	Fraction
Total production period	20	Years

Three dimension view of reservoir model illustrated by formation depth is shown in Figure 4.2 and top view is shown Figure 4.3.

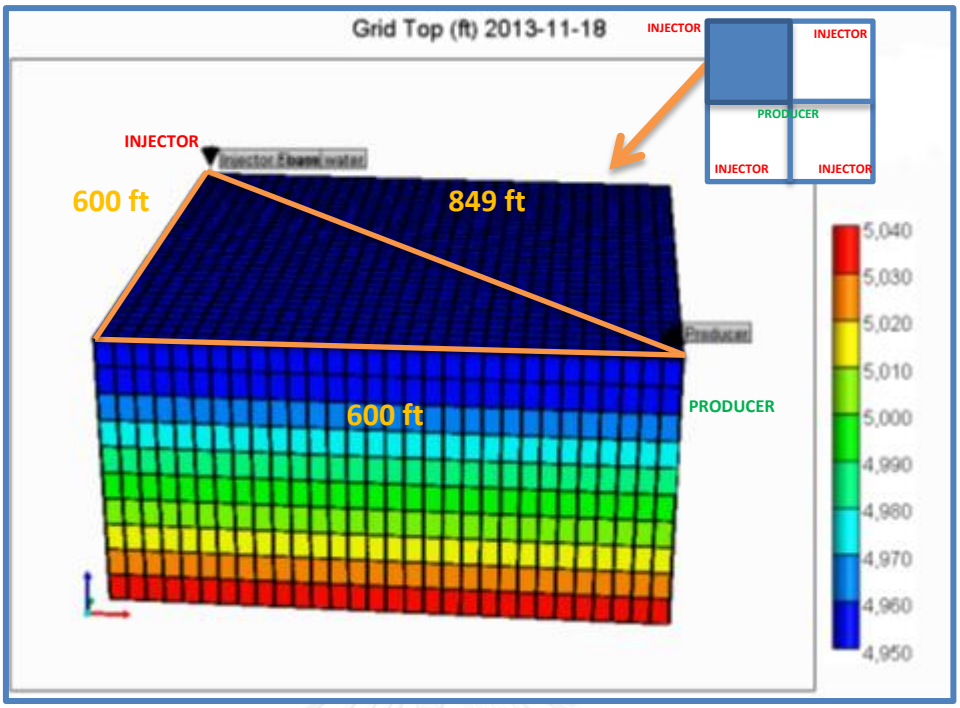

Figure 4.2 Three dimension view of reservoir model illustrating formation depth

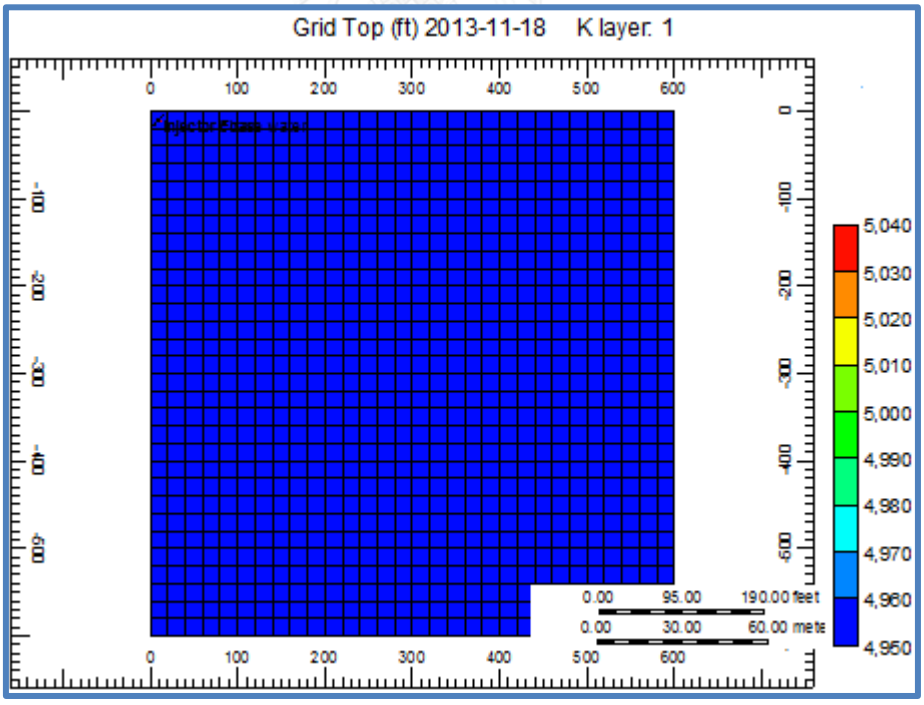

Figure 4.3 Top view of reservoir model

Reservoir model with Lorenz coefficient value of 0.35 is selected for initialized study. Injection and production wells are located at diagonal positions with distance of 1,555 ft away from each other. Reference depth is set at 5,000 ft. Based on reservoir dimensions; total volume of reservoir is 9MMbbl. Total effective pore volume is 2.25MMbbl which is corresponding to effective porosity of 0.25. In this study, connate water saturation which is also irreducible water saturation (no mobile water saturation) is 0.28, Original Oil in Place (OOIP) therefore equals to 1.68MMbbl in case of virgin reservoir.

4.2.1 Components of Black Oil

This section explains how fluid model is built on STARS. The PVT wizard generates new fluid model. Important values are input and together with analytical PVT correlations, final values are obtained. The black oil PVT graphical user interface (GUI) controls these correlations. From parameter selection, formation temperature is 145°F, bubble point pressure is 1,025 psi, oil gravity is 35 °API and gas specific gravity is 0.8. In this study Standing correlations are used to calculate oil properties. Gas properties are calculated using Standing correlations as well and all related descriptions are provided in appendix. Oil formation volume factor, oil density and oil viscosity are plotted as a function of reservoir pressure in Figures 4.4, 4.5 and 4.6, respectively. Dry gas formation volume factor and gas viscosity are also illustrated in Figures 4.7 and 4.8, respectively.

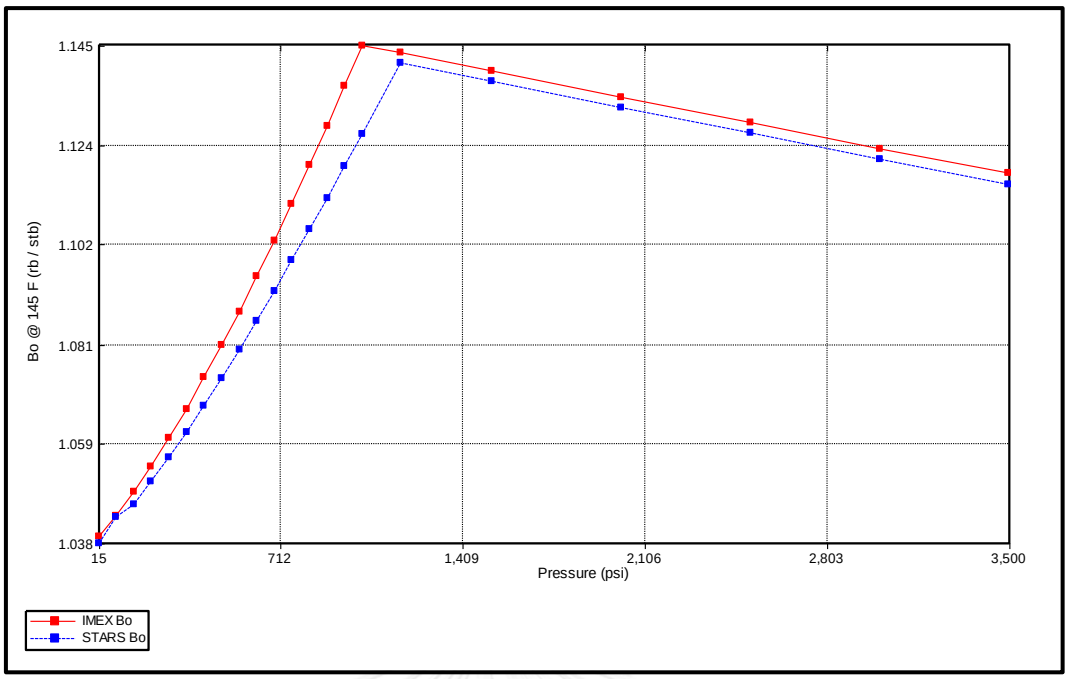

Figure 4.4 Oil formation volume factors as a function of reservoir pressure

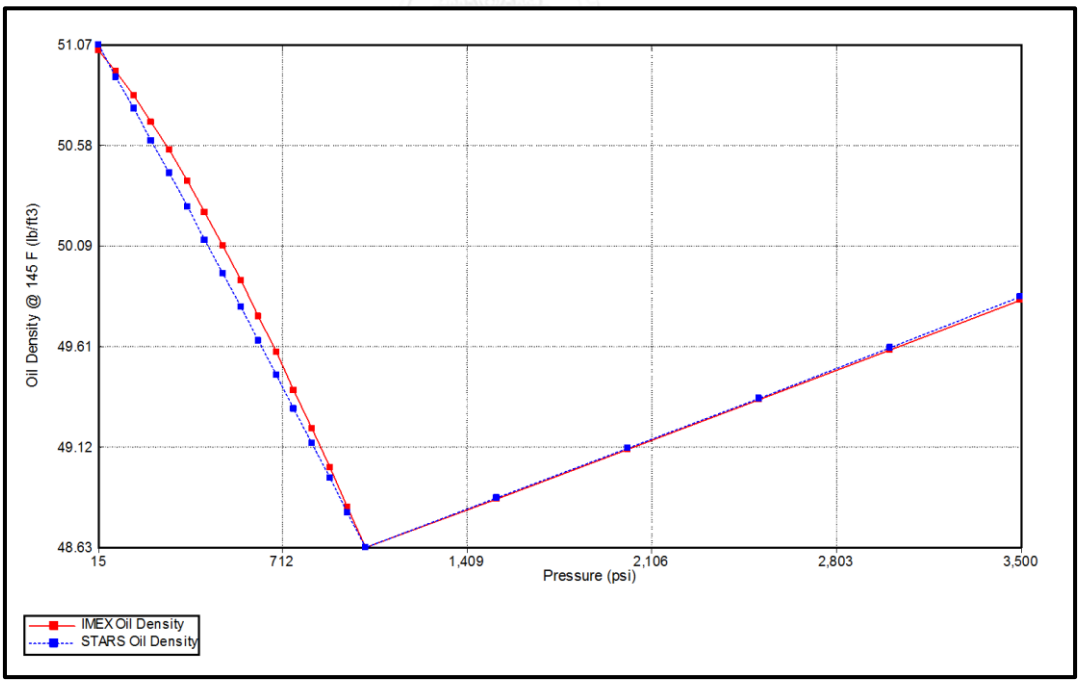

Figure 4.5 Oil densities versus as a function of reservoir pressure

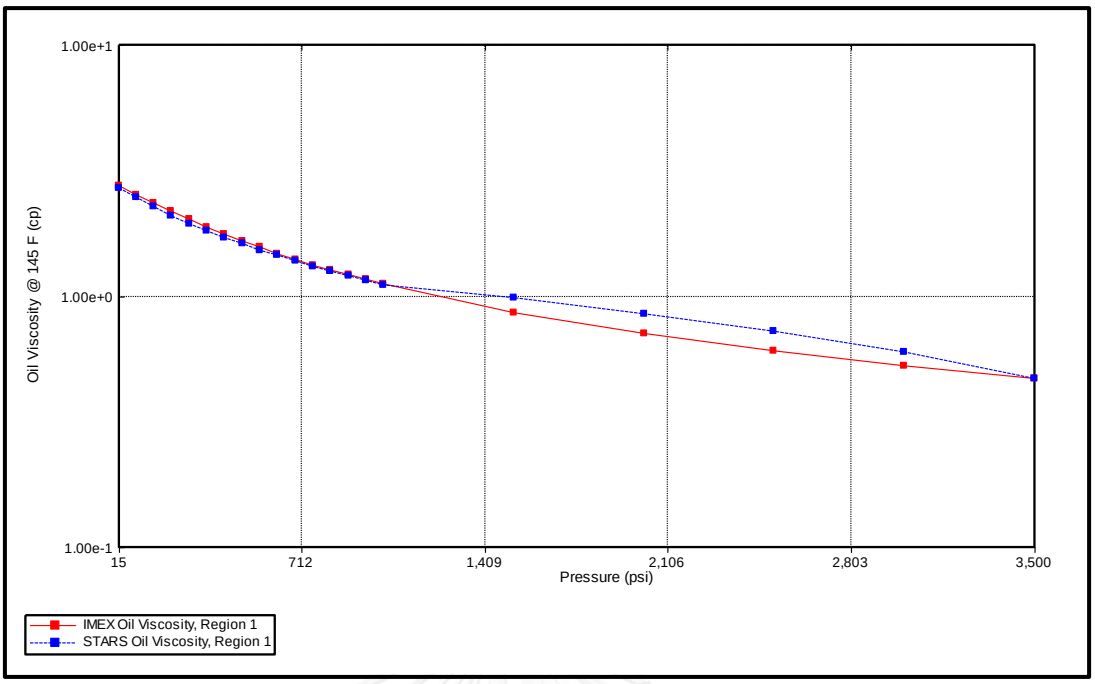

Figure 4.6 Oil viscosities as a function of reservoir pressure

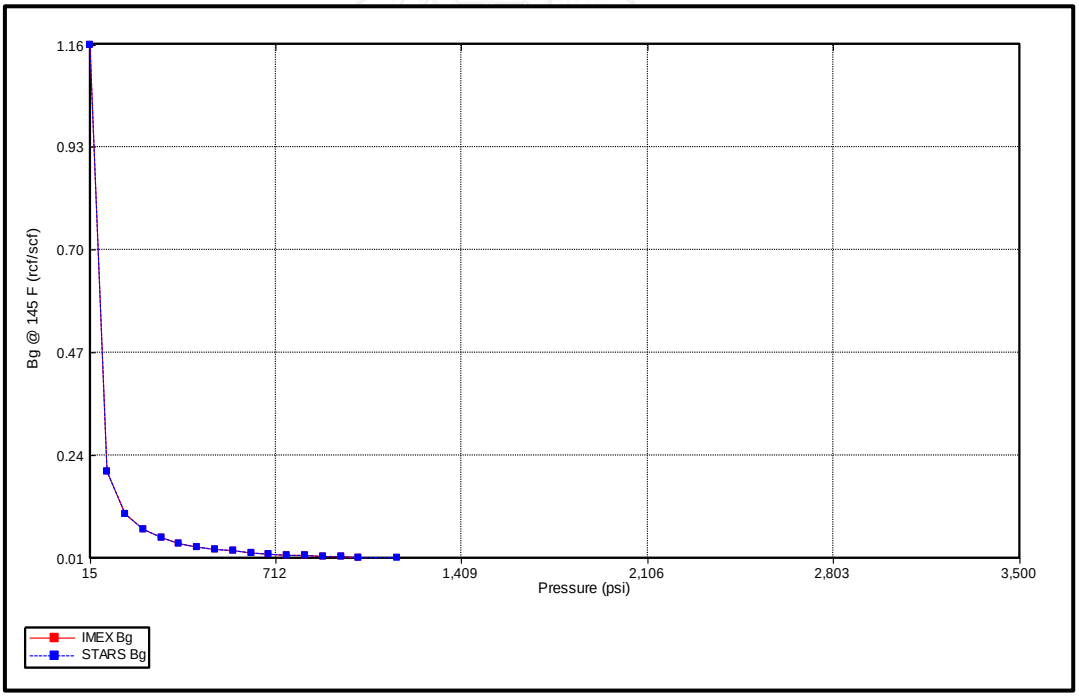

Figure 4.7 Dry gas formation volume factors as a function of reservoir pressure

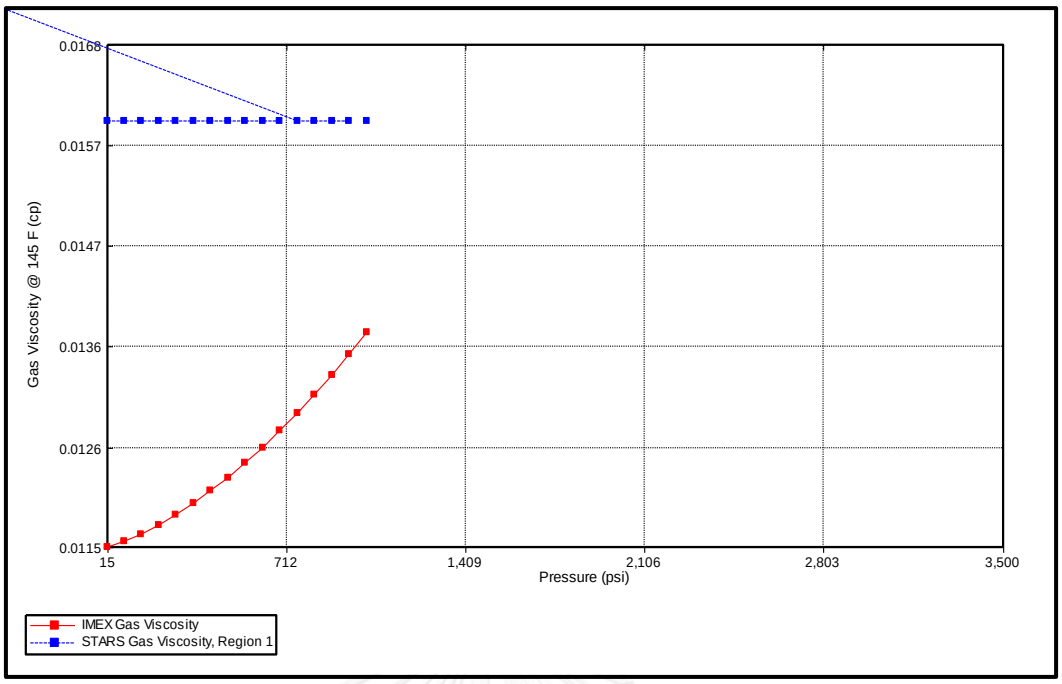

Figure 4.8 Gas viscosity as a function of reservoir pressure

4.2.2 Rock and Fluid Properties

Rock and fluid section defines petrophysical properties including wetting condition of rock. Selected formation lithology in this study is sandstone formation. As sandstone is mostly found as water-wet, relative permeability curves are constructed based on several rules of thumbs for distinguish type of wettability. Required data to construct relative permeability curves are shown in Table 4.5. Relative permeability curves are constructed using Corey's correlation, generating both oil-water and gas-liquid systems. Calculated relative permeability values are summarized in Table 4.6 for relative permeabilities oil-water system and Table 4.7 shows relative permeabilities of gas-liquid system. Values are plotted together with water saturation for oil-water system and liquid saturation for gas-liquid system, depicted in Figures 4.9 and 4.10, respectively. Three phase relative permeability is shown in Figure 4.11 which is generated by using Stone 2 model

Table 4.5 Required data for construction of permeability curves

Keywords	Description	Value
SWCON or S_{wcon}	Connate Water Saturation	0.28
SWCRIT or S_{wcrit}	Critical Water Saturation	0.28
SOIRW or S_{oirw}	Irreducible Oil Saturation for Water-Oil Table	0.24
SORW or S_{orw}	Residual Oil Saturation for Water-Oil Table	0.24
SOIRG or S_{oirg}	Irreducible Oil Saturation for Gas-Liquid Table	0.05
SORG or S_{org}	Residual Oil Saturation for Gas-Liquid Table	0.10
SGCON or S_{gcon}	Connate Gas Saturation	0.00
SGCRIT or S_{gcrit}	Critical Gas Saturation	0.15
KROCW or k_{rocw}	Kro at Connate Water Saturation	0.41
KRWIRO or k_{rwiro}	Krw at Irreducible Oil Saturation	0.13
KRGCL or k_{rgcl}	Krg at Connate Liquid Saturation	0.6
	Exponent for calculating Krw from k_{rwiro}	3
	Exponent for calculating Krow from k_{rocw}	3
	Exponent for calculating Krog from KROGCG	3
	Exponent for calculating Krg from k_{rgcl}	3

Table 4.6 Calculated relative permeability values for oil-water system

S_w	k_{rw}	k_{ro}
0.28	0	0.410
0.31	3.17×10^{-5}	0.338
0.34	2.54×10^{-4}	0.275
0.37	8.57×10^{-4}	0.220
0.40	2.03×10^{-3}	0.173
0.43	3.97×10^{-3}	0.133
0.46	6.86×10^{-3}	0.100
0.49	0.011	0.073
0.52	0.016	0.051
0.55	0.023	0.034
0.58	0.032	0.022
0.61	0.042	0.013
0.64	0.055	6.41×10^{-3}
0.67	0.070	2.70×10^{-3}
0.7	0.087	8.01×10^{-4}
0.73	0.107	1.00×10^{-5}
0.76	0.130	0

จุฬาลงกรณ์มหาวิทยาลัย
CHULALONGKORN UNIVERSITY

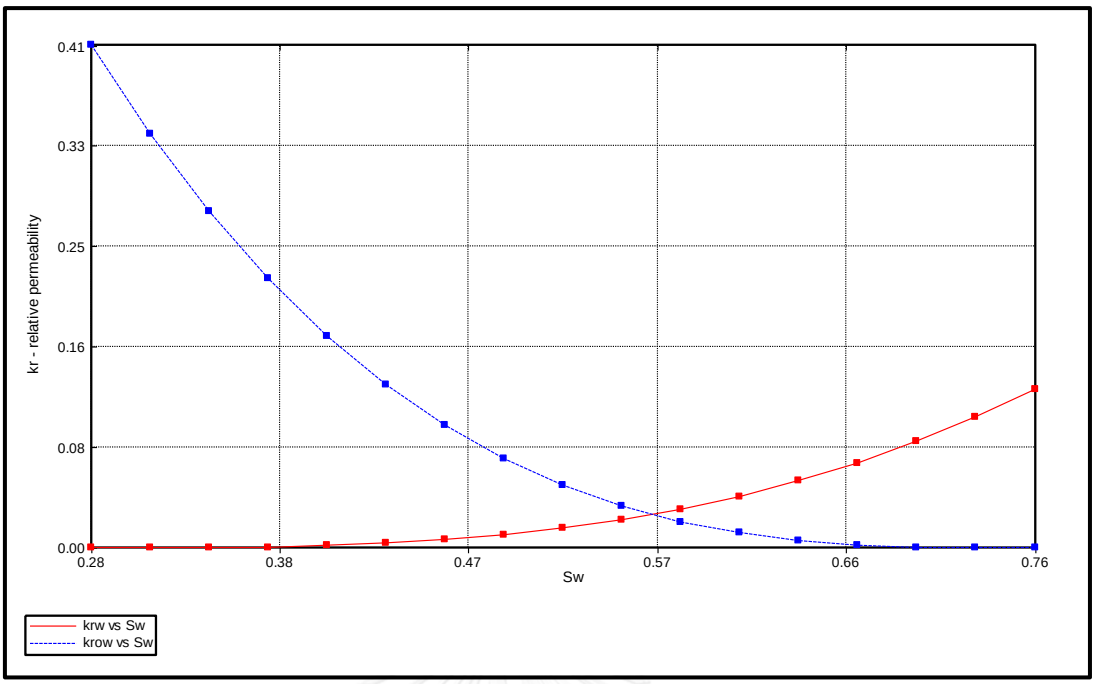

Figure 4.9 Relative permeabilities to oil and to water as a function of water saturation

Table 4.7 Gas - Liquid Relative permeability

S_l	k_{rg}	k_{rog}
0.33	0.600	0
0.36	0.518	0
0.38	0.443	0
0.41	0.365	4.36×10^{-5}
0.44	0.297	3.49×10^{-4}
0.47	0.238	1.17×10^{-3}
0.50	0.187	2.79×10^{-3}
0.53	0.144	5.45×10^{-3}
0.56	0.108	9.42×10^{-3}
0.59	0.079	0.015
0.62	0.055	0.022
0.64	0.037	0.032
0.67	0.023	0.044

S_l	k_{rg}	k_{rog}
0.70	0.014	0.058
0.73	6.92×10^{-3}	0.075
0.76	2.92×10^{-3}	0.096
0.79	8.65×10^{-4}	0.120
0.82	1.08×10^{-4}	0.147
0.85	0	0.179
0.93	0	0.278
1	0	0.41

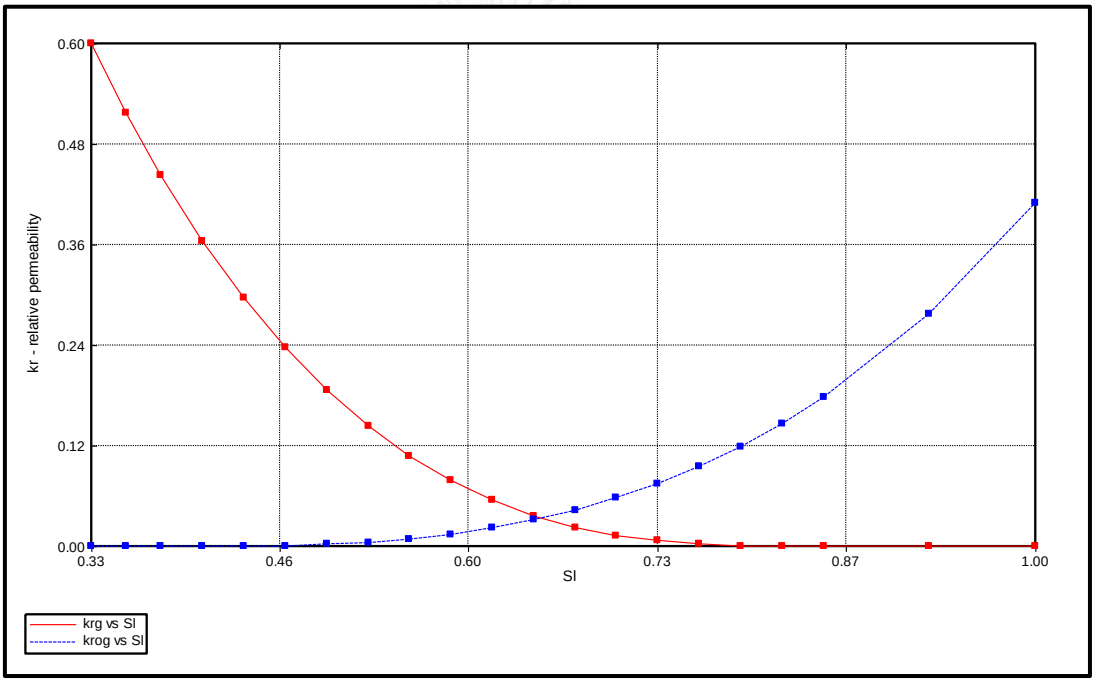

Figure 4.10 Relative permeabilities to liquid and to gas as a function of liquid saturation

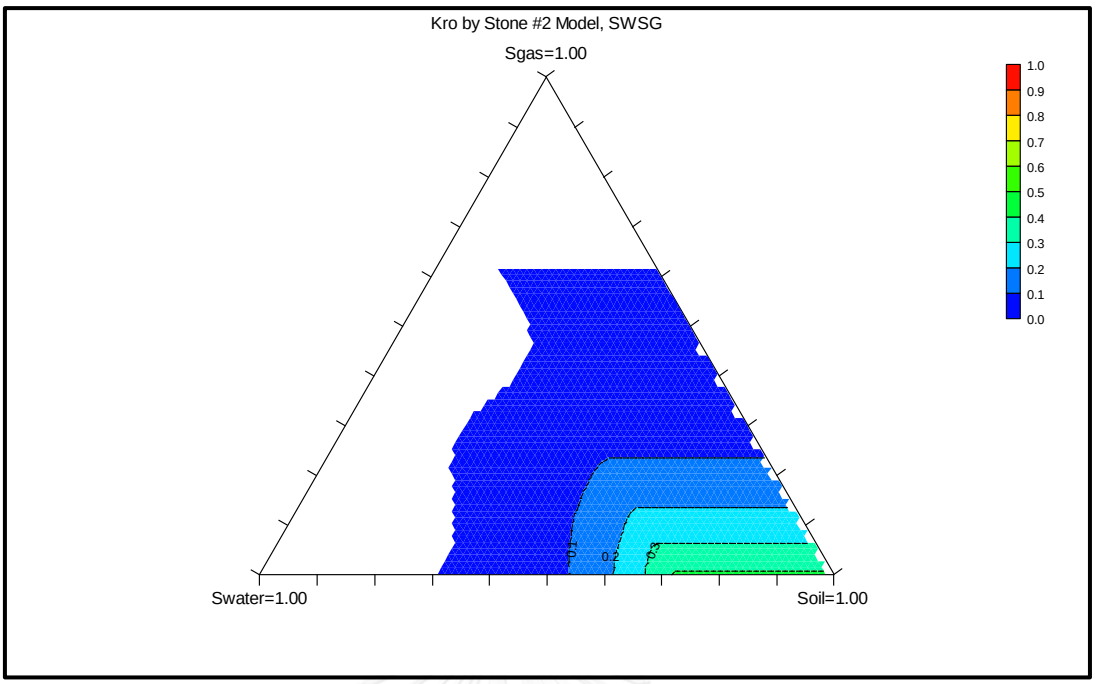

Figure 4.11 Three phase relative permeabilities constructed by Stone 2 model

4.2.3 Data of Well and Recurrent

Data and specifications that may vary with time are presented in Well and Recurrent section in STARS. In this section, wells are assigned to perform individual task. The keywords including *RUN, *TIME, *DATE,*WELL, *INJECTOR, *PRODUCER, *SHUTIN, *OPEN, *PERF are defined [23]. Injection and production wells are located diagonally with a distance of 1,555 ft. Injection well is placed at grid coordination (1, 1, 1) and production well is located at coordination (30, 30, 1) in (X, Y, Z) system. Wellbore radius of both injection and production wells is 0.28ft. All ten layers of reservoir are perforated. Skin effect is assumed to be zero. Constraints of injection well are shown in Table 4.8, whereas constraints and economic limits of production well are summarized in Table 4.9. Maximum bottomhole pressure of injection well is set at 3,500 psi to avoid undesired fractures. Total production period is 20 years. Injection data is obtained by volume fraction method which is described in the following sections.

Table 4.8 Injection constraints of injection well

Parameter	Value	Unit
Maximum bottomhole pressure	3,500	psi
Desired injection rate	varied	bbl/day

Table 4.9 Production constraints and economic limits of production well

Parameter	Value	Unit
Minimum bottomhole pressure	200	psi
Surface target liquid rate	varied	STB/day
Maximum water-cut	0.95	fraction
Minimum oil production	50	STB/day

4.2.4 Foam Parameters

Foam parameters play very important role in foam study especially in foam generation. As previously explained, foam is a mixture of gas, water and surfactant. For this purpose nitrogen gas is used which is available as an option in STARS. Oxygen is excluded in this study to avoid effect of oxidation reaction, resulting in changing of reservoir temperature. Molecular weight of nitrogen is 28.01 lb/lbmole. Anionic surfactant used for this study is commercially called Chaser SD 1,000, which has molecular weight of 310 lb/lbmole and it is commonly used surfactant in oil field. Surfactant concentration used in this study is 0.5% by weight [10] [12] [15]. Since formation is sandstone, smaller quantity of anionic surfactant is adsorbed on rock and so adsorption value is assumed to be 0.05 mg surf/g rock [32] which is relatively small compared to adsorption in carbonate formation . The co-injection method is used to deliver foam to formation where foam starts to form either in tubing string or immediately as gas and surfactant solution enter formation. Foam parameters used to create foam are shown in Table 4.10. The co-injection method is adopted to inject nitrogen and liquid as shown in Table 4.11 on volume fraction

basis. Foam flow behavior in CMG is designed as described in section 3.2.8 of chapter III. For this study, only F_1 (surfactant concentration) and F_2 (oil saturation) are used along with Fmmob in equation 3.2. As per Table 4.3, Input of foam parameters of function F_1 and F_2 will command CMG simulator to use equation 3.3 and 3.4 of Chapter III to calculate for F_1. The calculation of these functions will direct simulator to calculate FM which is an inverse mobility reduction factor, varying between 1 (no foam) and FM << 0 (strongest foam) [23]. This value is used to rescale relative permeability of gas by simulator.

Table 4.10 Foam parameters

Foam Parameter	Key word	value
Reference gas mobility reduction factor	fmmob	76,000
Critical component mole fraction	fmsurf	0.00001
Critical oil saturation	fmoil	0.2
Exponent for composition contribution	Epsurf	1
Exponent for composition contribution	Epoil	1
Lower limit of critical oil saturation	floil	0

จุฬาลงกรณ์มหาวิทยาลัย
Chulalongkorn University

Table 4.11 Calculation of injected fluid as per volume fraction basis

Component	Phase rate(P) (STB/day)	Fraction(F)	Comp. rate (C) = P* F	Volume Fraction = C/T
water	200	0.995	199	1.53×10^{-3}
surfactant		0.005	1	7.68×10^{-6}
nitrogen	130,000	1	130,000	0.998
total	130,200	-	130,200	1.00

4.2.5 Heterogeneous Reservoir Model

Most reservoirs are found heterogeneous instead of homogeneous. When any operation is performed in heterogeneous reservoir, difficulties may occur. Usually heterogeneity of permeability is mostly concerned as it affects flow ability of fluid in pore space as well as productivity. Hence, heterogeneous reservoir models are created by varying reservoir permeability in this study. Models are created as multi-layered sandstone reservoir having ten layers possessing different permeabilities. Porosity is constant in all layers. In order to quantify heterogeneity, several methods can be performed such as Schmalz and Rahme, Dykstra and Parson, and Warren and Price. In this study, Schmalz and Rahme method is chosen to represent heterogeneity. Procedure to calculate Lorenz coefficient is clearly described in section 3.3. Six models with different heterogeneities are generated by fixing minimum, maximum, median and average permeabilities. Permeability of layers is arranged in descending order. Calculated data for different six cases are shown in table form from Tables 4.12 to 4.17 and illustrated as Lorenz curves in Figures 4.12 to 4.18. Explanation of calculation is performed for the first case with Lorenz coefficient of 0.2.

จุฬาลงกรณ์มหาวิทยาลัย
Chulalongkorn University

Table 4.12 Summary of calculated parameters for Lorenz coefficient of 0.20

layer	k	h	kh	hϕ	Cum. kh	Cum. hϕ	$C_n(X)$	$F_n(X)$
1	300	10	3,000	2.5	3,000	2.5	0.083	0.200
2	170	10	1,700	2.5	4,700	5.0	0.167	0.313
3	165	10	1,650	2.5	6,350	7.5	0.250	0.423
4	160	10	1,600	2.5	7,950	10.0	0.333	0.530
5	150	10	1,500	2.5	9,450	12.5	0.417	0.630
6	145	10	1,450	2.5	10,900	15.0	0.500	0.727
7	140	10	1,400	2.5	12,300	17.5	0.583	0.820
8	135	10	1,350	2.5	13,650	20.0	0.667	0.910
9	125	10	1,250	2.5	14,900	22.5	0.750	0.993
10	10	10	100	2.5	15,000	30.0	1.000	1.000

From Table 4.12 k is horizontal permeability in mD, h is height of layer in ft, ϕ is porosity in fraction, $C_n(X)$ is fractional storage capacity, $F_n(X)$ is fractional flow capacity. After that fractional flow capacity is plotted over fractional storage capacity as illustrated in Figure 4.12.

จุฬาลงกรณ์มหาวิทยาลัย
Chulalongkorn University

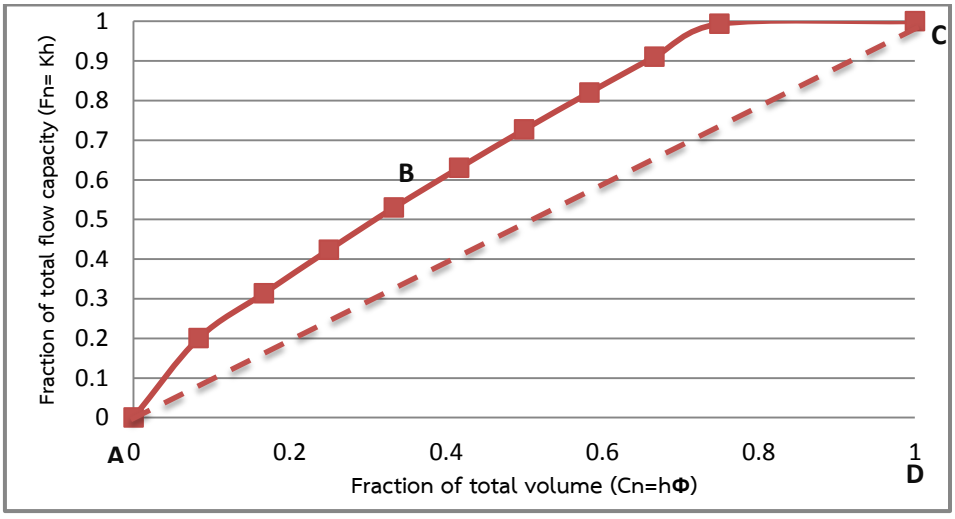

Figure 4.12 Relationship between C_n and F_n for Lorenz coefficient of 0.20

Total area under Lorenz curve is summation of area in Table 4.12 which is 0.603. Area is calculated using formula of trapezoidal. After subtraction area under diagonal (ACDA) of 0.5, area in between (ACBA) is 0.103. Lorenz coefficient is therefore calculated which is area ABCA divided by area ACDA, corresponding to 0.206 in this case. Similar to this case, Lorenz coefficients of 0.25, 0.30, 0.35, 0.40 and 0.45 are generated.

Table 4.13 Summary of calculated parameters for Lorenz coefficient of 0.25

layer	k	h	kh	hϕ	Cum. kh	Cum. hϕ	$C_n(X)$	$F_n(X)$
1	300	10	3,000	2.5	3,000	2.5	0.083	0.200
2	214	10	2,140	2.5	5,140	5.0	0.167	0.343
3	185	10	1,850	2.5	6,990	7.5	0.250	0.466
4	160	10	1,600	2.5	8,590	10.0	0.333	0.573
5	150	10	1,500	2.5	10,090	12.5	0.417	0.673
6	130	10	1,300	2.5	11,390	15.0	0.500	0.760
7	125	10	1,250	2.5	12,640	17.5	0.583	0.843
8	120	10	1,200	2.5	13,840	20.0	0.667	0.923
9	106	10	1,060	2.5	14,900	22.5	0.75	0.993
10	10	10	100	2.5	15,000	30	1	1.000

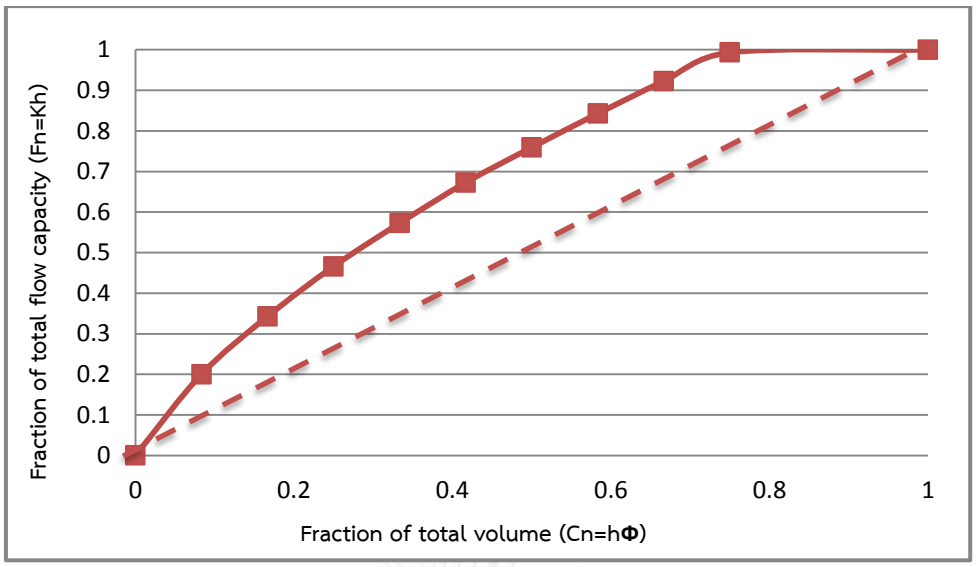

Figure 4.13 Relationship between C_n and F_n for Lorenz coefficient of 0.25

Table 4.14 Summary of calculated parameters for Lorenz coefficient of 0.30

layer	k	h	kh	hϕ	Cum. kh	Cum. hϕ	$C_n(X)$	$F_n(X)$
1	300	10	3,000	2.5	3,000	2.5	0.083	0.200
2	250	10	2,500	2.5	5,500	5.0	0.167	0.367
3	200	10	2,000	2.5	7,500	7.5	0.250	0.500
4	170	10	1,700	2.5	9,200	10.0	0.333	0.613
5	150	10	1,500	2.5	10,700	12.5	0.417	0.713
6	140	10	1,400	2.5	12,100	15.0	0.500	0.807
7	120	10	1,200	2.5	13,300	17.5	0.583	0.887
8	85	10	850	2.5	14,150	20.0	0.667	0.943
9	75	10	750	2.5	14,900	22.5	0.750	0.993
10	10	10	100	2.5	15,000	30.0	1.000	1.000

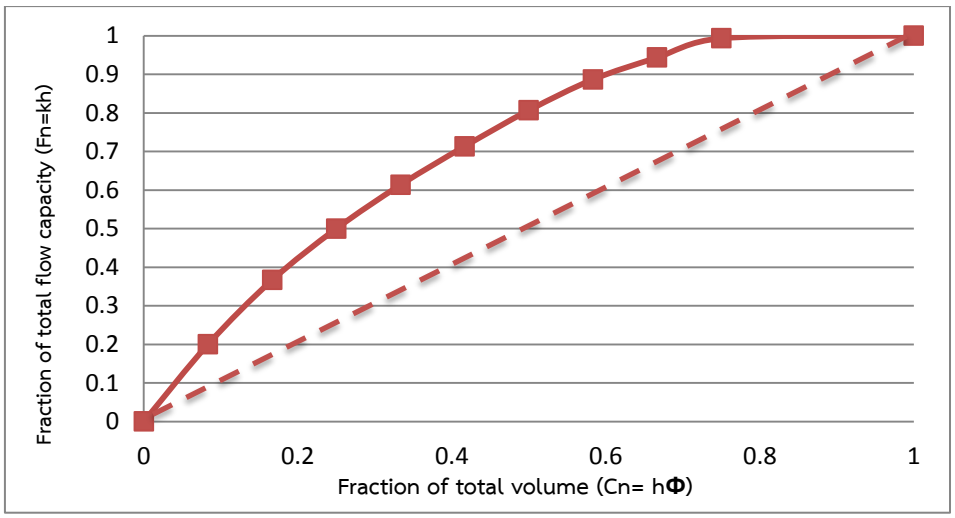

Figure 4.14 Relationship between C_n and F_n for Lorenz coefficient of 0.30

Table 4.15 Summary of calculated parameters for Lorenz coefficient of 0.35

layer	k	h	kh	hϕ	Cum. kh	Cum. hϕ	Cn(X)	Fn(X)
1	300	10	3,000	2.5	3,000	2.5	0.083	0.200
2	280	10	2,800	2.5	5,800	5.0	0.167	0.387
3	240	10	2,400	2.5	8,200	7.5	0.250	0.547
4	160	10	1,600	2.5	9,800	10.0	0.333	0.653
5	150	10	1,500	2.5	11,300	12.5	0.417	0.753
6	140	10	1,400	2.5	12,700	15.0	0.500	0.847
7	120	10	1,200	2.5	13,900	17.5	0.583	0.927
8	60	10	600	2.5	14,500	20.0	0.667	0.967
9	40	10	400	2.5	14,900	22.5	0.750	0.993
10	10	10	100	2.5	15,000	30.0	1.000	1.000

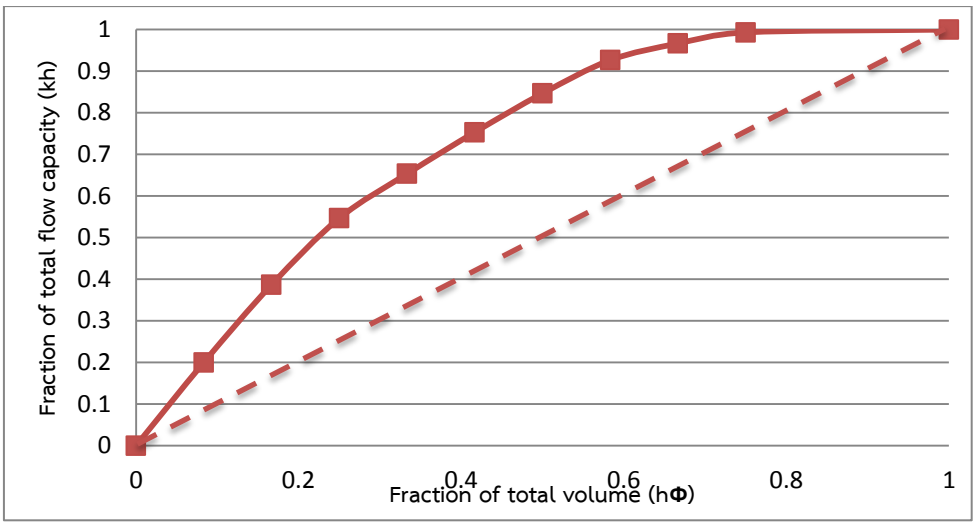

Figure 4.15 Relationship between C_n and F_n for Lorenz coefficient of 0.35

Table 4.16 Summary of calculated parameters for Lorenz coefficient of 0.40

layer	k	h	kh	hϕ	Cum. kh	Cum. hϕ	Cn(X)	Fn(X)
1	300	10	3,000	2.5	3,000	2.5	0.083	0.200
2	280	10	2,800	2.5	5,800	5.0	0.167	0.387
3	270	10	2,700	2.5	8,500	7.5	0.25	0.567
4	240	10	2,400	2.5	10,900	10.0	0.333	0.727
5	150	10	1,500	2.5	12,400	12.5	0.417	0.827
6	110	10	1,100	2.5	13,500	15.0	0.500	0.900
7	65	10	650	2.5	14,150	17.5	0.583	0.943
8	50	10	500	2.5	14,650	20.0	0.667	0.977
9	25	10	250	2.5	14,900	22.5	0.750	0.993
10	10	10	100	2.5	15,000	30.0	1.00	1.000

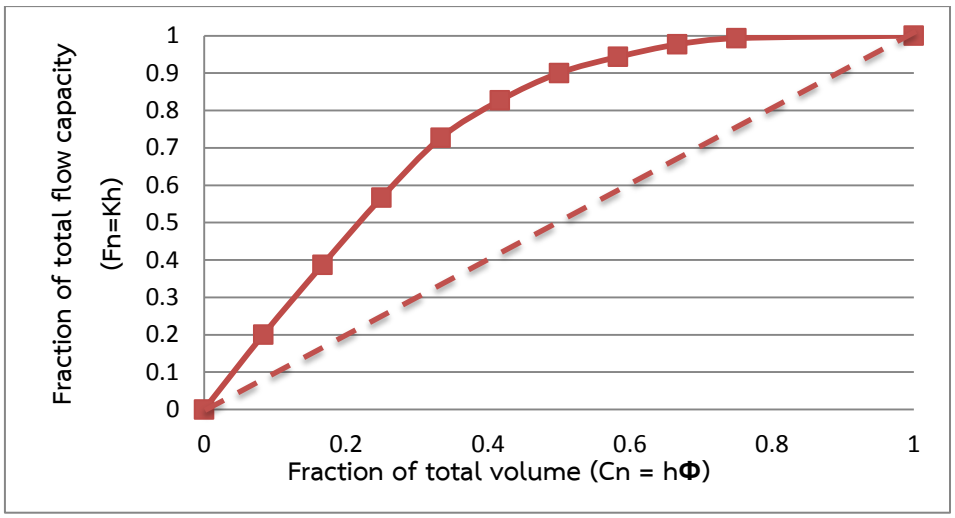

Figure 4.16 Relationship between C_n and F_n for Lorenz coefficient of 0.40

Table 4.17 Summary of calculated parameters for Lorenz coefficient of 0.45

layer	k	h	kh	hϕ	Cum. kh	Cum. hϕ	Cn(X)	Fn(X)
1	300	10	3,000	2.5	3,000	2.5	0.083	0.200
2	299	10	2,990	2.5	5,990	5.0	0.167	0.399
3	296	10	2,960	2.5	8,950	7.5	0.250	0.597
4	294	10	2,940	2.5	11,890	10.0	0.333	0.793
5	150	10	1,500	2.5	13,390	12.5	0.417	0.893
6	54	10	540	2.5	13,930	15.0	0.500	0.929
7	50	10	500	2.5	14,430	17.5	0.583	0.962
8	32	10	320	2.5	14,750	20.0	0.667	0.983
9	15	10	150	2.5	14,900	22.5	0.750	0.993
10	10	10	100	2.5	15,000	30.0	1.000	1.000

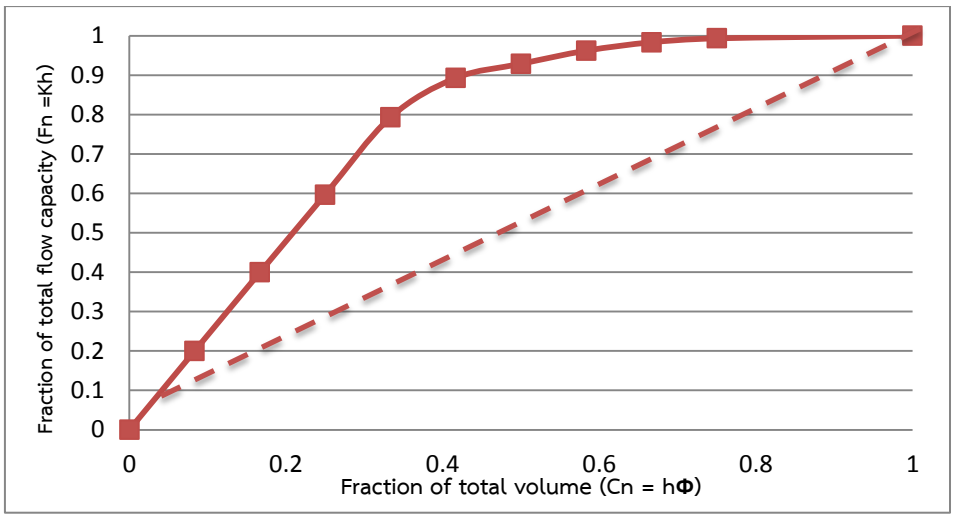

Figure 4.17 Relationship between C_n and F_n for Lorenz coefficient of 0.45

Variation in permeabilities is clearly shown in all tables. As Lorenz coefficient increases, distribution of permeability in each layer is less uniform. Value Lorenz coefficient or degree of heterogeneity is related to different area between cumulative curve and diagonal line. When Lorenz coefficient is increased, curve increasingly deviates from diagonal line Figure 4.18

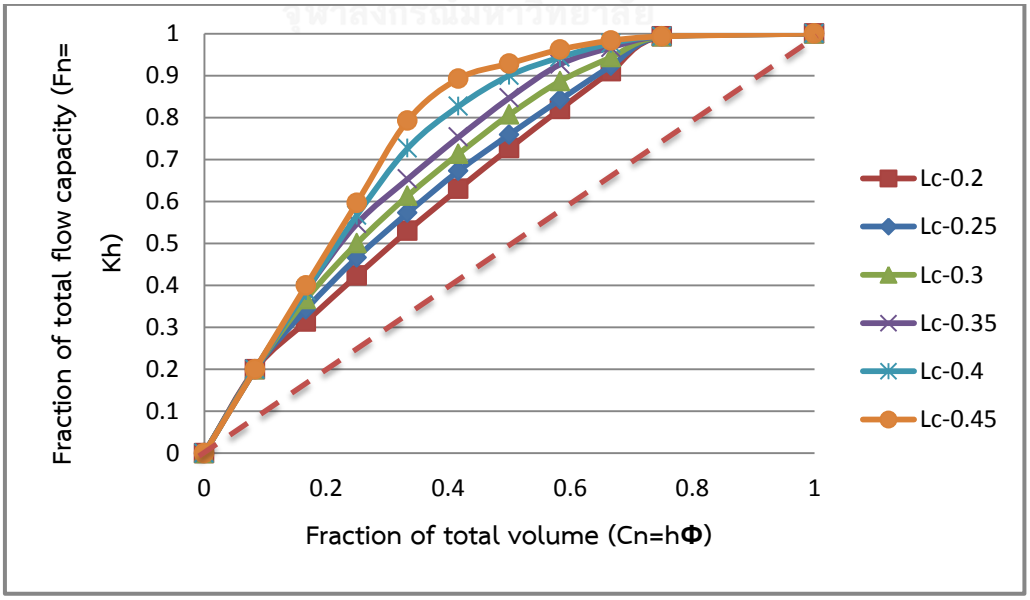

Figure 4.18 Summary relationships between C_n and F_n for all of all Lorenz coefficients

Case 4, representing Lorenz coefficient of 0.35 is chosen for initialized study. This model is simulated along with reservoir parameters selected to construct final base case model which will be described in section 4.1.

4.3 Detail methodology

4.3.1 Foam initialized case study

1. Construct the heterogeneous reservoir model consisting of ten layers with Lorenz coefficient value of 0.35 and simulate with foam flooding model for initial injection rate 1,000 rb/day, production injection ratio 1.5, gas-liquid ratio 4:1 and slug size 0.3 PV. Once 0.3PV slug size is reached, chasing water is injected at same fluid injection rate until one of the production constraints is attained. The simulations are performed from start of the set time for production. This study is the beginning of the rest studies and so, care is taken to check about errors and warning of simulation. This initialized case model is further labeled into case models 1 to 4 to study the following effects.
2. The case model 1 is performed to select fluid injection rate for the rest of study. The fluid injection rates selected after trials are 500, 800, 1,000, and 1,200 bbl/day. While studying by varying injection rate, other operational parameters are kept constant. The best injection rate for nitrogen-foam flooding is compared with results from conventional waterflooding. This case is labeled the case model 2 and used in the following step.
3. The case model 2 is performed to select production-injection ratio (P-I).The different ratios selected to study are 1.0, 1.5 and 2.0. Injection rate is kept constant at value obtained from previous step and only production rate is varied. The rest operational parameters are kept constant. The best production-injection ratio is selected and this will give the case model 3.

จุฬาลงกรณ์มหาวิทยาลัย
Chulalongkorn University

4. The case model 3 is performed to select the best gas-liquid ratio. Chosen values of gas-liquid ratios in this study are 0.6, 1.0, 1.5, 2.0, 3.0, and 4.0. The rest operation parameters are kept constant. The best gas-liquid ratio is selected in this step, leading to the case model 4.
5. The case model 4 is performed to select slug size with previous selected operation parameters. This is the final step for the finalized base case model. The chosen foam slug sizes for study are 0.1, 0.2, 0.25, 0.3 0.4 and 0.5 PV. At the end of this step, selected injection rate, production- injection ratio, gas-liquid ratio and slug size are fixed on one case for study of interest parameters.

4.3.2 Study of Interest Parameters

1. Heterogeneous reservoir models with selected operational parameters are form in this study. As explained previously, chosen value of heterogeneity representing by Lorenz coefficient are 0.2, 0.25, 0.3, 0.35, 0.4, and 0.45.
2. Effect of vertical permeability on nitrogen-foam flooding is investigated in this section. Only case with Lorenz coefficient of 0.35 is performed. Previously, vertical permeability is fixed at 0.1 time horizontal permeability. Ratio of vertical permeability to horizontal permeability is varied from 0.1 to 0.05, 0.2, 0.3 and 0.5.
3. Effect of wetting condition on nitrogen-foam flooding is performed by adjusting relative permeability. As mentioned earlier, the initial case study is performed on water-wet sandstone. This wetting condition is represented wetting condition no.1. Other three wetting conditions are generated to have a gradual increment in oil-wet characteristic by decreasing irreducible water saturation, increasing residual oil saturations and increasing of relative permeability to water.

จุฬาลงกรณ์มหาวิทยาลัย
Chulalongkorn University

4. Formation thickness is varied from 100 ft to 150 and 250 ft. In all cases, datum depth is kept at 5,000 ft and hence, top and bottom depths are varied as well as reservoir pressure in each layer.
5. Single slug mode is altered to double- and triple-slug. From previous step, selected slug size is divided into two and three slugs. Each slug is altered by chasing water and chasing water slug size is also obtained from base case by dividing total injected pore volume of chasing water into two or three slugs for double- and triple-slug modes, respectively. Comparisons are made in two ways, extension of chasing water and limited chasing water.
6. Conclusions and new findings are made based on simulations outcomes including oil recovery factor, oil and water production rates, fluid injection rate, and bottomhole pressure. Moreover, 3-dimentional illustration of lamellae (foam) flowing, oil saturation, water saturation etc. are also used to assist discussion and conclusion processes.

จุฬาลงกรณ์มหาวิทยาลัย
Chulalongkorn University

CHAPTER V
RESULTS AND DISCUSSIONS

This chapter consists of results of reservoir simulation performed by nitrogen-foam flooding. Results of waterflooding are first discussed, pertaining to construct basecase of foam flooding. Operational parameters including fluid injection rate, gas-liquid ratio, production-Injection ratio and slug size are adjusted and values are selected based on criteria. Each case is individually simulated under the same constraints. Various results of different operational parameters are summarized as well as 3-dimensional illustration of reservoir, showing location of lamella (foam) throughout flooding period. Effects of reservoir heterogeneity, ratio of vertical to horizontal permeability, number of slugs, rock wettability and formation thickness are studied.

5.1 Base Case Study

5.1.1 Initialization of Nitrogen-Foam Flooding Model

Reservoir physical model and foam model are initially constructed based on selected reservoir parameters and foam design method described in Chapter 4. After several trials, values are initially selected as follow: gas-liquid ratio 4:1, pore volume slug foam size 0.3, total fluid injection rate 1,000 rb/D, and production-injection ratio 1.5:1. This combination displaces light oil efficiently in heterogeneous (Lorenz coefficient of 0.35). Nitrogen gas and liquid on volume fraction basis is co-injected as a single slug to generate in-situ nitrogen-foam. Foam is generated as soon as it enters formation. To generate foam, there is foam regeneration model which consists of two foam formation reactions which is explained in Table 3.3. Similarly, foam degeneration model consists of reactions, resulting in foam coalesces. Once foam is created and reaches certain fixed pore volume, water is injected to chase foam at the same injection rate. Total fluid rate (foam), nitrogen gas rate, surfactant solution rate and chasing water rate at reservoir conditions as a function of time are shown in Figure 5.1, whereas all rates at surface conditions is shown in Figure 5.2.

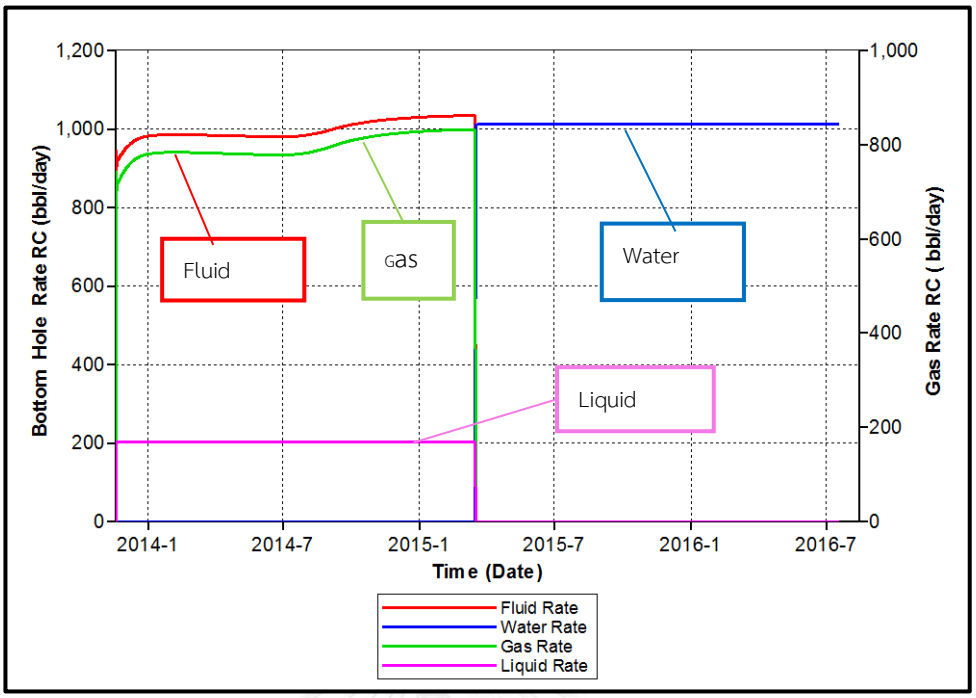

Figure 5.1 Total fluid (foam), nitrogen, surfactant solution and chasing water rates at reservoir conditions

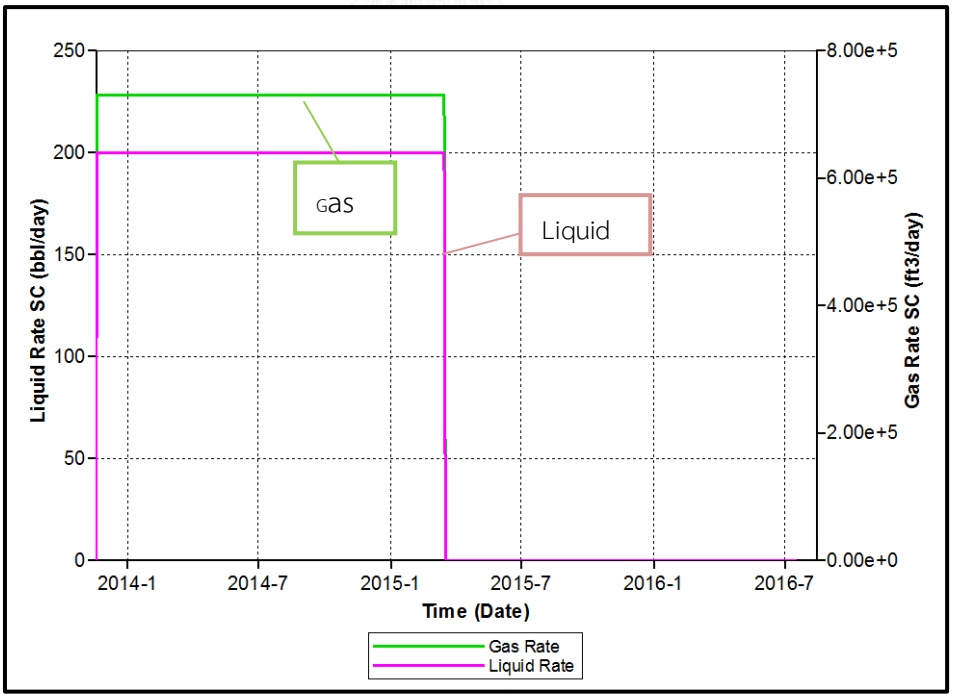

Figure 5.2 Nitrogen and surfactant solution rates at surface conditions

Total fluid rate at surface conditions is 130,200bbl/day. This rate is summation of nitrogen and surfactant solution rate as shown in Figure 5.2. Many trials are attempted to set surface rate which is equal to bottom fluid rate at reservoir conditions of 1000rb/D. Total fluid rate and chasing water rate at surface conditions as a function of time is shown in Figure 5.3.

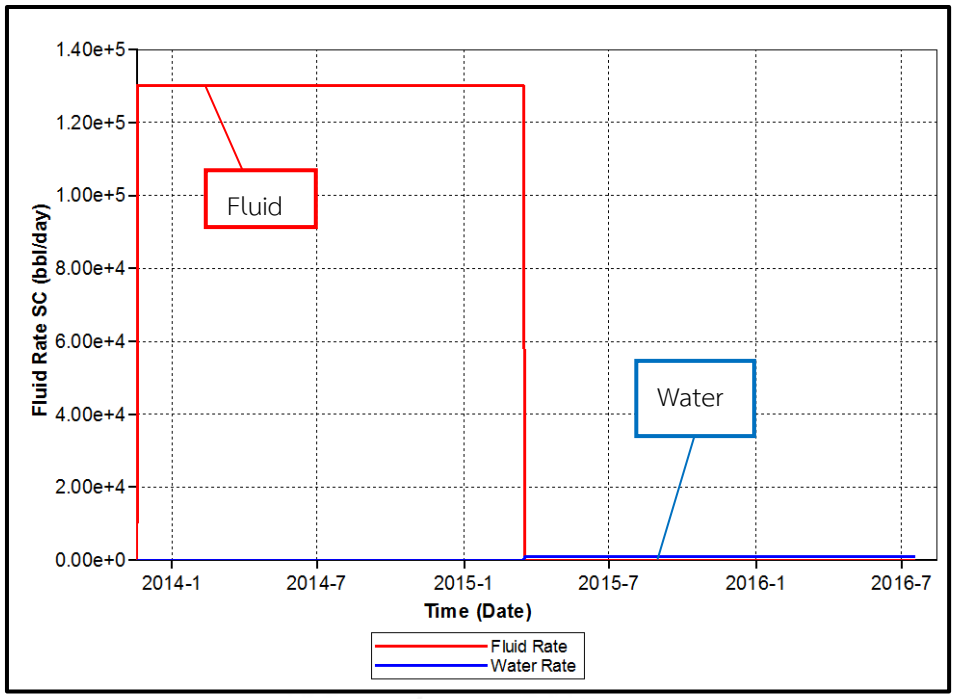

จุฬาลงกรณ์มหาวิทยาลัย
CHULALONGKORN UNIVERSITY

Figure 5.3 Comparison of total fluid rate and chasing water rate Injection rate at surface conditions as a function of time

The lamella (foam) created in reservoir after nitrogen gas and surfactant solution enter the formation is 3-dimensionally illustrated in Figure 5.4. Foam is injected from the first day of simulation for 483 days, reaching slug size of 0.3 PV which is shown graphically in Figure 5.5. It can be observed from Figure 5.4a and 5.4b that foam advancement is less in layer 1 (high permeability) compared to layers 2 and 3. At starting of foam generation before gas is liberated foam flow is best in layer 1. But as foam propagates into formation in the same time of continuing of oil production, gas is liberated due to reduction of reservoir pressure below bubble point pressure and this liberated gas accumulated at layer 1, reducing total effective

permeability due to presence of immiscible gas phase. This results in flow resistance and hence foam flow better in layers 2 and 3. Later, chasing water is injected at the rate of 1,000 bbl/day to chase foam until production constraints are attained and this is depicted by lamella concentration profile in Figure 5.5(b). Once foam is created, it starts to displace light oil in high permeability zones.

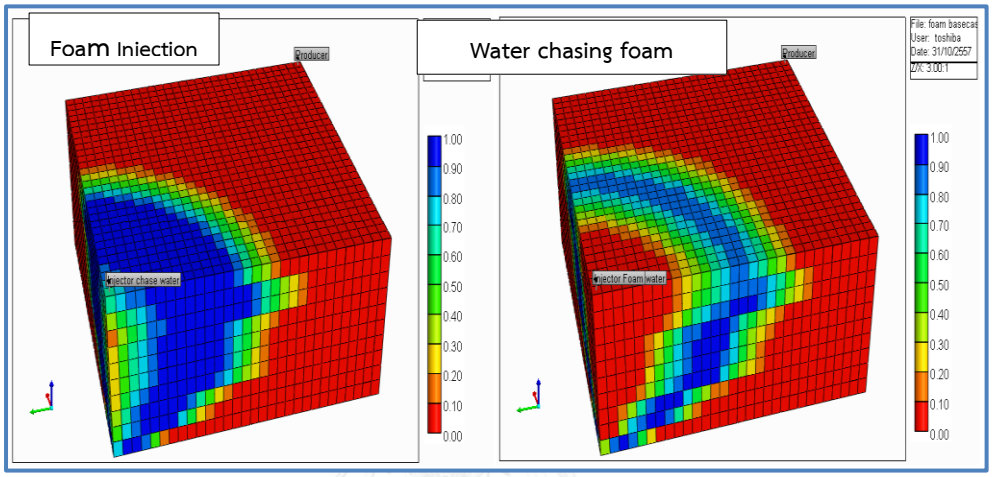

(a) (b)

Figure 5.4 Lamella profile (a) during foam injection (b) during chasing water injection

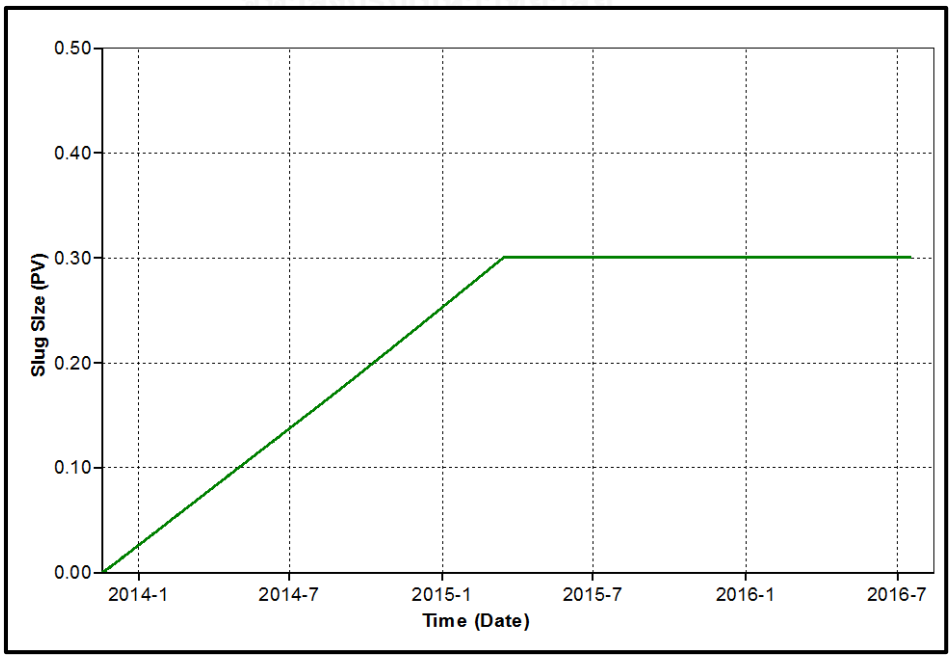

Figure 5.5 Foam slug size as a function of time

Oil, water and gas production rates from initial nitrogen-foam flooding case are shown in Figure 5.6. Total production duration is 973 days. From the figure, oil production rate is maintained mostly constant for 285 days. It can be observed that early breakthrough of gas (solution gas and nitrogen) occurs at upper layers of reservoir around day 209th. It is observed that reservoir pressure adjacent to production well at day 209th is below bubble point pressure (1,025 psi) in layer 1, whereas pressure in the rest layers is still higher than bubble point pressure. Therefore, solution gas and nitrogen gas breakthrough occurs in layer 1 and gas rate increases due to expansion. Oil rate is constantly maintained at plateau rate until day 285th and as bottomhole pressure of production well cannot be further reduced, oil rate suddenly drops. Solution gas rate reduces as oil rate drops but nitrogen gas that is kept produced. At the same time water which does not involve in foam generation is bypassed and so breakthrough of this water occurs at 477th day, whereas breakthrough of lamella does not occur as shown in Figures 5.7a and 5.7b. It can be observed Figure 5.7a that water breakthrough occurs first at upper layers of reservoir.

At 483rd day slug size reaches 0.3PV and chasing water is injected at the same rate of 1,000 bbl/day in order to chase lamella. Foam breakthrough occurs around day 669th as shown in Figure 5.7d and water saturation increases as shown in Figure 5.7c. Therefore, nitrogen starts to be produced in high rate along (with trace amount of solution gas) and so, total gas rate sharply increases after foam breakthrough as illustrated in Figure 5.6.

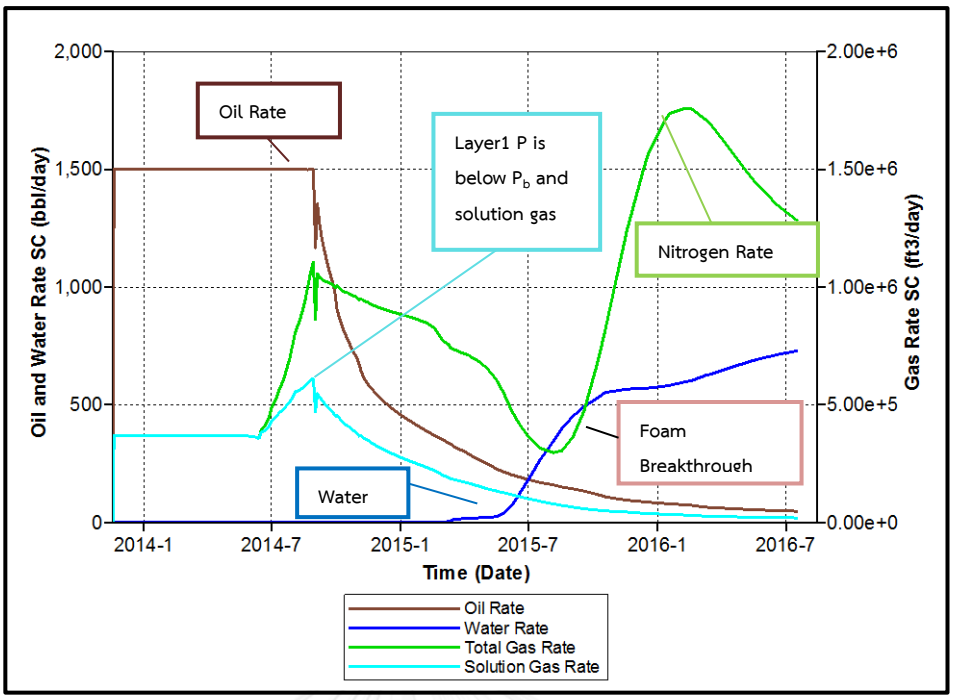

Figure 5.6 Oil, water, total gas and solution gas production rates as a function of time

Oil saturation profile is illustrated in Figure 5.8 in a 3D model at the end of production period. Remaining oil left in bottom layers is due to low permeability and displacement of oil by foam is difficult. Lamella formation is obvious in upper layers of reservoir where permeability is higher and therefore oil can be easily displaced. Eventually, production period is terminated due to oil rate reaching minimum oil production rate which is one of the constraints of production well.

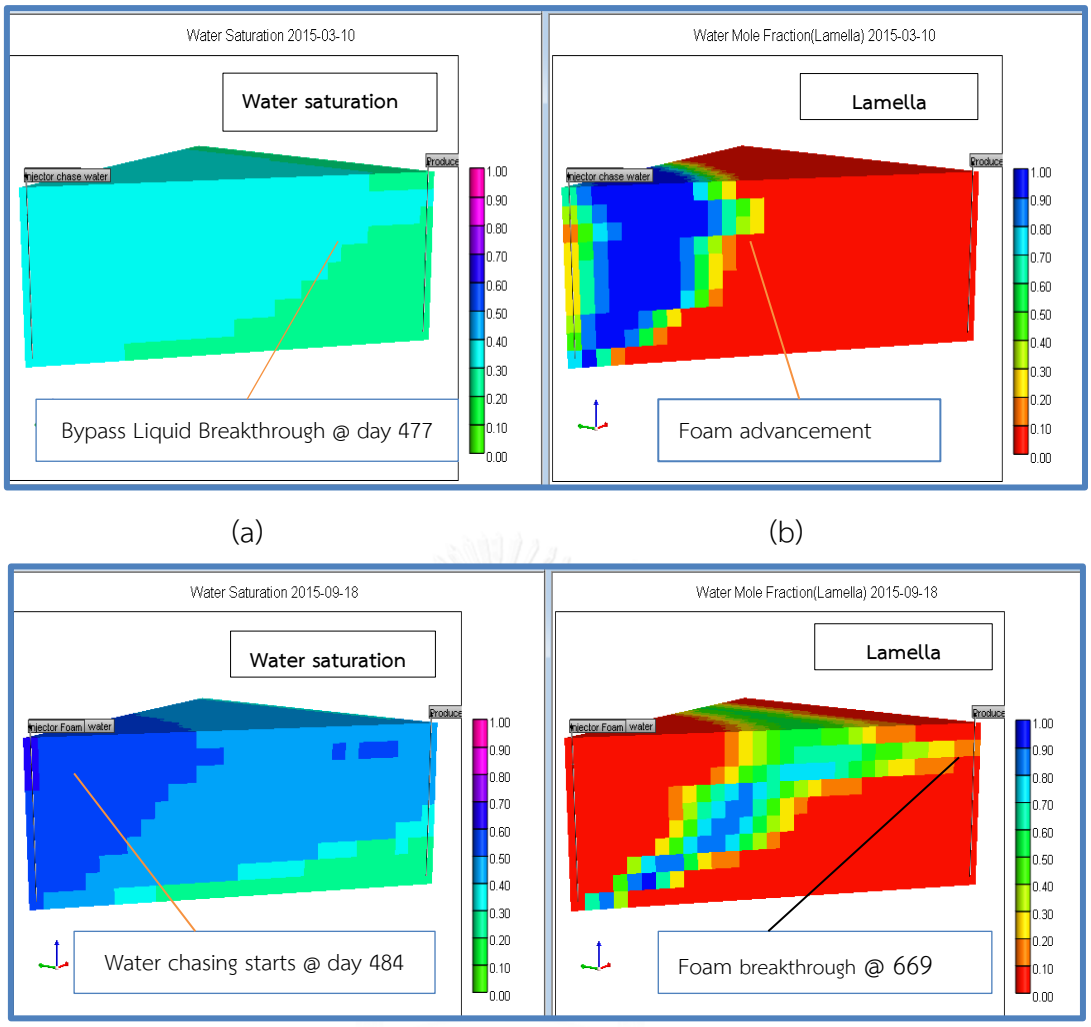

Figure 5.7 (a) Water saturation profile at water breakthrough, (b) existence pf lamella profile, (c) water saturation profile at lamella breakthrough (d) lamella profile at lamella breakthrough

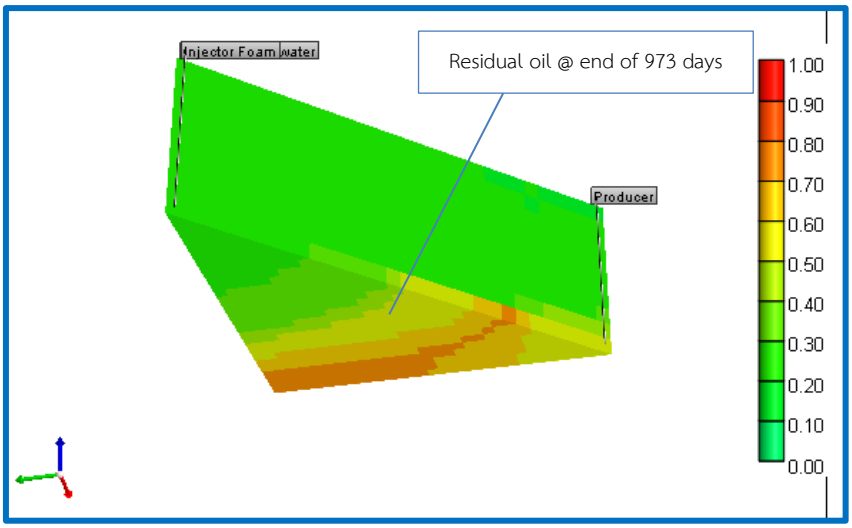

Figure 5.8 Oil saturation profile at the end of production showing oil remaining at bottom layer of reservoir model

Oil recovery factor obtained from initialized foam flooding as a function of time until the end of production is shown in Figure 5.9. At the end of production, nitrogen-foam flooding yields oil recovery factor of about 59.39% with is equivalent to 607.78 MSTB of total oil production in a total production period of 973 days.

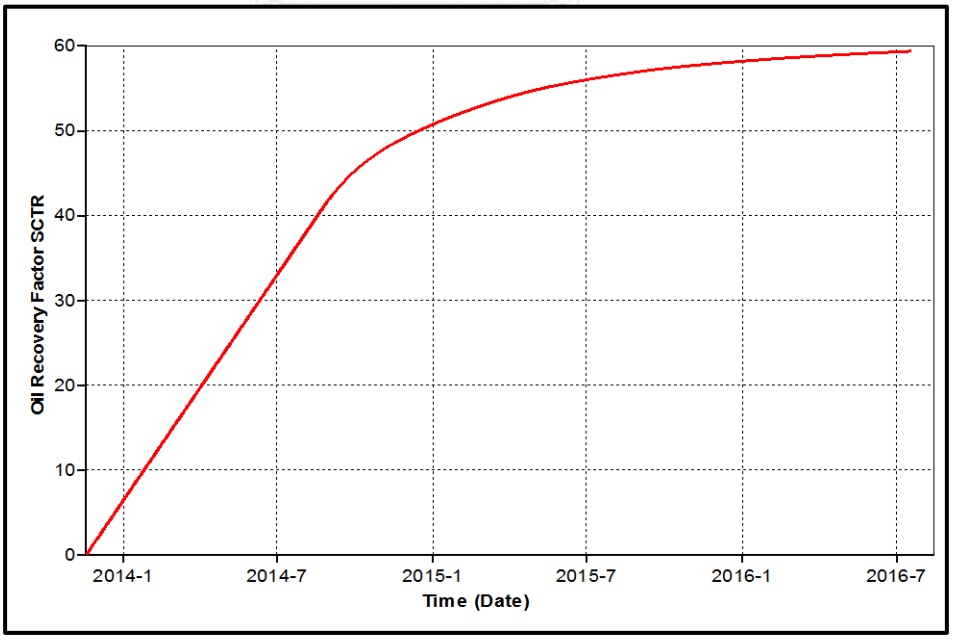

Figure 5.9 Oil recovery factor of initialized nitrogen-foam flooding as a function to time

As initialized nitrogen-foam flooding is performed on a quarter of five-spot pattern, the following step is to perform reference waterflooding. In this study, waterflooding is performed to ensure that, nitrogen-foam flooding would be a more applicable technique for reservoir containing heterogeneity. Results obtained from waterflooding are also useful to compare in terms of investment since alternative techniques are usually more expensive than just injecting of water.

5.1.2 Waterflooding Case

Injection of nitrogen-foam in previous section is replaced by conventional waterflooding. Water is injected at same rate as fluid injection rate in nitrogen-foam flooding which is 1,000 bbl/day. Bottomhole pressure is fixed at 3,500 psi as same as in case of nitrogen-foam flooding to prevent fracture pressure. Production constraints are also kept similar. Water is injected from day one of oil production and water injection rate as a function of time is shown graphically in Figure 5.10. From the figure, water injection rate is stable for the entire production period. The 3-D view of waterflooding is illustrated in Figure 5.11, showing water saturation profile at the end of production.

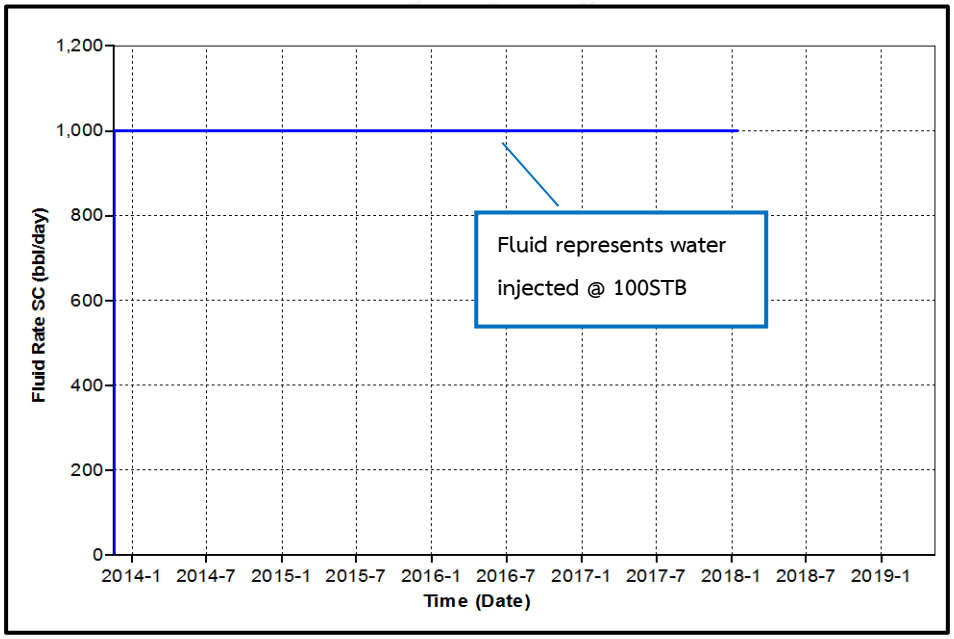

Figure 5.10 Water injection rate at surface conditions as a function of time

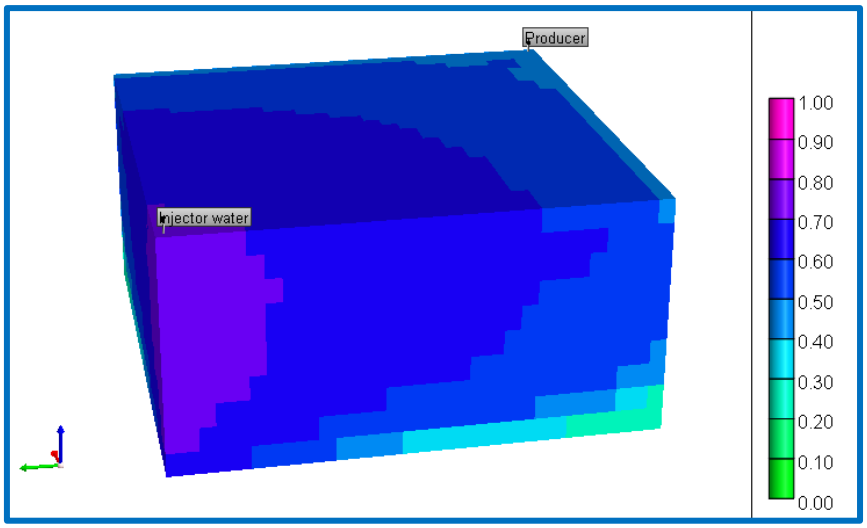

Figure 5.11 water saturation profiles at the end of production period for waterflooding case.

Oil, water and gas production rates obtained from waterflooding is shown in Figure 5.12. Total production period is 1,522 days in this case of waterflooding. As same as nitrogen-foam flooding case, formation pressure in top layer pressure firstly reaches bubble point pressure and solution gas starts to liberate out from oil phase. Oil production rate is as high as 1,500 bbl/day for a few days due to desire maximum oil production rate. Oil rate starts to drop after 22 days because well bottomhole pressure of production well starts to drop gradually. Oil rate reaches equilibrium of 1,000 bbl/day which is equal to injection rate. Injection water starts to be produced from day 192 and oil production rate starts to decline. Production period is terminated after 1,522 days due to water cut reaching 95% which is one of the preset production constraints at production well (not due to minimum oil production rate). By means of waterflooding, high amount of oil is left in reservoir which is not recovered as illustrated in 3-D view of oil saturation profile Figure 5.13.

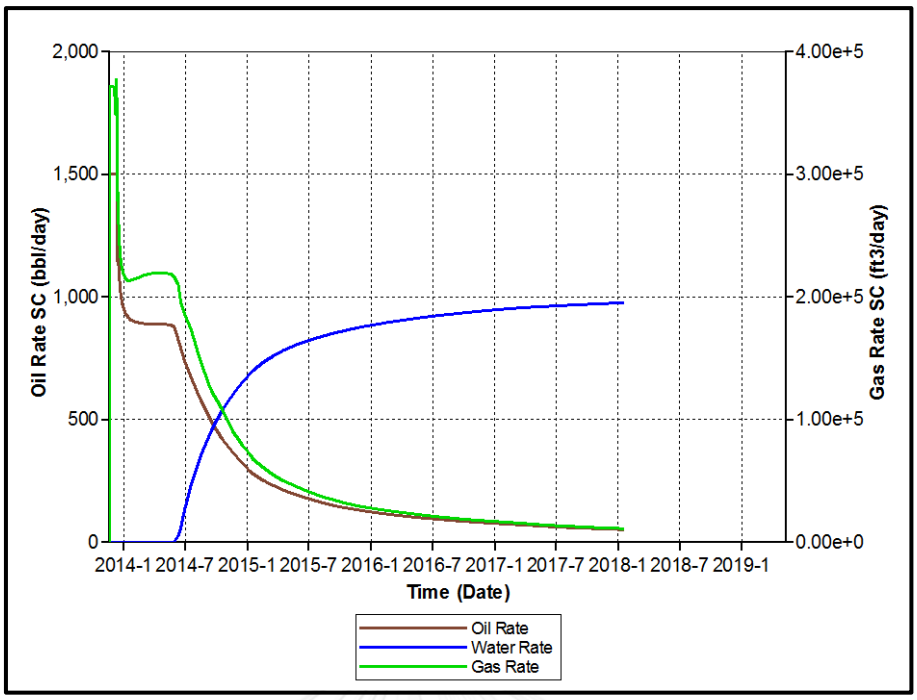

Figure 5.12 Oil, water and gas production rates at surface conditions for waterflooding as a function of time

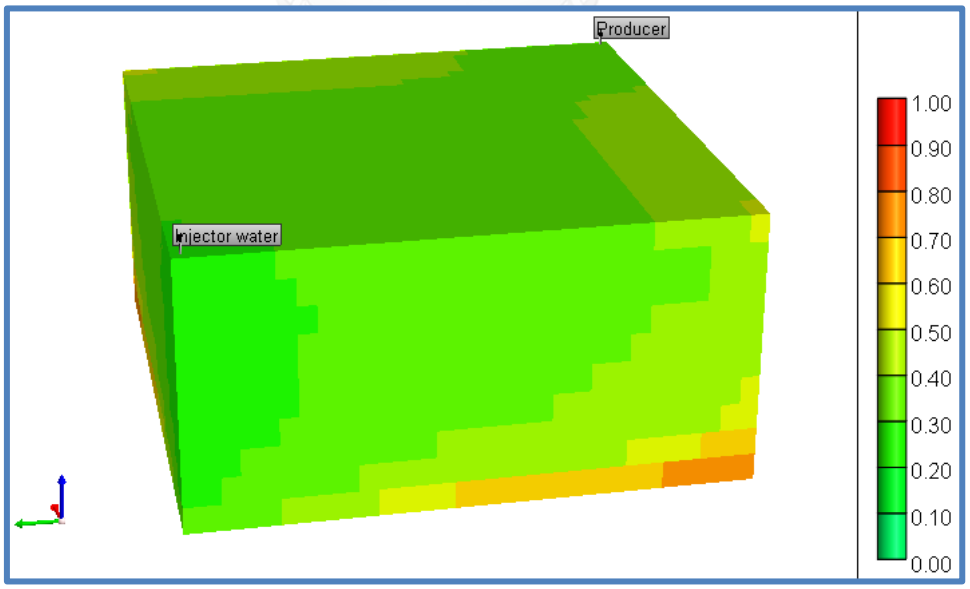

Figure 5.13 Oil saturation profile at the end of production period for waterflooding case

From Figure 5.13 it can be noticed that oil is recovered from upper layers efficiently compared to bottom layers. Effects of heterogeneity are clearly shown in the reservoir. Water displaces oil easily in high permeability layers compared to bottom layers. Since oil cannot be efficiently displaced in bottom layers, it can be seen in Figure 5.13 that oil saturation left is more in bottom layers particularly the vicinity of production well (showing orange-yellow color compared to green color to the rest of reservoir). Early water breakthrough occurs in upper layers, causing oil production rate starts to drop. Total oil recovery factor is about 41.07% as depicted in Figure 5.14 which is the combined recovery from upper layers as well as bottom layers.

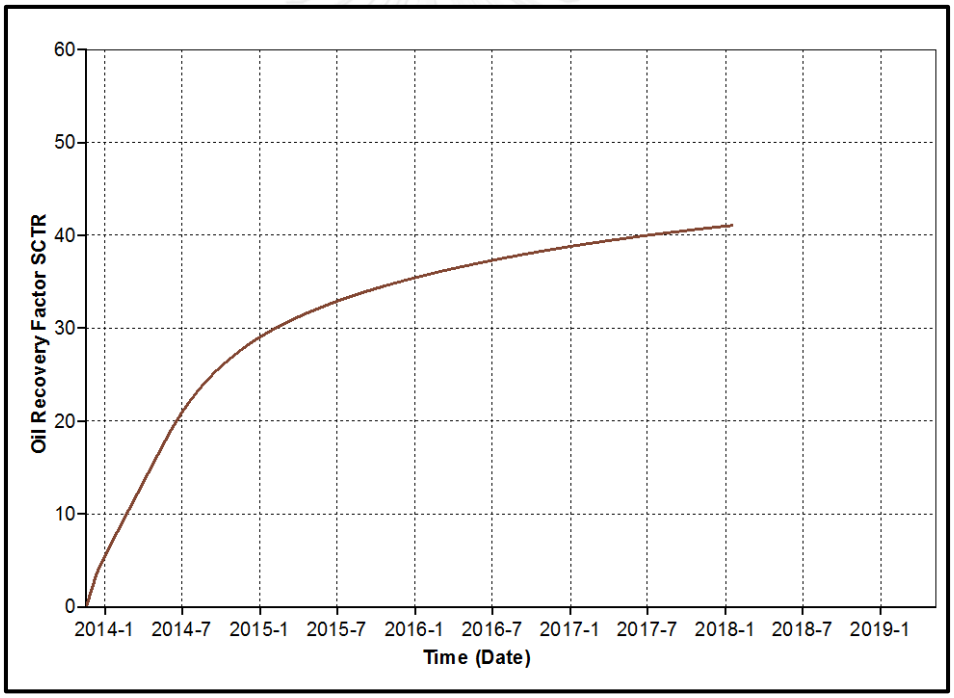

Figure 5.14 Oil recovery factor of waterflooding case as a function of time

5.1.3 Comparison between Waterflooding and Initialized Nitrogen-Foam Flooding

Initialized nitrogen-foam flooding case is framed and the results are discussed on effectiveness on heterogeneous reservoir. The only operational parameter similar

is total fluid injection rate in both cases which 1,000 bbl/day. In nitrogen-foam flooding, total fluid rate includes nitrogen gas and surfactant solution. Production constraints are the same and production-injection ratio is fixed at 1:1.5. Table 5.1 shows the summary of various results.

Table 5.1 Summary of nitrogen-foam flooding and waterflooding cases

Flooding Type	**Nitrogen-foam Flooding**	**Waterflooding**
Total production period (day)	973	1,522
Cumulative oil production (MSTB)	607.48	420.24
Oil recovery factor (%)	59.39	41.07
Cumulative gas injection (BSCF)	0.353	-
Cumulative gas production (BSCF)	0.832	0.101
Cumulative liquid injection (MSTB)	96.6	1,522
Cumulative water production (MSTB)	277.15	1,097.87
Cumulative surfactant injected (STB)	483	-
Oil recovered per surfactant (STB/STB)	1,278	-

จุฬาลงกรณ์มหาวิทยาลัย
Chulalongkorn University

Table 5.1 summarizes important reservoir simulation outcomes such as cumulative oil production, cumulative water production and oil recovery factors. In waterflooding process, water can displace very fast in high permeability layer and reach production well. This slows down oil recovery process and oil production is prolonged to 1,522 days in total with 420.24 MSTB of cumulative oil production and oil recovery factor of about 41.07%. In case of nitrogen-foam flooding, when nitrogen gas and surfactant solution are injected, nitrogen is easily dispersed in surfactant solution, turning to lamella formation and improving flow resistance. When flow resistance is improved in high permeability layers, displacing fluid which is lamella is forced to flow towards the direction of higher resistance zone which is low permeability layers, sweeping oil from un-swept zone and recovering large quantity

of residual oil. Sweep efficiency is improved by using foam. As nitrogen gas is dispersed in liquid, lamella is formed by capturing gas inside liquid films. Mobility of nitrogen gas is decreased, diminishing gas overriding as well as viscous fingering problems. When the lamella is formed, water breakthrough time is increased, resulting in plateau production rate of oil for longer time. When well bottomhole pressure keeps reducing until to minimum bottomhole pressure is reached, oil rate gradually declines in both flooding until one of production constraints is reached. In nitrogen-foam flooding, termination is provoked from minimum oil rate of 50 bbl/day. Cumulative oil production at the end of 973 days is 607.48 MSTB and oil recovery factor is 59.39%.

From initialized nitrogen-foam flooding, fluid injection rate, production-injection ratio, gas-liquid ratio and slug size are not adjusted yet. The following step is performed to choose of operational parameters that yield favorability.

5.1.4 Selection of Fluid Injection Rate

Reasonable design with favorable operating conditions is a prime concern. In this section, an attempt is made to control total fluid (gas, water and surfactant) from surface to downhole. To obtain exact injection rate from surface, bottomhole fluid rate is maintained at desired rate by adjusting ratio between production and injection rates. The selected fluid injection rates (rb/D) for this study are 500, 800, 1,000, and 1,200, whereas gas-liquid ratio is fixed at 4:1, foam pore volume is 0.3. First, production–injection ratio is fixed at 1.5 to identify the best injection rate and this step is performed only in reservoir with Lorenz coefficient of 0.35. For all cases, nitrogen gas and surfactant solution are injected through tubing from September 18, 2013, using volume fraction basis and once fluids enter formation, lamella is generated. Fluid injection rate along with chasing water rate at reservoir conditions are shown graphically in Figure 5.15, whereas fluid injection rates at surface conditions are shown in 5.16. Injected gas rates and injected liquid rates are illustrated in Figures 5.17 and 5.18, respectively.

จุฬาลงกรณ์มหาวิทยาลัย
Chulalongkorn University

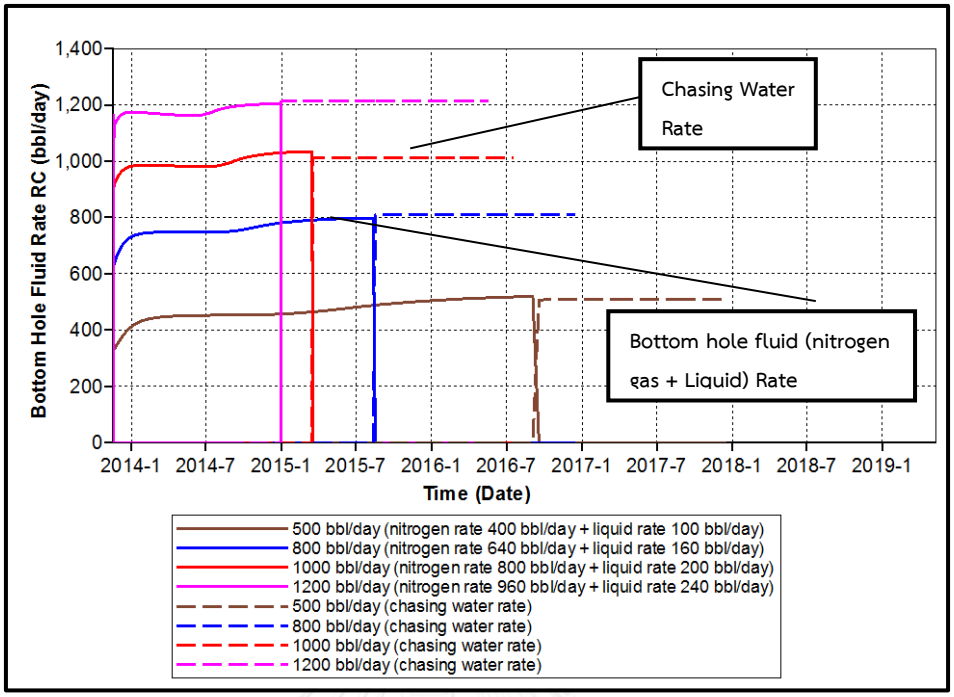

Figure 5.15 Fluid injection rates along with chasing water rates at reservoir conditions as a function of time

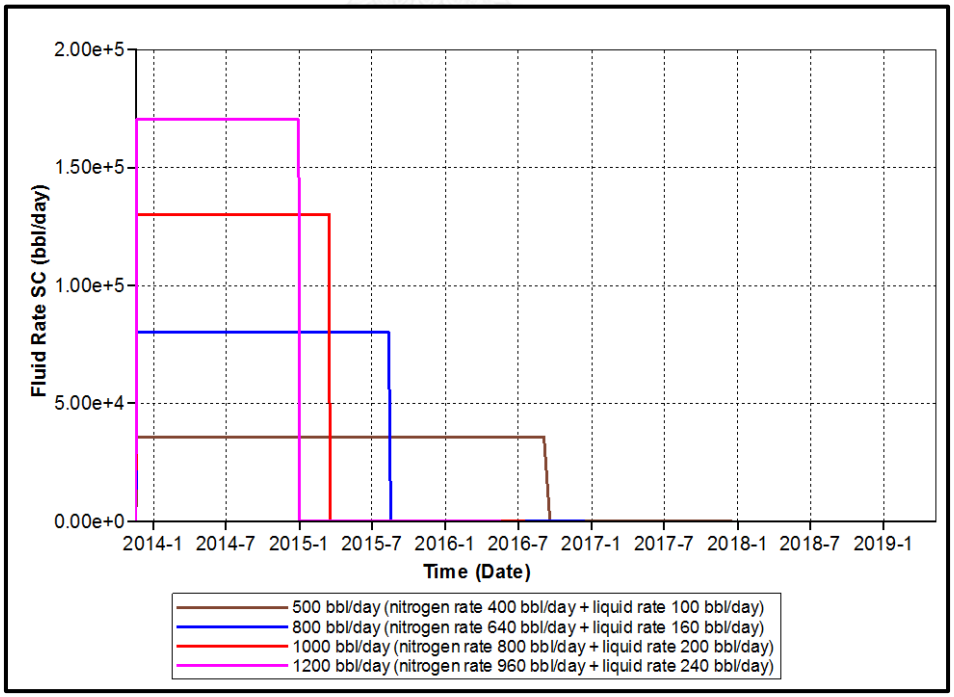

Figure 5.16 Fluid Injection rates at standard conditions as a function of time

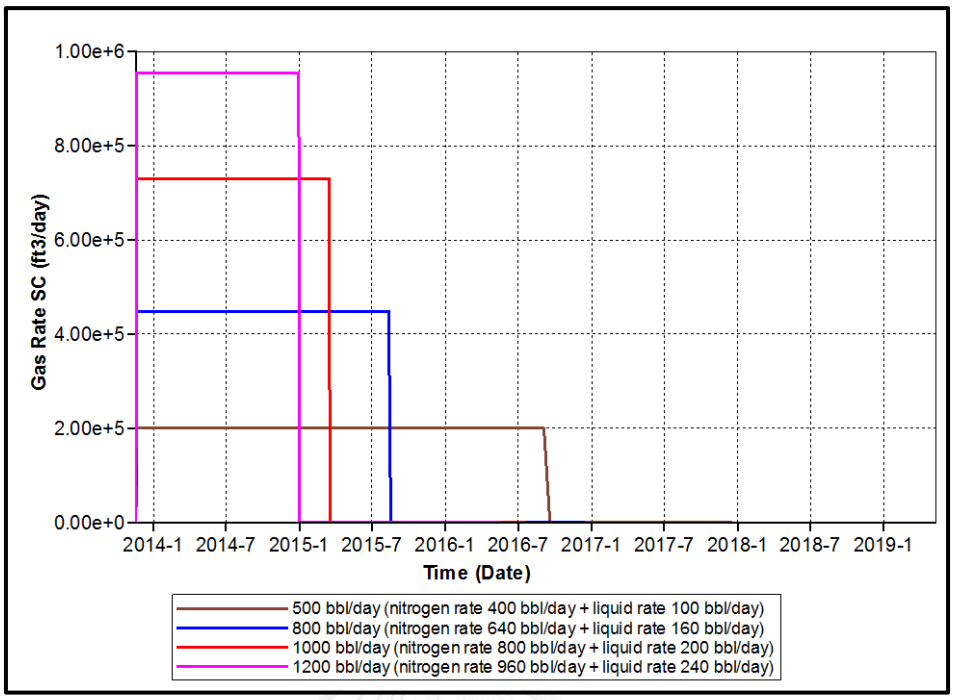

Figure 5.17 Nitrogen Injection rates at surface conditions as a function of time

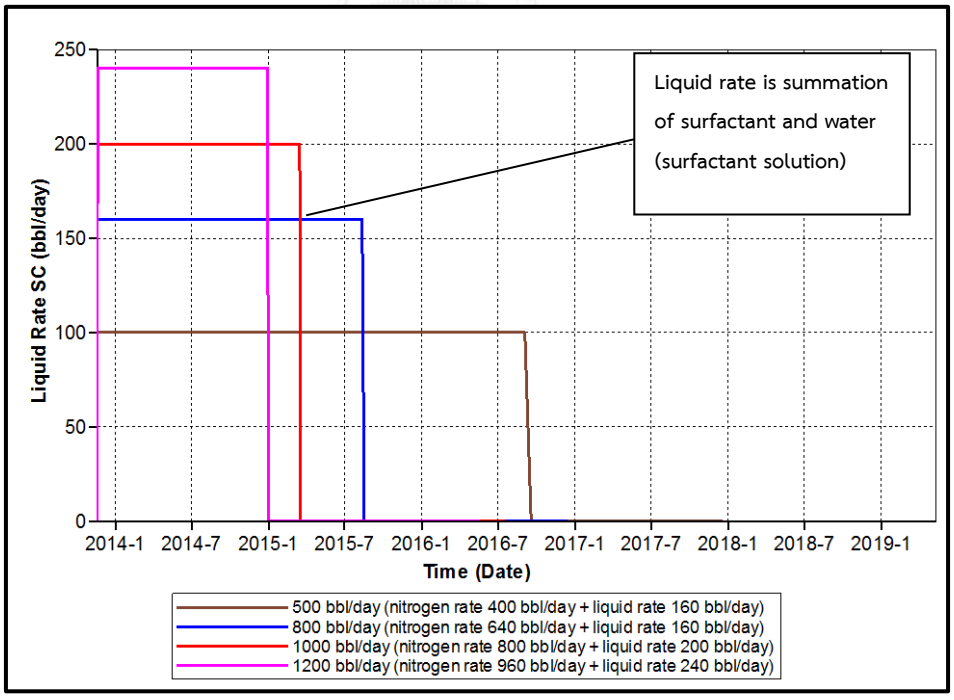

Figure 5.18 Liquid Injection rates at surface conditions as a function of time

Volume of nitrogen is large at surface conditions and when it injected into well, it is compressed to much smaller volume due to effect of pressure. Bottomhole fluid injection rate is firstly fixed to correct injection rate at surface conditions. In STARS, nitrogen gas and surfactant solution can be co-injected from the same injection well. Adjusting bottomhole fluid rate as shown in Figure 5.15 is very difficult task. Once designed value is attained, injection rate at surface conditions are obtained as shown in Figure 5.16. Fluid rate at the bottomhole condition is combination of nitrogen gas injection rate as shown in Figure 5.17 and surfactant solution injection rate from Figure 5.18. These two rates are fixed based on gas-liquid ratio of 4:1. Fluid injection rate is maintained constant, indicating that well bottomhole pressure of injection well is still below fracture pressure.

For example, fluid injection rate at surface condition of 35,843 STB/day is equivalent to downhole fluid rate of 500 rb/D of which 100 rb/D is contributed by surfactant solution. Downhole fluid rates of 500, 800, 1,000 and 1200 rb/D are injected for 1,020, 632, 483 and 407 days, respectively depending on time required to attain one of the production constraints at production well. In each case cumulative bottomhole fluid of 0.483 MM reservoir barrels is maintained constant but at different periods as shown in Figure 5.19. This amount of cumulative bottomhole fluid represents the slug size 0.3 PV obtained from dividing by total reservoir pore volume.

Chulalongkorn University

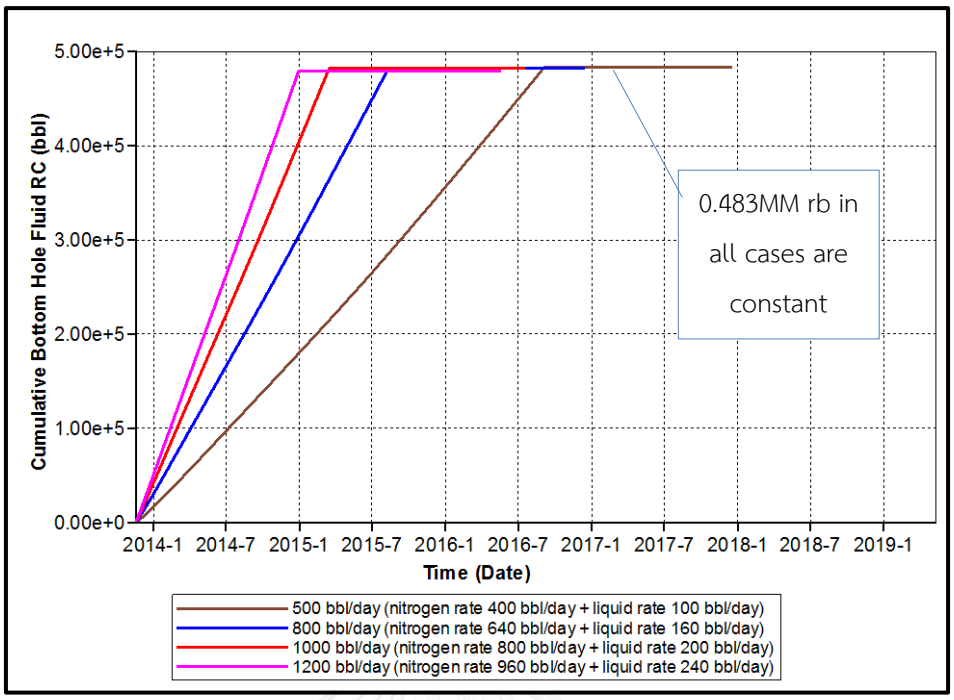

Figure 5.19 Cumulative bottomhole fluids at reservoir conditions a function of time

Lamella creation starts to displace oil from the 1st day. It can be observed in Figure 5.19 that oil production rate is constantly maintained for about 546, 334, 285, and 232 days for downhole fluid injection rates of 500, 800, 1,000, and 1,200, respectively. Water breakthrough starts from 872, 583, 457, and 392 days in the same sequence shown in Figure 5.21. Gas breakthrough occurs first in every case as can be seen in Figure 5.22. Even though gas breakthrough occurs early, the oil rate is maintained constant due to the fact that gas is highly compressible and pressure decline from gas breakthrough is low. Gas production rate is a summation of injected nitrogen and solution gas liberated out from oil when reservoir pressure is below bubble point pressure. Extremely high gas production before termination of production is injected nitrogen that is previously in a form of foam. When foam breakthroughs, nitrogen returns to gaseous form.

After well bottomhole pressure of production well reaches minimum bottomhole pressure of 200 psi, oil rates cannot be maintained at plateau rate due to insufficient different pressure. This results in declining of oil production rate until minimum oil production rates pre-set as one of the production constraints. Summary of simulation outcomes including cumulative oil production, cumulative water production etc. is shown in Table 5.2.

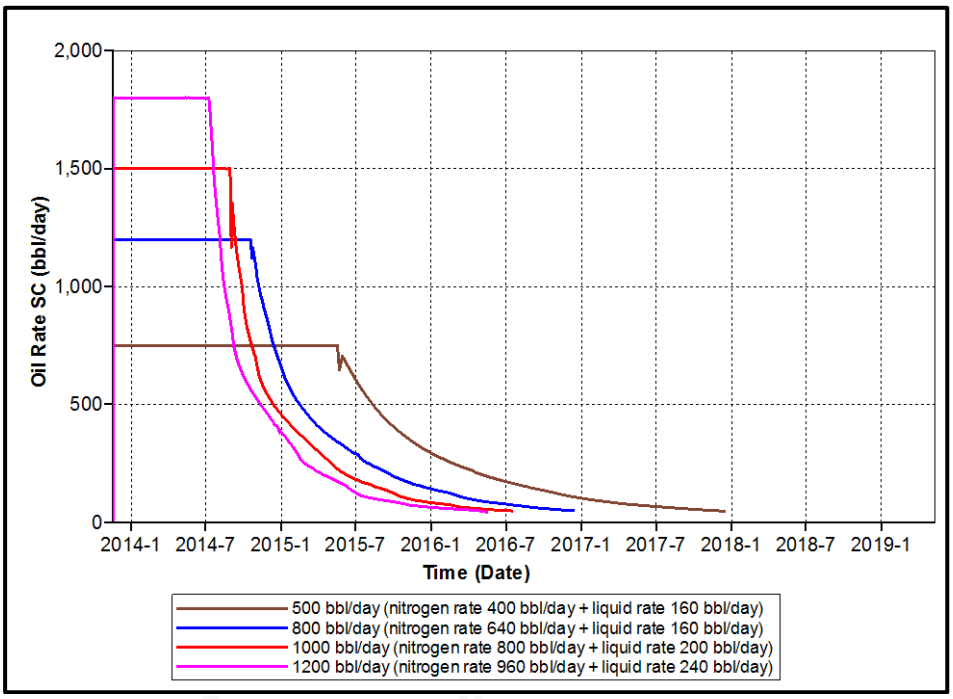

Chulalongkorn University

Figure 5.20 Oil production rates at standard conditions as a function of time for the study of fluid injection rate

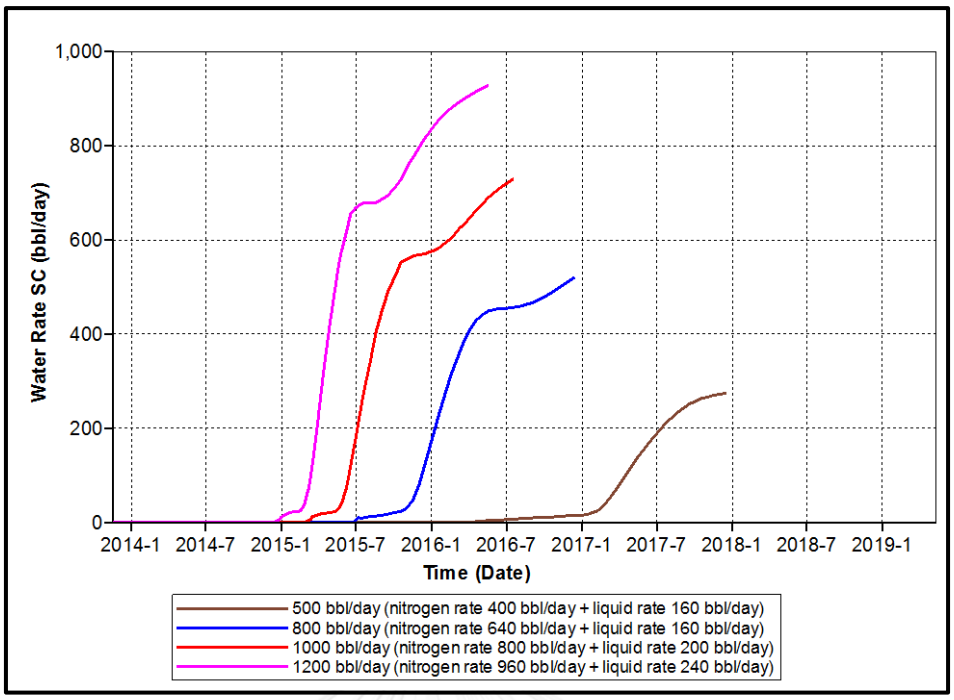

Figure 5.21 Water production rates at standard conditions as a function of time for the study of fluid injection rate

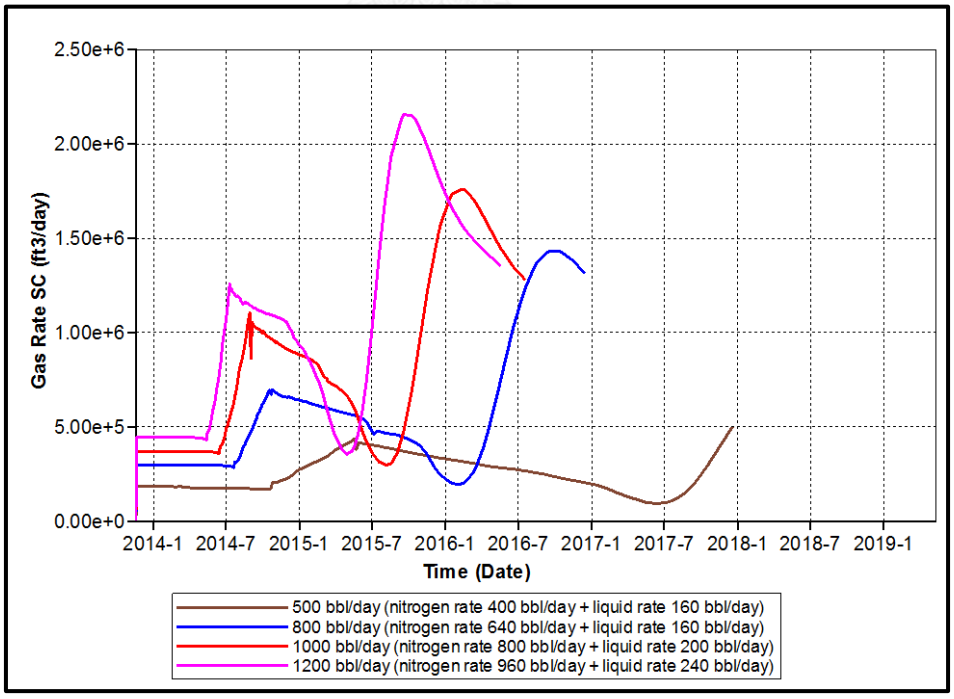

Figure 5.22 Gas production rates at standard conditions as a function of time for the study of fluid injection rate

Oil saturation profile at the end of production is shown 3-dimensionally in Figure 5.23 for all pre-selected rates and water saturation profile at the end of production is shown in Figure 5.24. From Figure 5.24, it is clearly shows that when fluid is injected at 500 rb/D, oil is remaining at bottom layers as can be seen from yellow color, indicating that this injection rate is not adequate to displace oil in bottom layers. Fluid injection rates higher than 800 rb/D show mostly the same remaining oil saturation at bottom layers. From water production profiles in Figure 5.24, it can be seen that at higher water saturation is observed in case of higher fluid injection rates, resulting in smaller water production is case of low small total fluid injection rate compared to higher fluid injection rate as water production rate is controlled from rate of chasing water. Summary of simulation outcomes various are shown in Table 5.2 and this is an aid to select injection rate for the following steps.

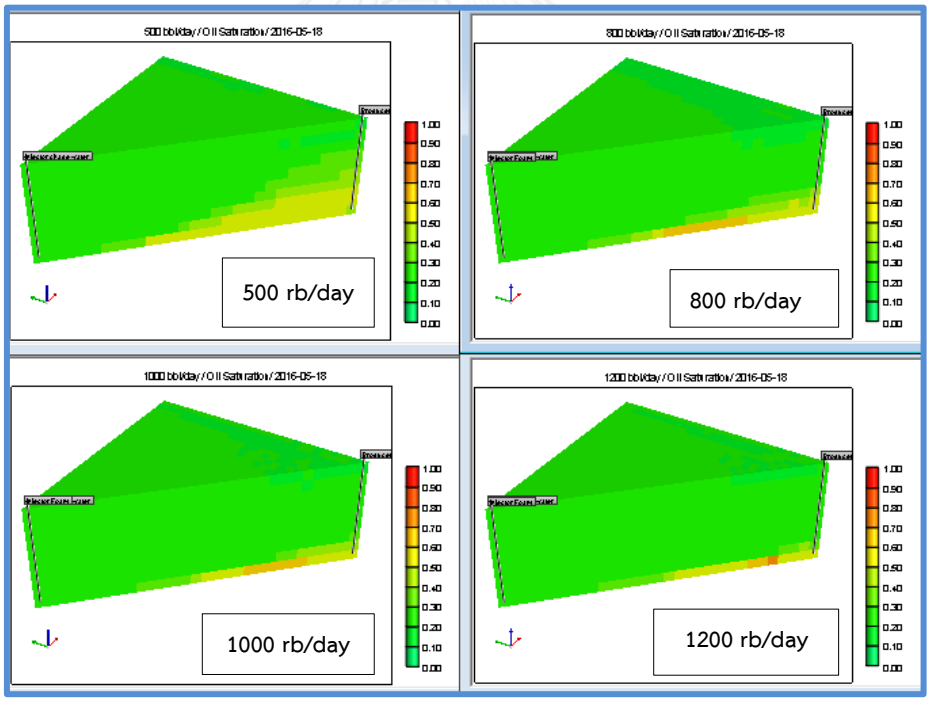

Figure 5.23 Oil saturation profiles at the end of production from different fluid injection rates

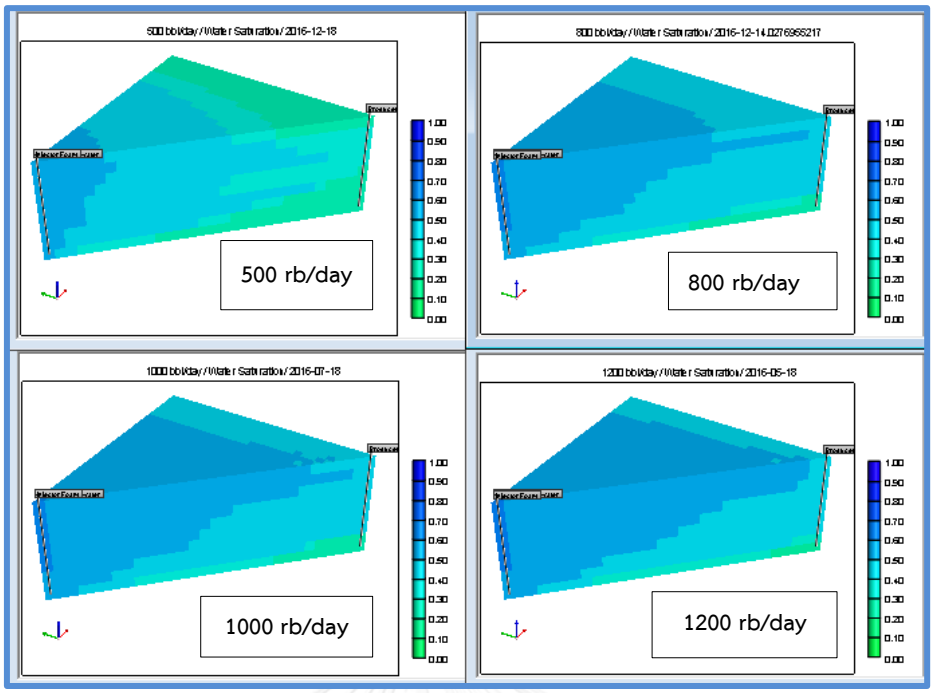

Figure 5.24 Water saturation profiles at the end of production from different fluid injection rates

Table 5.2 Summary of simulation outcomes in the study of at fluid injection rates

Fluid injection rates (rb/D)	**500**	**800**	**1,000**	**1,200**
Total production period (days)	1,491	1,123	973	912
Cumulative oil production (MSTB)	601.51	607.48	607.78	611.83
Oil recovery factor (%)	58.77	59.36	59.39	59.78
Cumulative gas production (BSCF)	0.380	0.667	0.832	0.985
Cumulative water production (MSTB)	62.73	159.18	227.15	313.65
Slug size period (days)	1,020	632	483	407
Oil recovered per surfactant (STB/STB)	1,277	1,290	1,291	1,299

From Table 5.2, based on oil recovery factor it can be seen that sudden increment is found from 500 to 800 rb/D. After the rate of 800 rb/D, oil recovery factor just slightly increases. Injection rates of 1,000 and 1,200 rb/D yields very good results as well since oil recovered is high within short period and also oil recovered per surfactant is observed to be the highest at higher rate and decreases as fluid injection rate decreases. However, selection of injection rate is based on oil recovery factor. Hence, oil recovery factors of all cases as a function of time are shown in Figure 5.25.

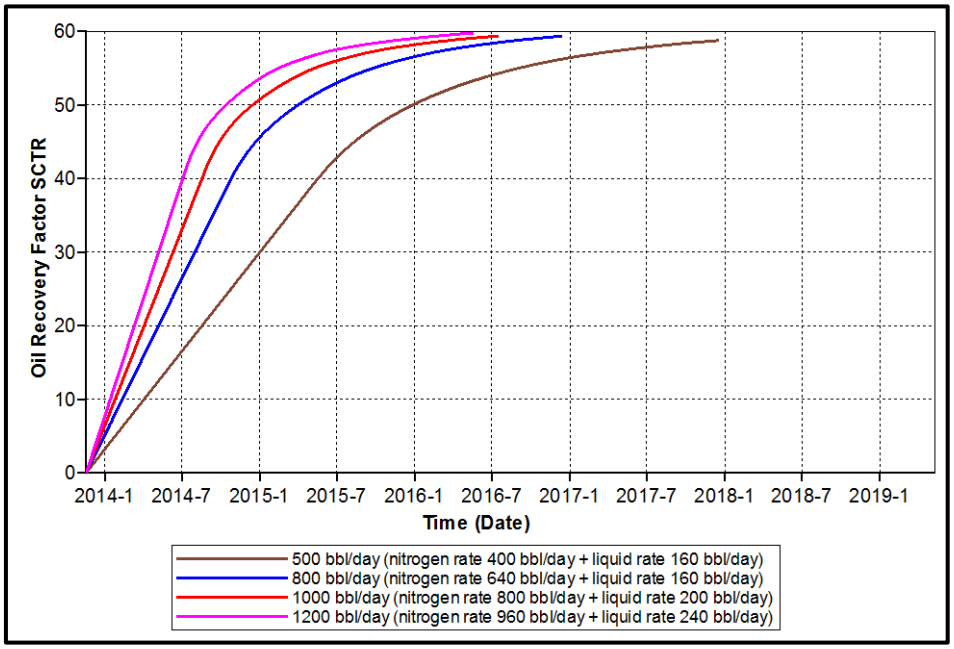

Figure 5.25 Oil recovery factors from different fluid injection rates as a function of time

As explained previously, a change is obviously found from the rate of 500 to 800 rb/D. Relationship between oil recovery factor and total fluid injection rate is also plotted and shown in Figure 5.26 and this helps to select reasonable Injection rate.

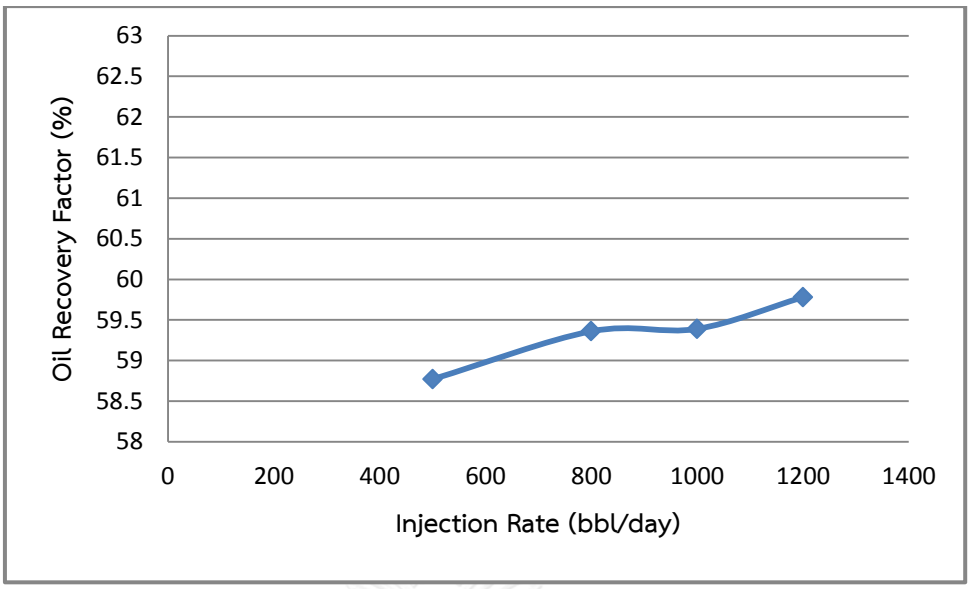

Figure 5.26 Oil recovery factors from different fluid injection rates

As injection rate increases, total production period decreases. From Figure 5.26 an intercept of two trends of oil recovery factor lays in between 800 to 1000 rb/D. The total fluid injection rates of 500 and 800 requires longer production periods. Injection rate of 1,000 rb/D minimizes production period. When total fluid injection rate is further increased to 1,200, oil recovery is almost the same but substantial water production is obtained due to higher rate of chasing water.

In general, higher production rate might be favorable for foam creation . The total fluid injection rate of 1,200 rb/D is however too high. As production-injection ratio is fixed at 1.5, high injection rate of 1,200 rb/D will cause production rate correspond to 1,800 BPD per quarter of well or 7,200 per well which is too high for real implementation.

Total fluid injection rate of 1000 rb/D is therefore selected for the following steps since this rate yields high oil recovery in short period with moderate water production. This rate corresponds to surface rate of 130,200 STB/day at the surface conditions.

5.1.5 Selection of Production-Injection (P-I) ratio

This section is performed to selected production rate from the previously obtained total fluid injection rate. In this study, total fluid injection rate is kept constant at 1,000 rb/D, gas-liquid ratio is 4:1 with also 0.3 PV of slug size. Chosen P-I ratios are 1.0, 1.5 and 2.0. The main aim for setting higher P-I ratios is to partial deplete reservoir pressure and according to this, fluid injection and foam generation may be favored. The 3-D view of lamella profiles at day 483 and at the end of production are illustrated in Figure 5.27a and b, respectively for P-I ratios of 1.0, 1.5, 2.0.

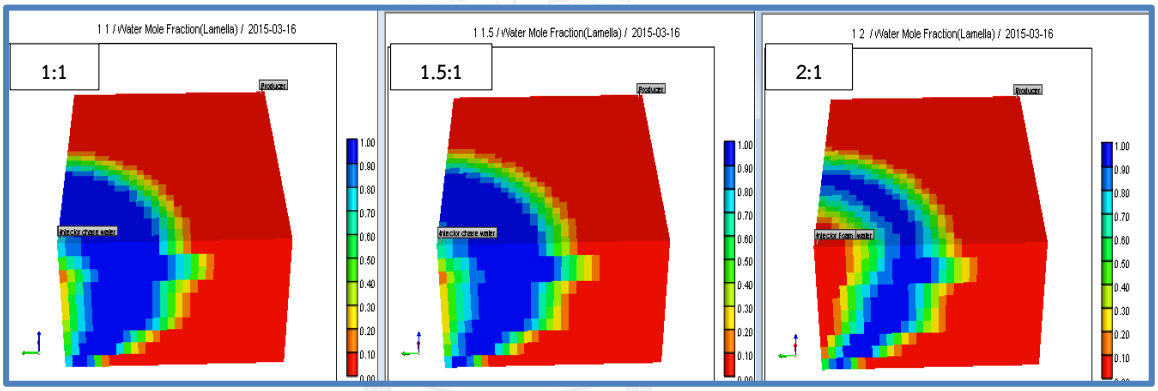

(a)

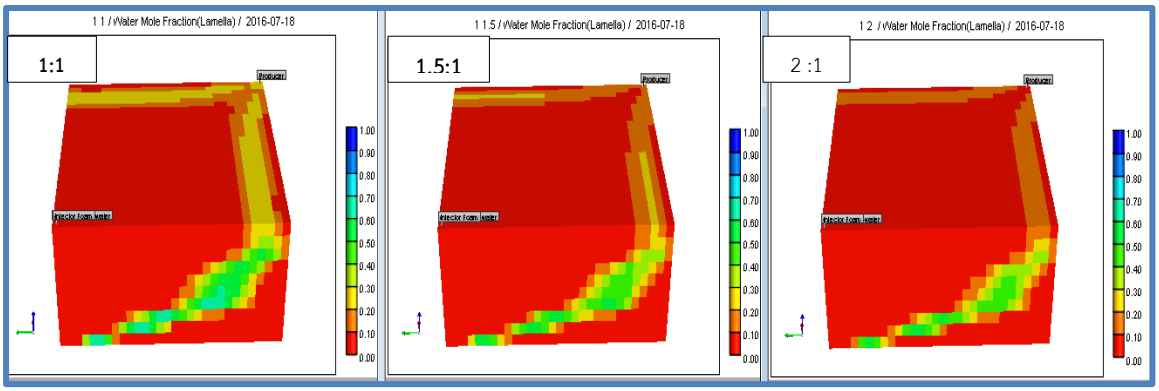

(b)

Figure 5.27 Lamella profiles from different P-I ratios at a) day 483 and b) the end of production

From Figure 5.27a, it can be observed that at day 483 surfactant solution and nitrogen gas are already injected into formation and chasing water partially propagates in case of P-I ratio of 2.0. Time required for completing foam slug size of 0.3 PV are 559, 483, and 462 days for P-I ratios of 1, 1.5 and 2, respectively.

Reservoir pressure is high and it is not drained proportionally with fluid injection rate when P-I ratio equals to 1. When foam is generated, reservoir pressure starts to build up and reaches maximum bottomhole pressure of 3,500 psi as can be observed in Figure 5.28. This pressure is maintained constant from day 51 to 390. Due to this limitation, injection rates of nitrogen gas and surfactant concentration are lower than expected as in Figure 5.29. The P-I ratio of 1.5 and 2.0 maintain bottomhole pressure of injection well below the constraint value and high injectivity results in constant fluid injection as shown in Figure 5.29. But in case of P-I equals to 2.0, reservoir pressure is depleted at higher rate, causing lower bottomhole. Cumulative fluid injection of 0.3 PV is attained earlier than other two cases and hence, starting of chasing water is earlier.

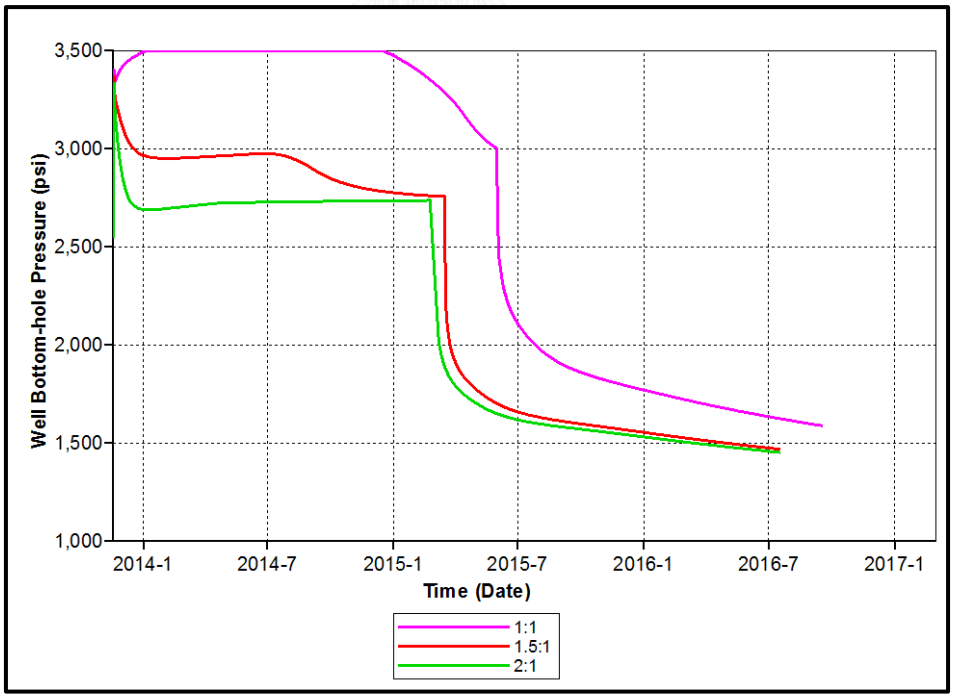

Figure 5.28 Bottomhole pressures of injection well from different P-I ratios as a function of time

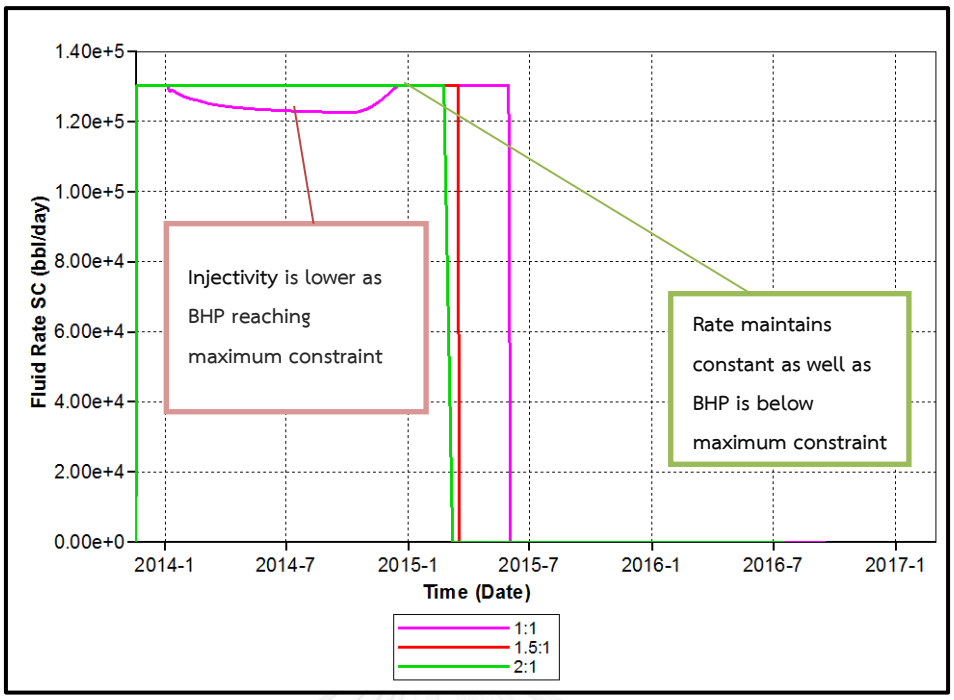

Figure 5.29 Fluid injection rates at surface conditions from different P-I ratios as a function of time

As foam generation period is delayed, it also delays in oil recovery process. Effects of P-I ratio on oil production rate are shown graphically in Figure 5.30, whereas effects on water production rate and gas production rate are consecutively illustrated in Figures 5.31 and 5.32. Oil production rate is generally maintained constant during early stage of oil recovery. For P-I ratios of 1.0, 1.5 and 2.0, oil production rates are maintained constant for 503, 285, and 158 days, and water breakthrough starts from day 538, 457, and 452, respectively. Gas breakthrough in all cases occurs before water breakthrough due to declining of reservoir pressure below bubble pressure. For P-I ratios 1.0, 1.5 and 2.0 gas breakthrough occurs at day 149, 212, and 318 as shown in Figure 5.32, respectively. After bottomhole pressure of producer reaches the minimum pre-set value (200 psi) and cannot be further reduced, oil rates declines until one of the production constraints is attained.

Summary of simulation outcomes such as cumulative oil production, cumulative water production etc. is shown in Table 5.3.

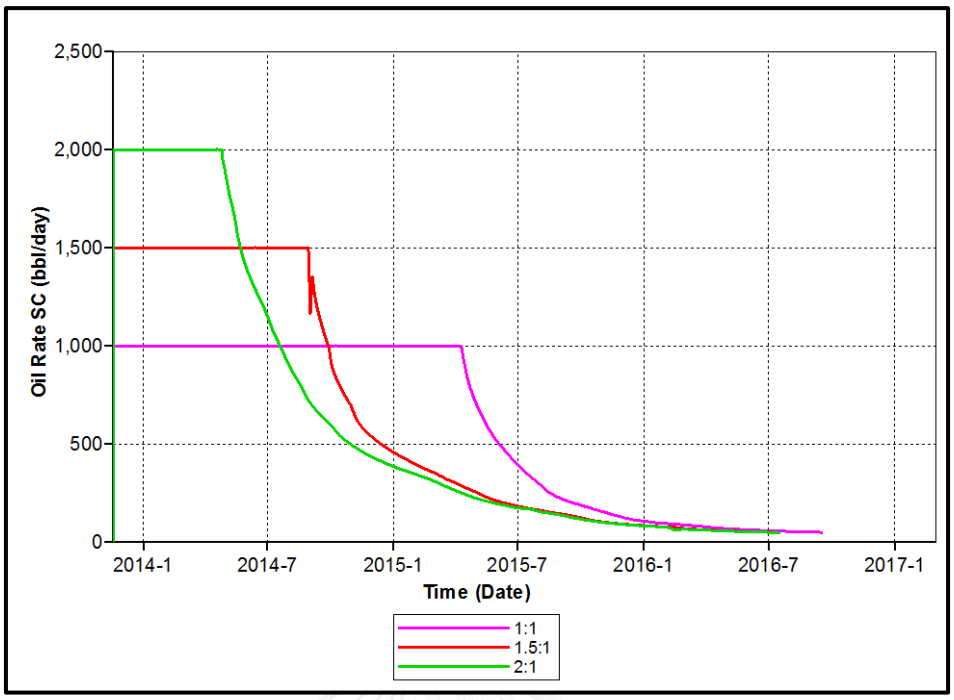

Figure 5.30 Oil production rates from different P-I ratios as a function of time

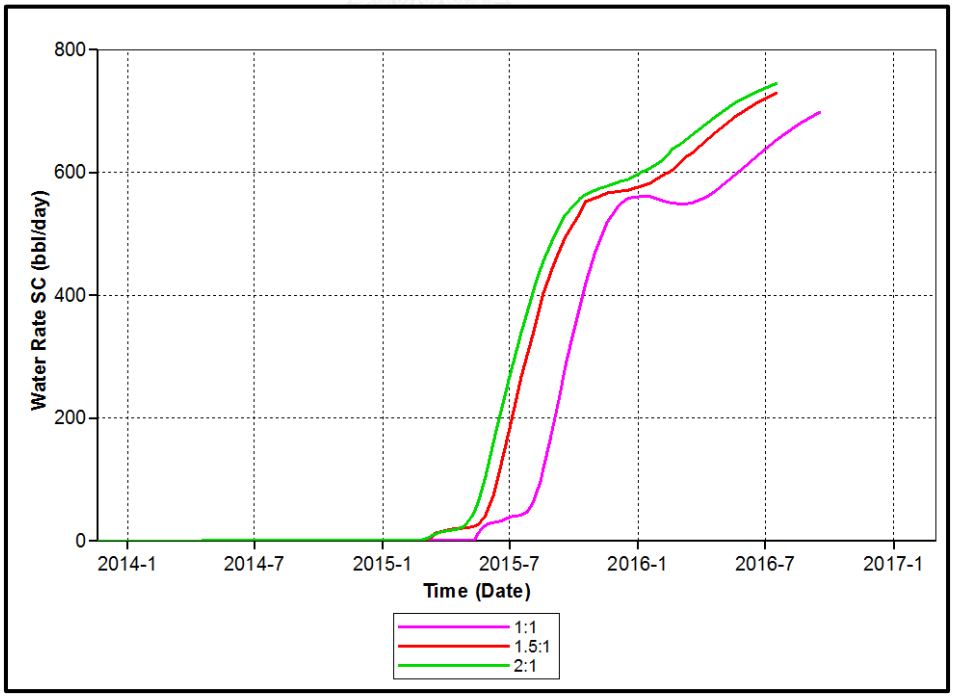

Figure 5.31 Water production rates from different P-I ratios as a function of time

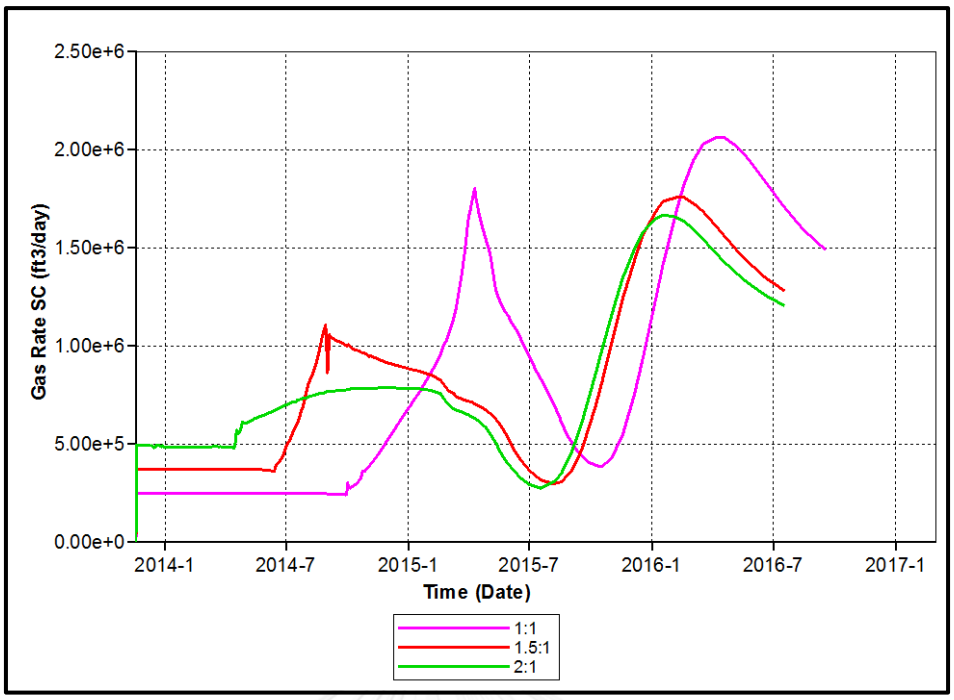

Figure 5.32 Gas production rates from different P-I ratios as a function of time

Table 5.3 Summary of results for different P-I ratios

Production-Injection ratio	1.0	1.5	2.0
Total production period (days)	1035	973	973
Cumulative oil production (MSTB)	610.27	607.78	611.36
Oil recovery factor (%)	59.32	59.39	59.74
Cumulative gas production (BSCF)	0.917	0.832	0.854
Cumulative water production (MSTB)	221.33	227.15	242.58
Slug size period (days)	559	483	462
Oil recovered per surfactant (STB/STB)	1,296	1,291	1,298

Oil saturation profile at the end of production is shown in 3-D views for both top-side and bottom-side views in Figure 5.33 for different P-I ratios and also water saturation profile is consecutively illustrated in Figure 5.34 at the end of production period.

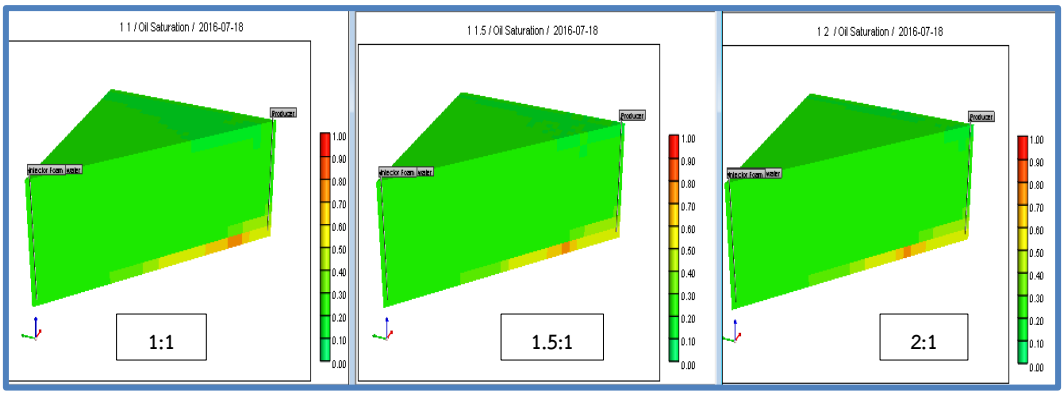

(a)

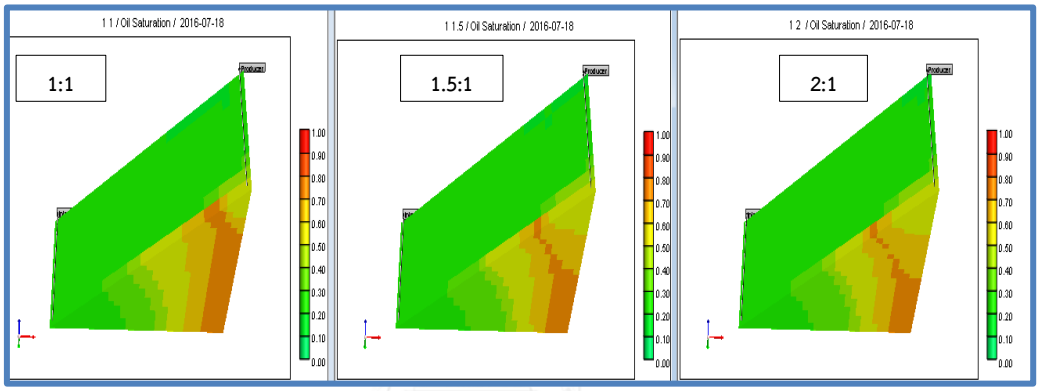

(b)

Figure 5.33 Oil saturation profiles at the end of production period for different P-I ratios showing a) top-side view and b) bottom-side view

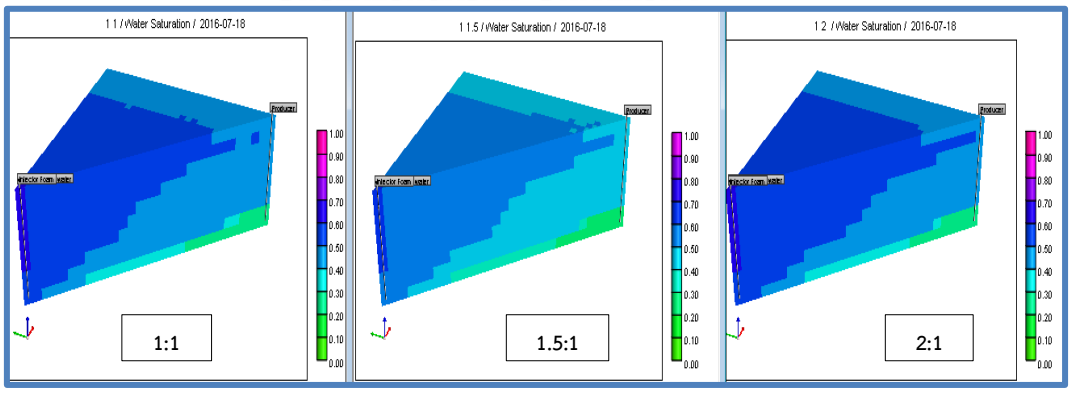

Figure 5.34 Water saturation profiles at the end of production different P-I ratios

Figures 5.33a and b, oil recovered by P-I ratio of 1.0 is slight less compared to P-I ratios of 1.5 and 2.0 when observing the bottom-side view that shows higher portion of orange color. Water saturation profiles do not show much different at the

end of production. However, advancement of chasing water is higher in case of P-I of 2.0 as nitrogen gas and surfactant solutions are switched to chasing water earlier. As production rate is increased, different pressure between injection well and production well increases, resulting in higher flow rate of fluids. As oil and water saturation profiles are detected at the end of production, dynamic change is hardly detected. Therefore, several plots with production time are performed. . Figure 5.35 illustrates oil recovery factor obtained as a function of time. Figure 5.36 illustrates oil recovery factor obtained from various P-I ratios as a function of time.

From Figure 5.36, it can be observed that there is a big gap between P-I ratio of 1.0 and 1.5. As desired injection rate cannot be attained together with smaller different pressure in case of P-I ratio of 1.0, displacement mechanism occurs slowly and hence, cumulative oil recovery factor increases slowly compared to other two cases where desired injection rate can be attained. Comparing between P-I ratio of 1.5 and 2.0, it can be seen that increase of oil recovery is faster in case of 2.0. As explained earlier, higher production rate results in fast depletion of reservoir pressure and hence, displacement mechanism occurs at higher rate. A plot between final oil recovery as a function of P-I ratio is shown in 5.36 before final decision.

จุฬาลงกรณ์มหาวิทยาลัย
Chulalongkorn University

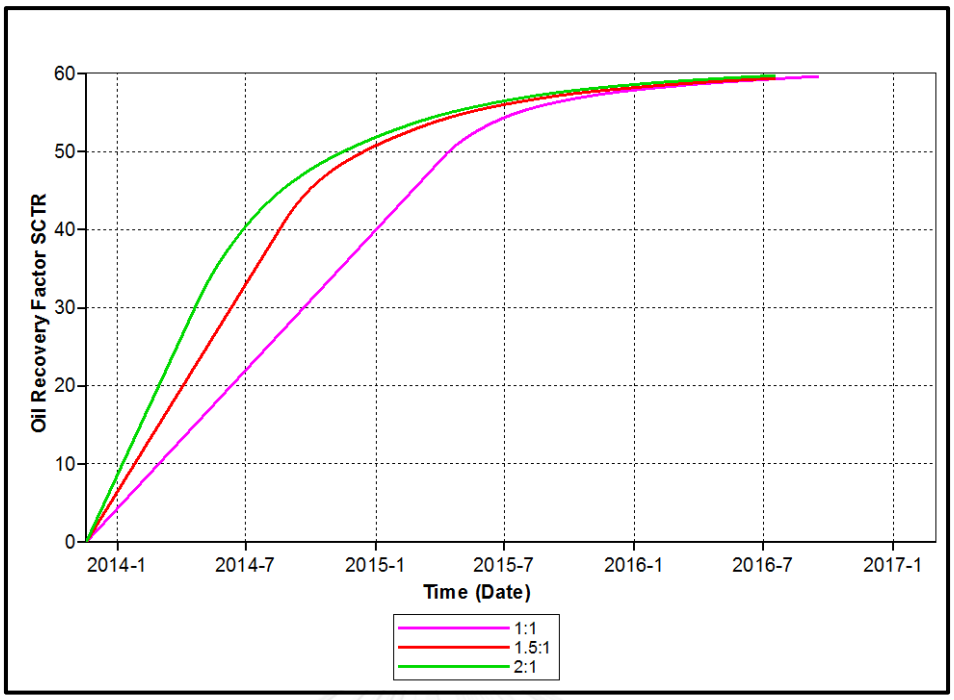

Figure 5.35 Oil Recovery Factors from different P-I ratios as a function of time

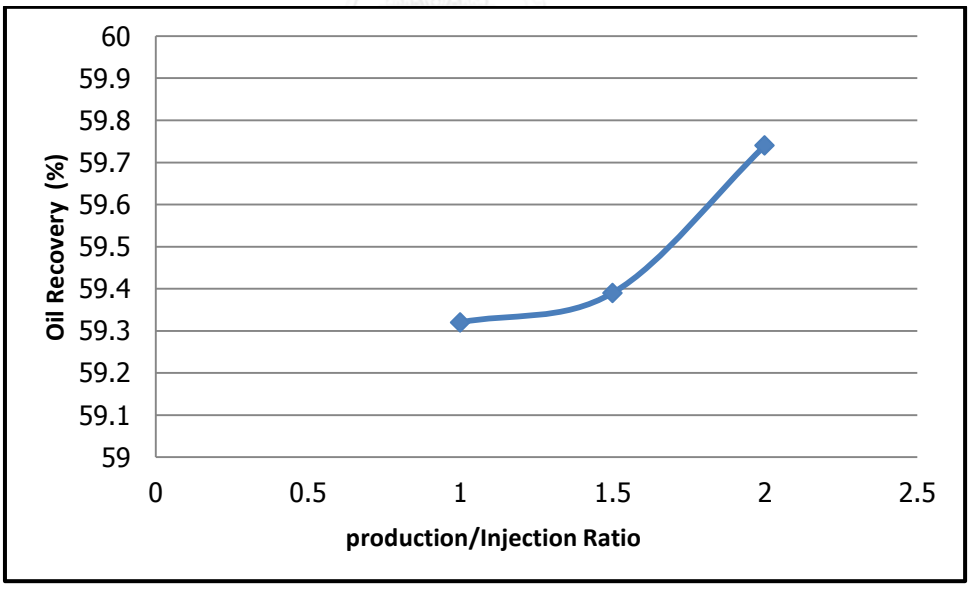

Figure 5.36 Oil recovery factors as a function of P-I ratio

The main purpose of adjusting P-I ratio is to maintain well bottomhole pressure since foam injection is performed in virgin reservoir where pressure is still high. Increasing of production rate helps to deplete high reservoir pressure, increasing

injectivity of both nitrogen has and surfactant solution. From Figure 5.36 final oil recoveries slightly changes. Nevertheless, higher P-I ratio tends to yield more oil recovery and also oil recovered per surfactant. But total production period is quite different in P-I ratio 1 and rest two are same. Even though oil recovered per surfactant in case of P-I ratio 1 and 2 is obtained more, P-I ratio of 1.0 could lead to bottomhole pressure of injection well above fracture pressure and P-I ratio of 2.0 will result in total production rate of 8,000 bbl/day (for a full flood pattern), this number is too high for reality and hence, P-I ratio of 1.5 is selected to help in partial depletion of reservoir pressure and improve fluid injectivity. A production rate of 1,500 bbl/day for a quarter of full pattern corresponds to total production rate of 6,000 bbl/day which is still reasonable number for real implementation.

5.1.6 Selection of Gas- Liquid Ratio

Gas-liquid ratio is operational factor that directly control foam quality that consecutively controls gas mobility and also water breakthrough which is possible when proper amount of nitrogen is mixed with right amount of surfactant. For example when high amount of nitrogen gas is co-injected with very small amount of liquid, light foams will be formed, which cannot resolve gravity overriding and gas channeling problems. If high surfactant solution is used with too small nitrogen gas, these fluids might not turn into foam, resulting in early breakthrough of surfactant solution as well as nitrogen gas

The study in this section aims to identify target gas-liquid ratio at reservoir conditions that will result in high oil recovery factor under minimum amount of surfactant consumption. In process of simulations, total fluid injection rate is 130,200 STB/D, P-I ratio 1.5, foam slug size is 0.3 PV. The chosen gas-liquid ratios are 0.6, 1.0, 1.5, 2.0, 3.0, 4.0 and 5.0. It is noted that, these gas-liquid ratios are expected gas-liquid ratio at reservoir conditions for entire study.

The 3-D view of lamella at day 492 for selected gas-liquid ratios is shown in Figure 5.37. In order to complete foam slug size, numbers of day in nitrogen gas and liquid injection are 406, 417, 437, 453, 472, 483 and 492 for gas-liquid ratio of 0.6, 1.0,

1.5, 2.0, 3.0, 4.0 and 5.0, respectively. As ratio of nitrogen gas increases, liquid portion decreases, resulting in reduction of surfactant quantity. As gas is very compressible fluid, higher gas-liquid ratios require more time to complete injection of 0.3 PV. Once injected slug reaches 0.3 PV, foam is chased by water. Summary of cumulative liquid injected, cumulative production and amount of surfactant consumed are shown in Table 5.4.

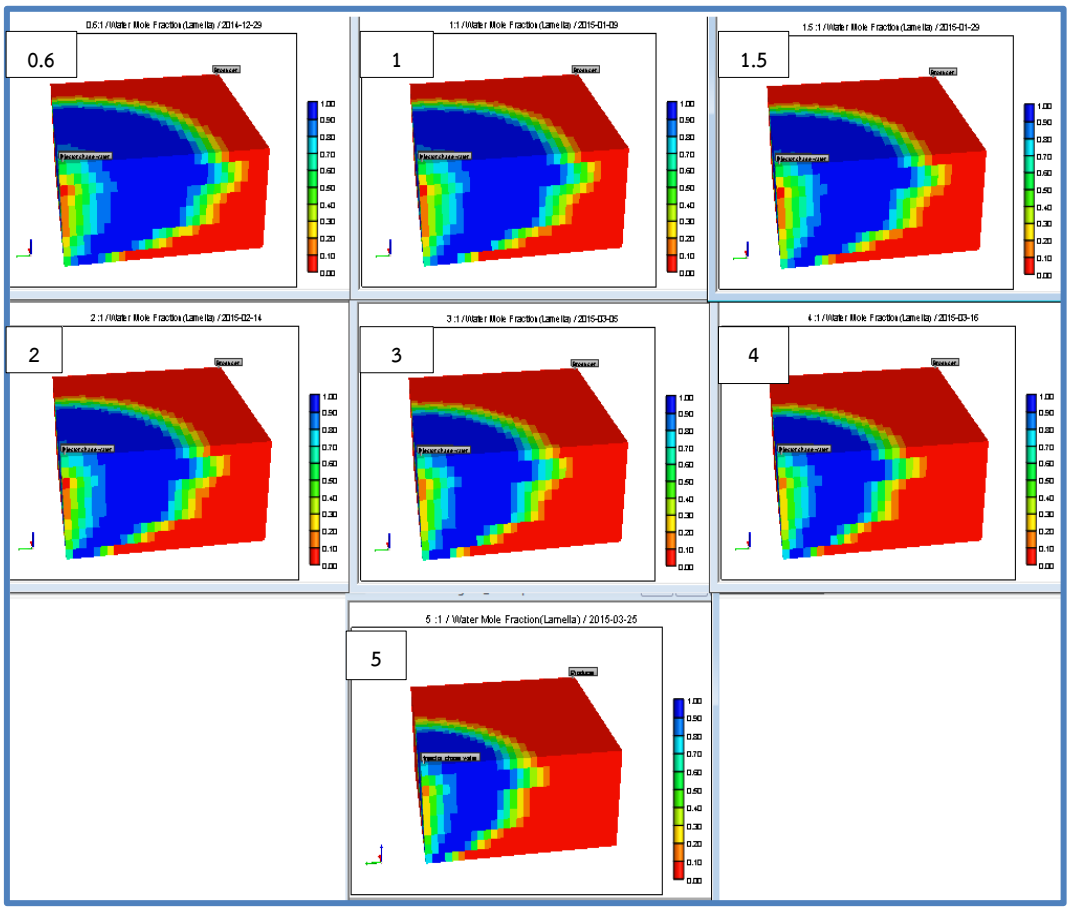

Figure 5.37 Lamella profile from different gas-liquid ratios at day 492

Oil, water, and gas production rates for different gas-liquid ratios are shown in Figures 5.38, 5.39 and 5.40, respectively. From Figure 5.38, oil production rates are maintained at constant rate of 1,500 bbl/day for 302, 327, 330, 313, 293, 285 and 279 days for ratios of 0.6, 1.0, 1.5, 2.0, 3.0, 4.0, and 5.0. Oil production rate is maintained constant for the longest time in ratios between 1.5 and 2.0. For the smallest gas-liquid ratio of 0.6, quantity of surfactant solution is high and that results in early

breakthrough of water at day 293 as seen in Figure 5.39. On the other hand, the highest gas-liquid ratio composing of large quantity of gas, gas cannot totally form foam, resulting in early breakthrough of gas at day 200 as can be observed from Figure 5.40. From the reasons of early breakthrough of surfactant solution and nitrogen gas, there should be gas-liquid ratio that mitigate both effects and could result in the highest oil recovery.

Table 5.4 Summary of simulation outcomes from different gas-liquid ratios

Gas-liquid ratio	0.6	1.0	1.5	2.0	3.0	4.0	5.0
Total production period (days)	840	840	791	870	943	973	1004
Cumulative oil production(MSTB)	611.18	615.43	615.43	615.50	611.57	607.78	601.87
Oil recovery factor (%)	59.80	60.13	60.14	60.22	59.76	59.39	59.15
Cumulative gas production (BSCF)	1.23	1.13	0.83	0.93	0.90	0.83	0.76
Cumulative water production (MSTB)	227.60	211.24	165.39	191.79	217.81	227.15	237.10
Cumulative liquid injection (MSTB)	230.80	204.19	174.77	150.07	118.00	96.60	75.77
Cum. surfactant injected(STB)	1154	1021	874	749	590	471	379
Slug size period (days)	406	417	437	453	472	483	492
Oil recovered per surfactant (STB/STB)	530	603	705	822	1,037	1,291	1,589

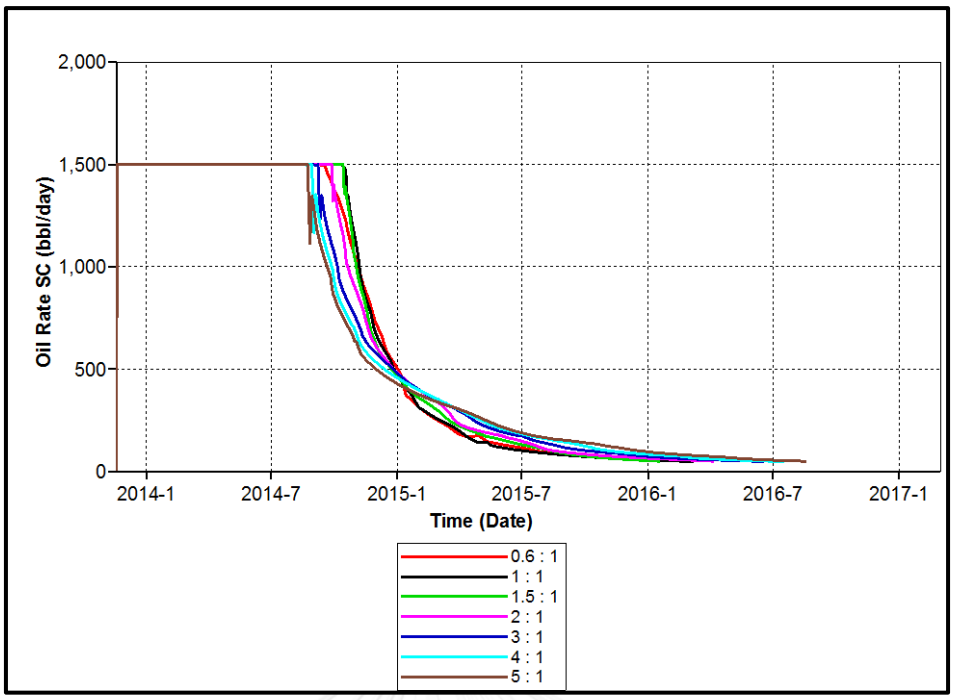

Figure 5.38 Oil production rates from different gas-liquid ratios as a function of time

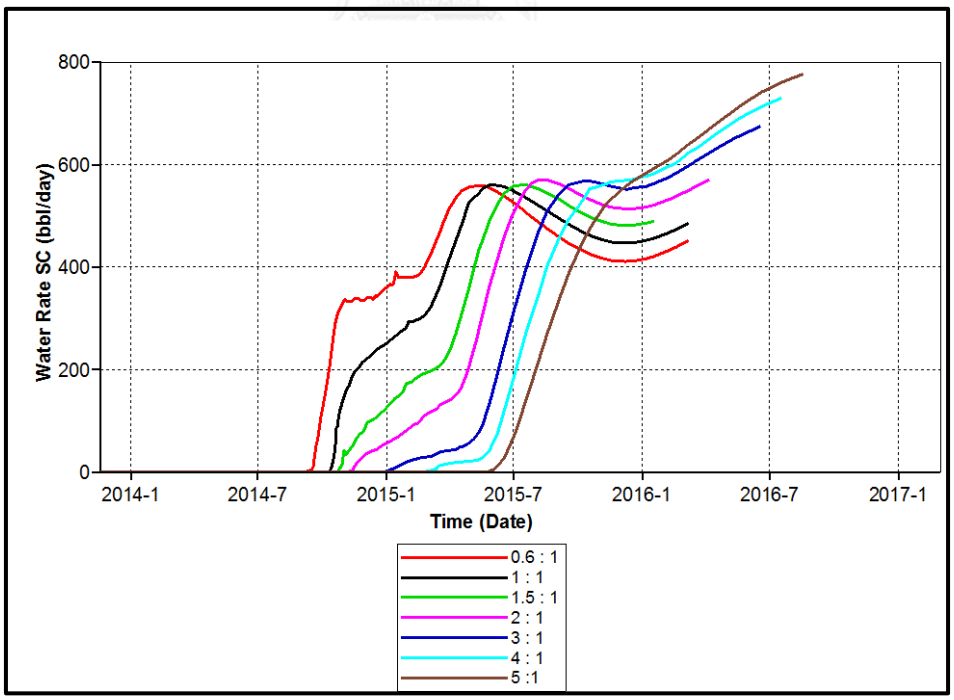

Figure 5.39 Water production rates from different gas-liquid ratios as a function of time

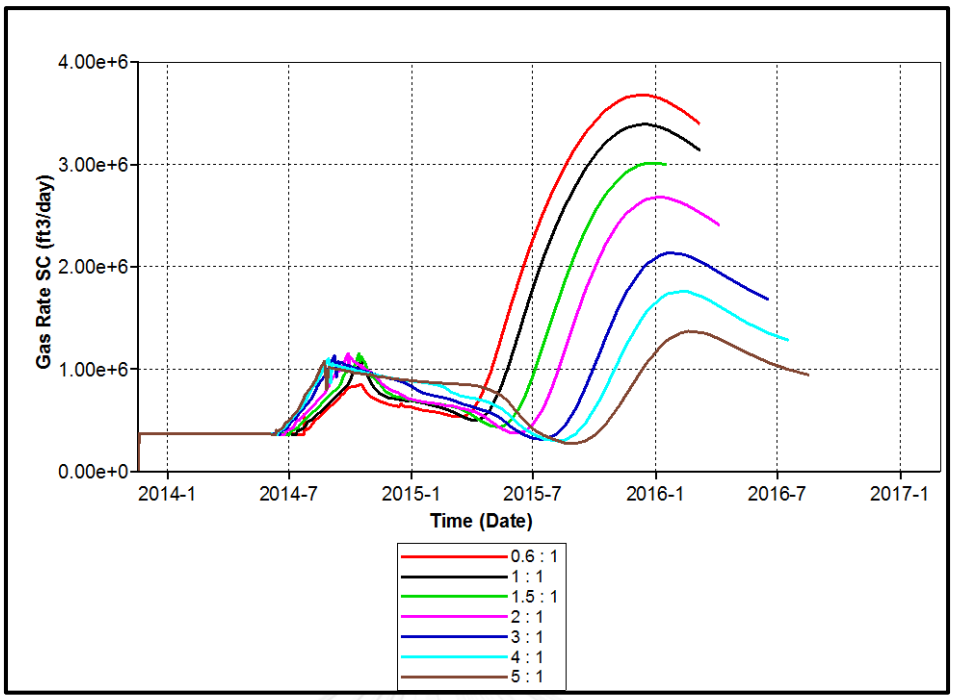

Figure 5.40 Gas production rates from different gas-liquid ratios as a function of time

As explained in initialized nitrogen-foam section, water and gas production rates show similar trends but with different breakthrough time and magnitude of rate. Higher water production rates are observed from this section compared to initialized case since different gas-liquid ratio is changed. First, water breakthrough is due to surfactant solution that does not undergo foam generation. Water production rate is small at first because surfactant solution breakthrough occurs only in high permeability layers on top of reservoir. Later, slug of surfactant solution reaches production well in all layers, causing higher water production rate. At foam breakthrough, water production rates decreases and before the end of production, chasing water reaches production well, re-increasing water production again. It can be obviously seen that, higher gas-liquid ratio results in smaller hump of water production during foam breakthrough period. This can be explained that, higher gas-liquid ratio yields quite low amount of foam. Amount of nitrogen gas that is released after foam breakthrough is also small as can be seen in Figure 5.40.

Relationship between oil recovery factor and time for various gas-liquid ratios is shown in Figure 5.41. From the figure, it can be seen that most gas-liquid ratio

yields almost the same final oil recovery factor. But due to different oil production rates, oil recovery is slightly different with time. From the figure, it can be obviously seen that lower gas-liquid ratio tends to yield higher oil recovery within shorter time.

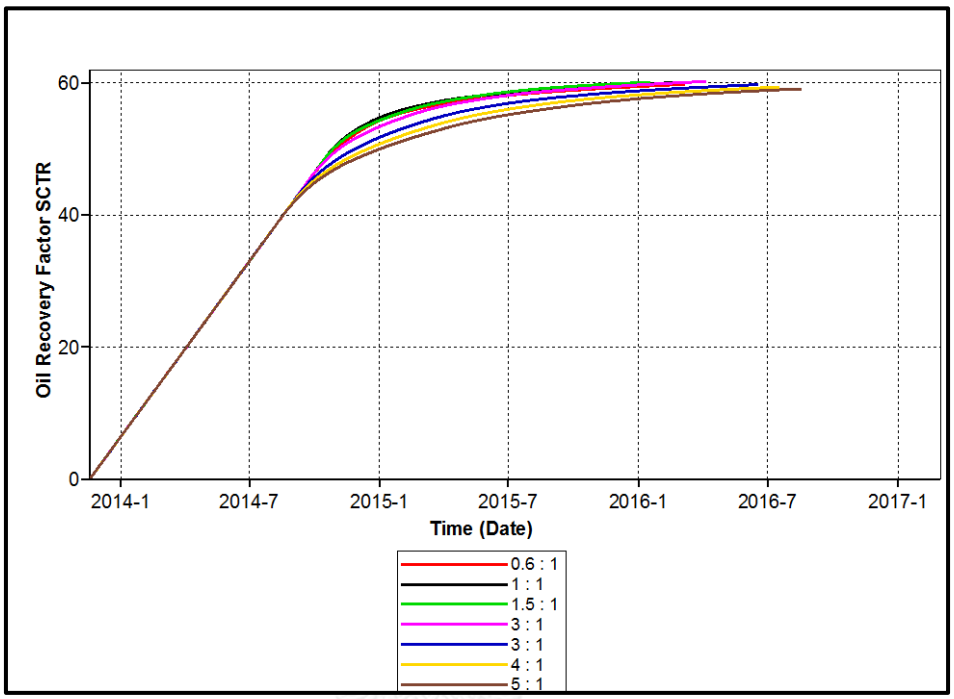

Figure 5.41 Oil recovery factors from various gas-liquid ratios as a function of time

จุฬาลงกรณ์มหาวิทยาลัย
CHULALONGKORN UNIVERSITY

As gas-liquid ratio is varied in this study, it is obvious that amount of surfactant is differentiated. A plot of oil recovery factor against cumulative surfactant solution is illustrated in Figure 42.

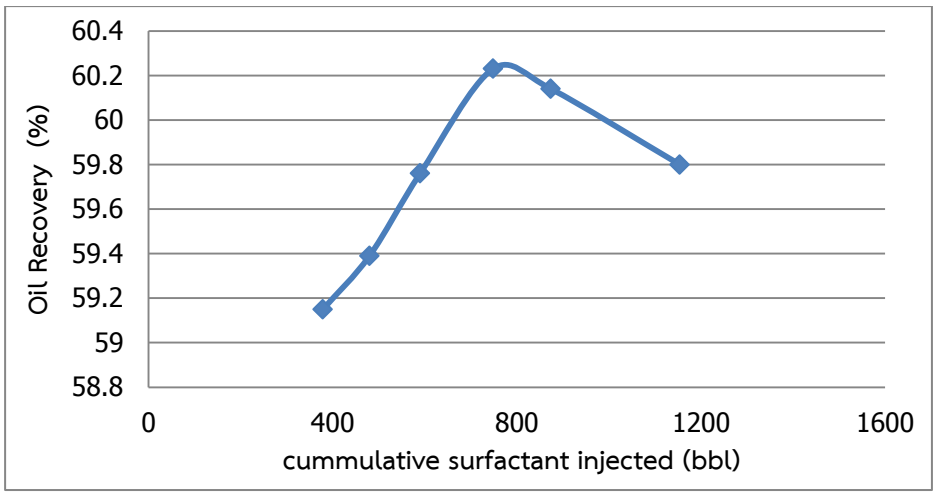

Figure 5.42 Oil recovery factor as a function of cumulative surfactant injected

From Figure 5.42, it can be seen that oil recovery factor increases with amount of surfactant solution or reduction of gas-liquid ratio. However, oil recovery starts to decrease when cumulative surfactant injected is higher than 800 bbl. The highest oil recovery is obtained from gas-liquid ratio of 2.0. Higher amount of surfactant solution leads to less oil recovery because nitrogen gas volume is too small and too much surfactant solution causes higher water production. As explained previously, too small and too high gas-liquid ratios might cause in improper foam quality and foam amount. From this study, gas-liquid ratio of 2.0 is selected and is used for the following steps.

5.1.7 Selection of Slug Size

Slug size is quantity of cumulative displacing fluid required to displace oil in the reservoir. Commonly used slug size is smaller number since to continuous injection would increase capital investment controls this factor. After smaller pore volume is injected, chasing water is followed until the end of oil production period since water is abundant (sea water or produced water). In this section, slug size is varied from previously fixed value of 0.3 PV. Several technical papers review different slug size for different techniques varying from 0.1 to 0.9 PV. Higher slug size is applied to the case of heavy oil where displacement requires a huge amount of additional

energy. As this study is mainly focused on light oil, a few percentage of total PV is required.

This section is performed to selected proper slug size that yield high oil recovery and at the same time, consumes to small amount of surfactant. To achieve this selection, six cases of single slug size including 0.1, 0.2, 0.25, 0.3, 0.4, and 0.5 are performed with selected parameters from previous sections which are fluid injection rate 1,000 rb/D, P-I ratio 1.5, and gas-liquid ratio 2.0. Each slug size is injected at varied total duration with different cumulative fluid in barrels to reach to particular pore volume. Complete foam generation in reservoir from different slug sizes is shown in Figure 5.43. Total times required to complete whole single slug are 152, 304, 379, 453, 601, 752 days for 0.1, 0.2, 0.25, 0.3, 0.4, and 0.5. Cumulative fluid required is shown in Figure 5.44 and summary of values in are in Table 5.5.

Table 5.5 Summary of simulation outcomes for different slug size

Slug size (PV)	**0.1**	**0.2**	**0.25**	**0.3**	**0.4**	**0.5**
Total production period (days)	912	851	876	870	870	894
Cumulative oil production(MSTB)	589.83	607.97	613.65	616.43	620.55	623.33
Oil recovery factor (%)	57.63	59.41	59.96	60.23	60.64	60.91
Cumulative gas production (BSCF)	0.50	0.78	0.91	0.92	0.76	0.60
Cumulative water production (MSTB)	427.93	265.04	235.11	191.78	142.64	119.12
Cumulative liquid injection (MSTB)	50.69	101.38	126.39	151.07	200.43	250.79
Cum. surfactant injected(STB)	254	507	632	755	1002	1254
Slug size period (days)	152	304	379	453	601	752
Oil recovered per surfactant (STB/STB)	2,322	1,200	971	817	620	498

จุฬาลงกรณ์มหาวิทยาลัย
Chulalongkorn University

From Figure 5.43 size of generated foam is increased with foam slug. Advancement of foam with larger foam slug size is affected from reservoir heterogeneity, causing higher instability of flood front.

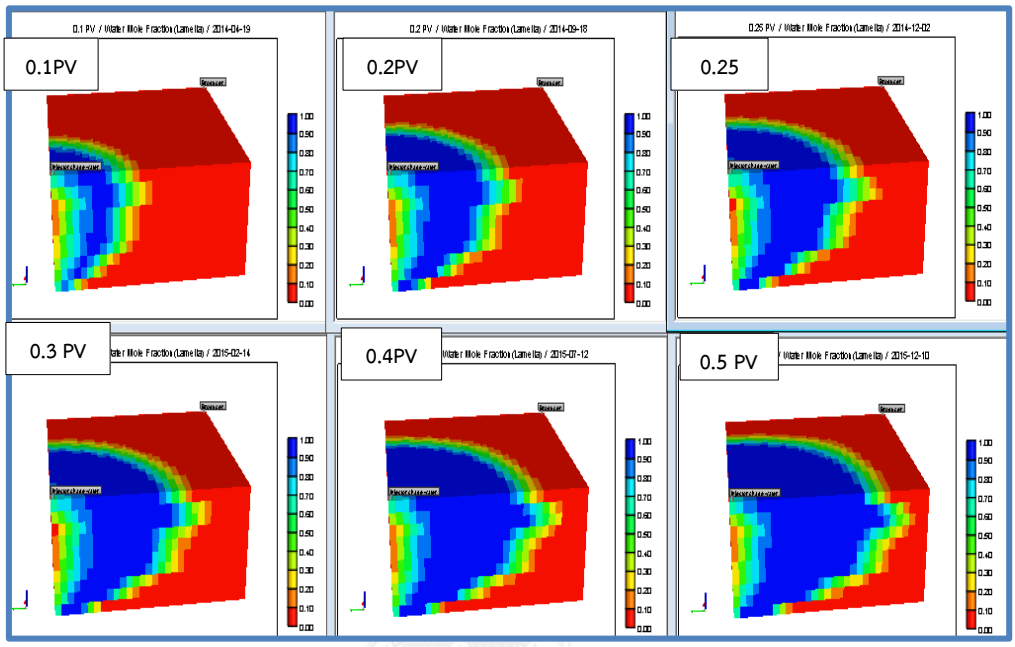

Figure 5.43 Lamella profiles from different slug sizes at duration required to complete foam slug size

จุฬาลงกรณ์มหาวิทยาลัย
Chulalongkorn University

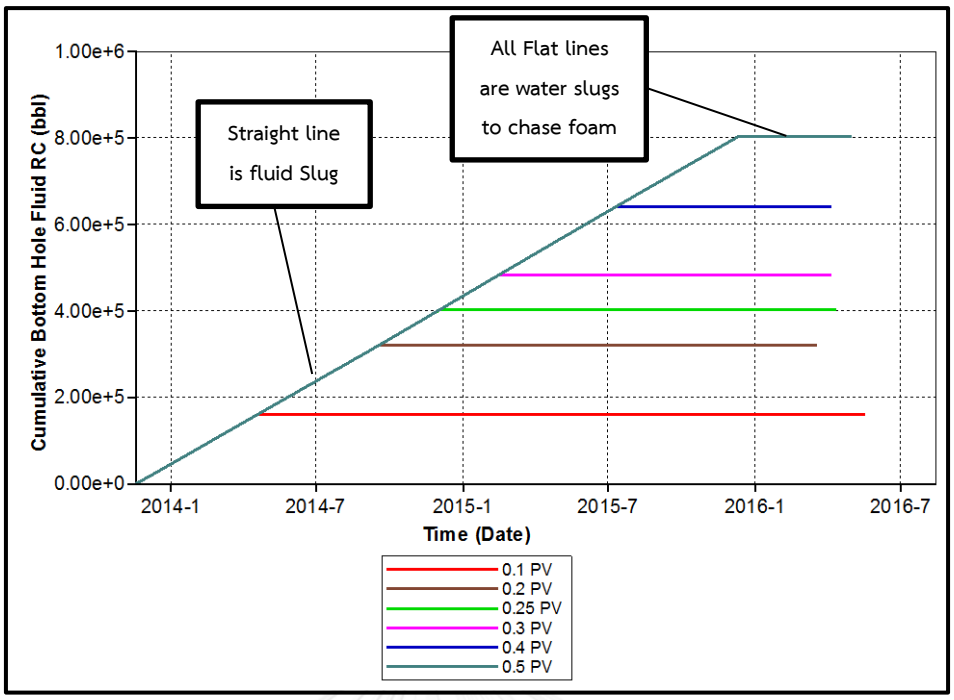

Figure 5.44 Cumulative bottomhole fluids injected for different slug sizes as a function of time

Oil and water production rates are graphically shown in Figures 5.45 and 5.46, respectively.

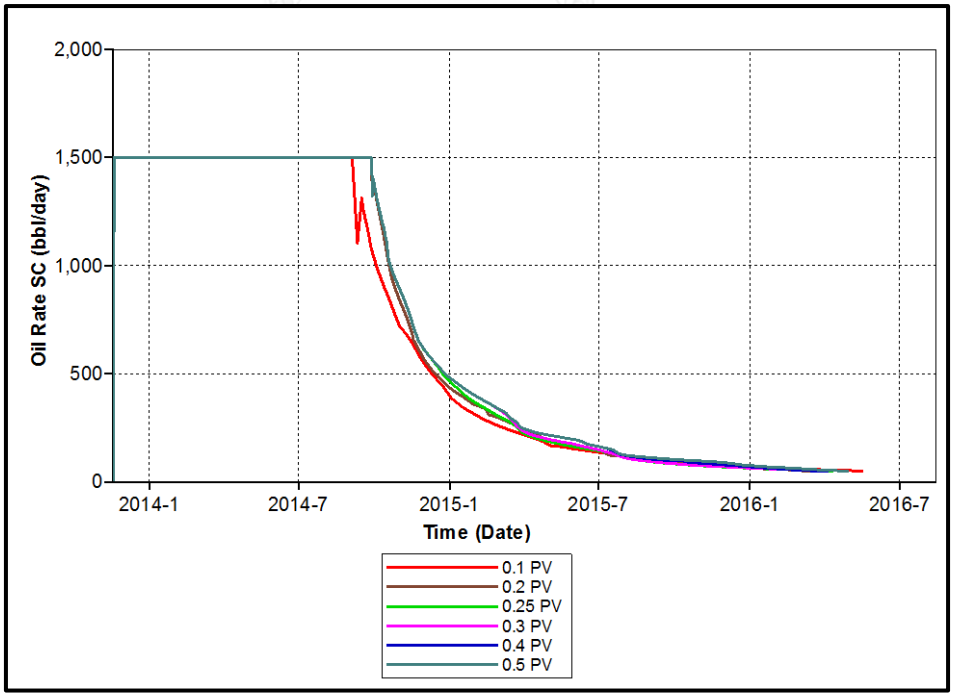

Figure 5.45 Oil production rates from different foam pore volumes as a function of time

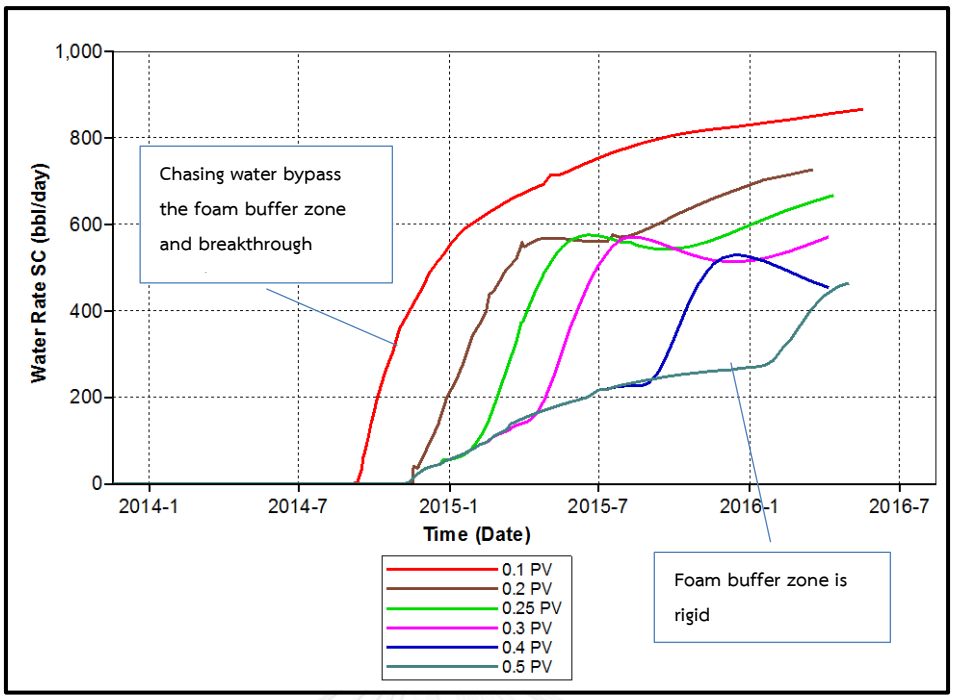

Figure 5.46 Water production rates from different pore volumes as a function of time

From Figure 5.45, oil production rates are mostly the same in all case, remaining constant for 290 days for 0.1 PV, 313 days for 0.2 and 0.25 PV, and 314 days for 0.3, 0.4 and 0.5 PV. Oil production rates are almost the same after declining. From water production rate in Figure 5.46, water starts to be produced from 293days in 0.1 PV which is the same date of drop of oil production rate. An interesting observation in this case is that there is no fluctuation of water production rate. This is due to small pore volume cannot maintain mobility control buffer. As chasing water is kept injected, this water bypasses small pore volume of foam and breakthrough together. Figure 5.47 illustrates breakthrough of lamella in case of 0.1 PV compared to 0.3 PV. Small foam slug leaves upper layers for water to bypass. The foam breakthrough therefore, cannot be seen by water production rate. Hence, too small foam slug should not be selected since it cannot form a buffer zone when chasing water is injected. Water production rates for higher slug size starts to show fluctuation in rates due to arrival of foam slug and chasing water slug.

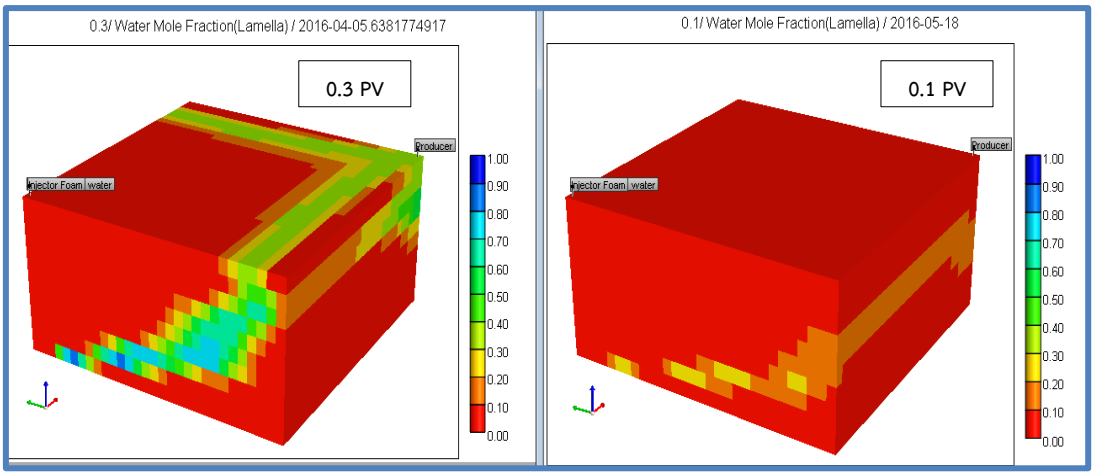

Figure 5.47 Comparison between lamella breakthroughs in cases of 0.1 and 0.3 PV

Oil saturation profiles after total foam is injected for each slug size are shown in Figure 5.48. Oil saturation profiles clearly show that as slug size increases, remaining oil is decreased. As explained earlier, smaller slug size cannot control mobility of injectant effectively. Hence, oil cannot be swept especially in lower layers of reservoir. Water saturation profiles at the end of production shown in Figure 5.49 also show that chasing water breakthrough occurs before well termination in case of 0.1 PV. As larger PV of foam is injected, chasing water advancement is smaller. This results in a benefit of less water production.

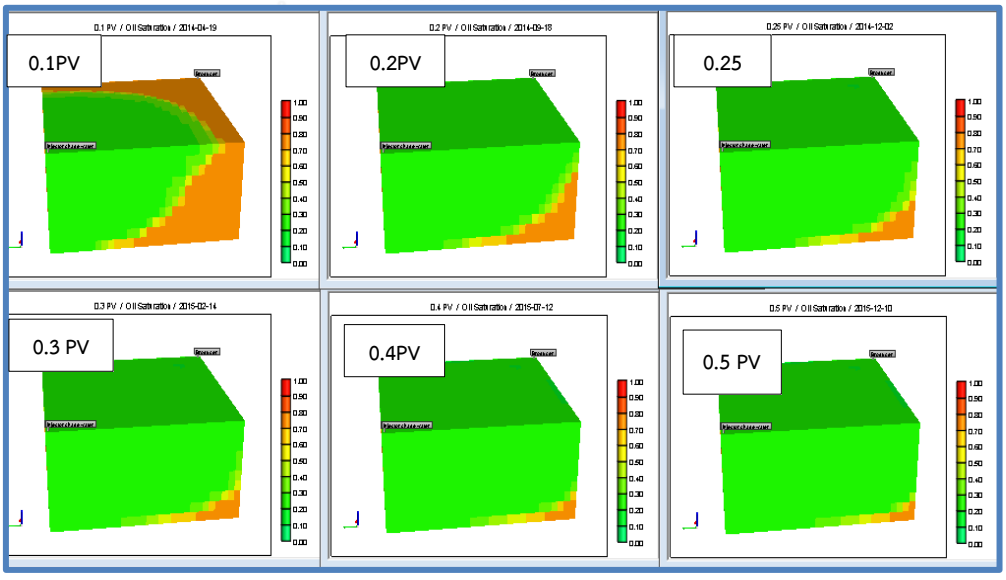

Figure 5.48 Oil saturation profiles from different slug sizes at complete foam injection

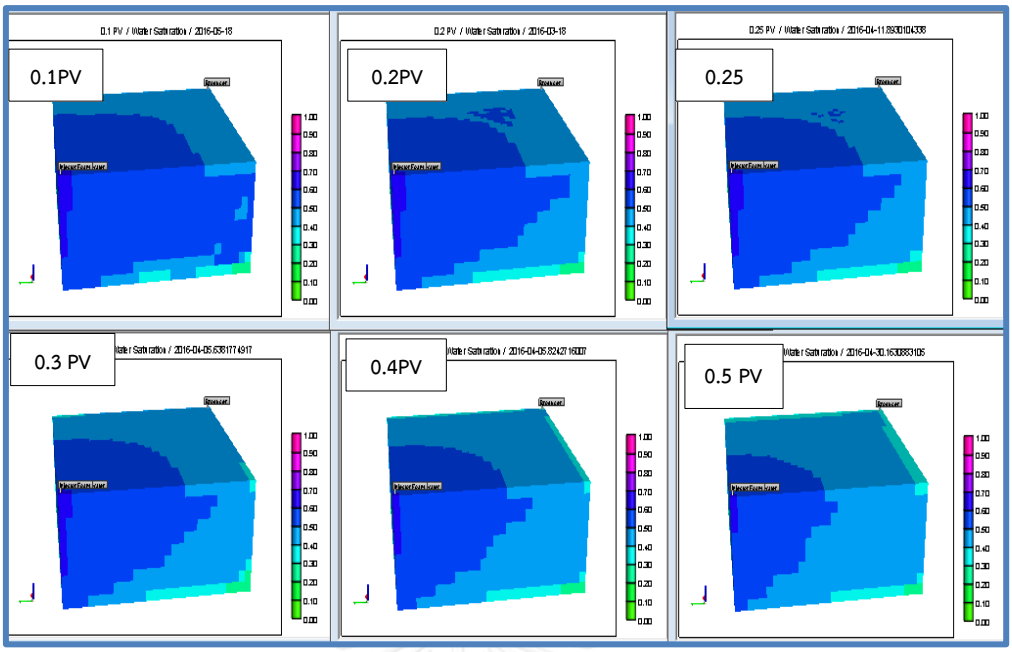

Figure 5.49 Water saturation profiles from different slug sizes at the end of production period

Oil recovery factors from different slug sizes are plotted with time and shown in Figure 5.50. From the figure, oil recovery factors are almost the same excluding the case of 0.1 PV. As explained earlier, this slug size is too small to create mobility control slug. In order to select proper slug size, final oil recovery factor is plotted versus slug size and shown in Figure 5.51.

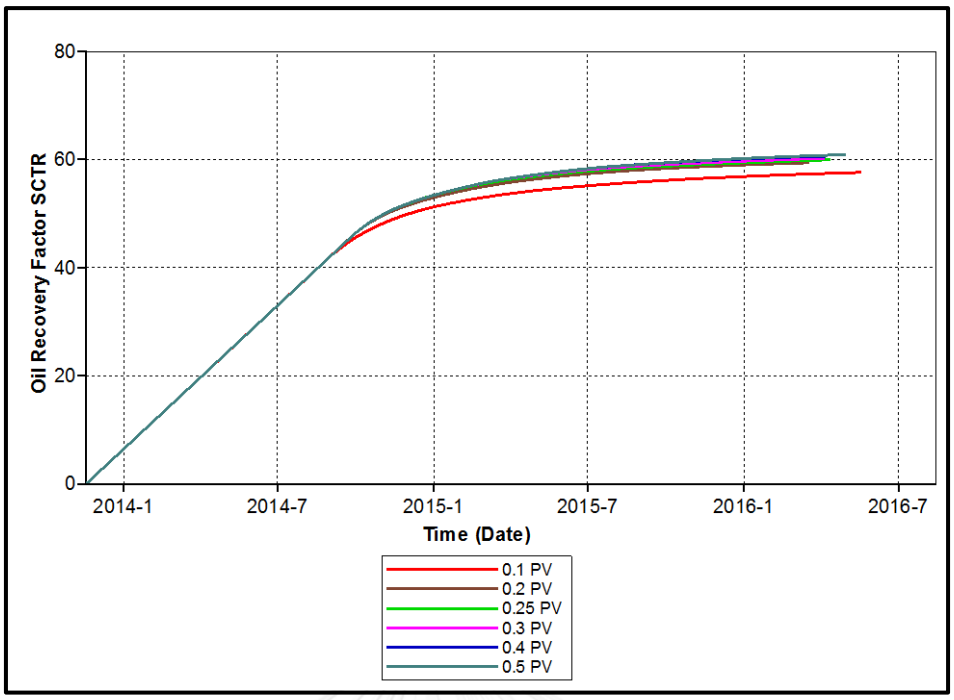

Figure 5.50 Oil recovery factor from different slug sizes as a function of time

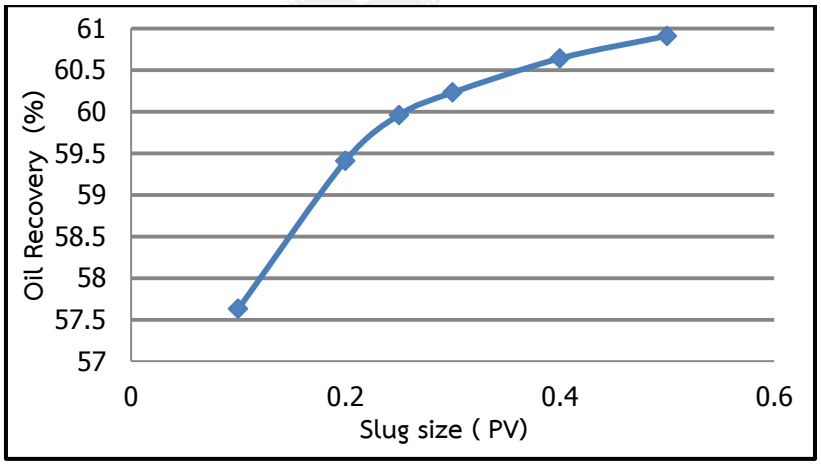

Figure 5.51 Oil recovery factor from different slug size as a function of foam slug size in pore volume

From Figure 5.51, it shows that oil recovery factor increases sharply from 0.1 to 0.2 PV and changing of tendency starts 0.25PV. This means that increment of oil recovery reduces from foam slug size of 0.25PV. So, this foam slug size is selected for the following steps.

At the end of operational parameter selection, the foam base case consists of total fluid injection rate 1000rb/D, production-injection ratio 1.5, gas-liquid ratio 2.0 and slug size 0.25PV. Oil recovery factor from this selected case is 59.96.

5.2 Study of Parameters

Study of parameter is performed on several reservoir uncertainties affecting output of the process. Uncertainty of reservoir cannot be deteriorated as it comes totally by nature. But adopting suitable methods will reduce these effects and help recover more oil. Heterogeneity is mainly discussed in this study. Co-effects of heterogeneity together with ratio of vertical to horizontal permeability, wettability condition, formation thickness are discussed. At the end, injection in different modes including double and triple slugs is considered.

5.2.1 Effect of Heterogeneity

Heterogeneity is very important factor that controls performance of any reservoir operation. Generally, heterogeneity of permeability is mostly concerned since it affects flow ability as well as productivity. Heterogeneous models are constructed to have average permeability equal to 150 mD and are generated by varying reservoir permeability in ten layers to represent multi-layered sandstone reservoir. Chosen heterogeneity values in this study are 0.2, 0.25, 0.3, 0.35, 0.4, and 0.45. Construction of various heterogeneous models is previously discussed in chapter IV. Selected operational parameters are gathered in this study.

First, lamella profiles of all heterogeneous models are tracked and in 2-D (diagonal between injector and producer) and 3-D views and shown in Figures 5.52a and b, respectively. Both figures are tracked when slug size of 0.25PV is completed injected into reservoir formation.

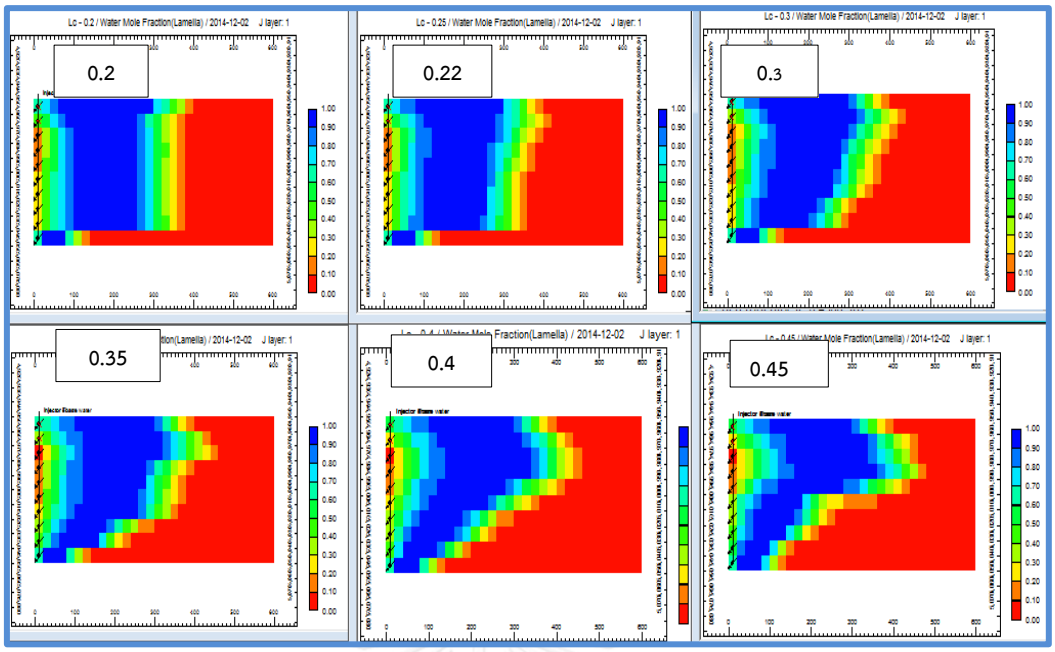

(a)

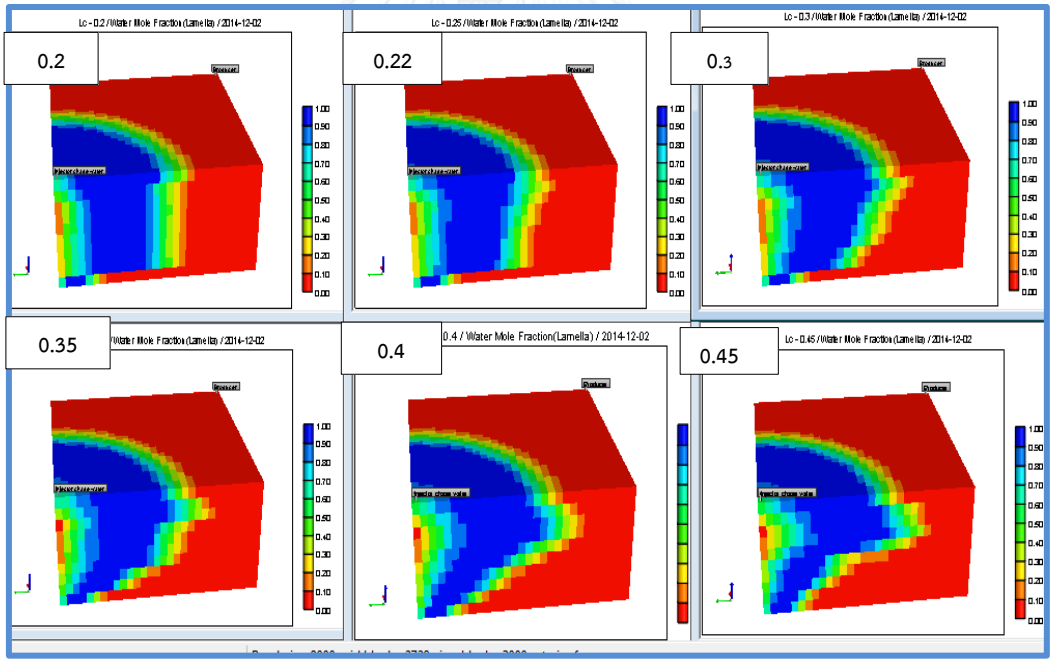

(b)

Figure 5.52 Lamella profile from models with different Lorenz coefficients when foam slug of 0.25 PV is injected a) 2-D view and b) 3-D view

From Figure 5.52a and b, it can be observed that foam can maintain stability of flood front efficiently in low heterogeneity values (L_c from 0.2 to 0.3) as flood front is maintained mostly vertical. This is due to uniformly distribution of heterogeneity. As Lorenz coefficient increases, flood front starts to deviate its vertical profile to a more overriding pattern as variation in permeability among layers is pronounced. In high permeability zones, generation of lamella is higher than lower permeability zones as fluids tend to propagate into higher permeability areas. Uneven foam front is clearly seen in reservoir model with L_c of 0.45 where top five layers possess high permeability and advancement of foam lamella is very high in these layers.

Oil production rates as a function of production time of all cases are shown in Figure 5.53 and it clearly shows that oil rate is maintained constant for different periods. The earliest drop of oil rate is found in case of high Lorenz coefficient value of 0.45 and the longest plateau rate is observed from case of Lorenz coefficient of 0.2. Nevertheless, crossover of oil production rates occurs. This can be explained that even in high heterogeneity value, oil production rate drops earlier, oil recovery from bottom layers as foam displaces oil from lowers section and hence, drop of oil production is gradual. Differently, foam displaces uniformly in low heterogeneity reservoir and hence, oil drops rapidly after foam breakthrough. It can be noticed that, foam flooding in low heterogeneity reservoir terminates much earlier compared to case with high heterogeneity values.

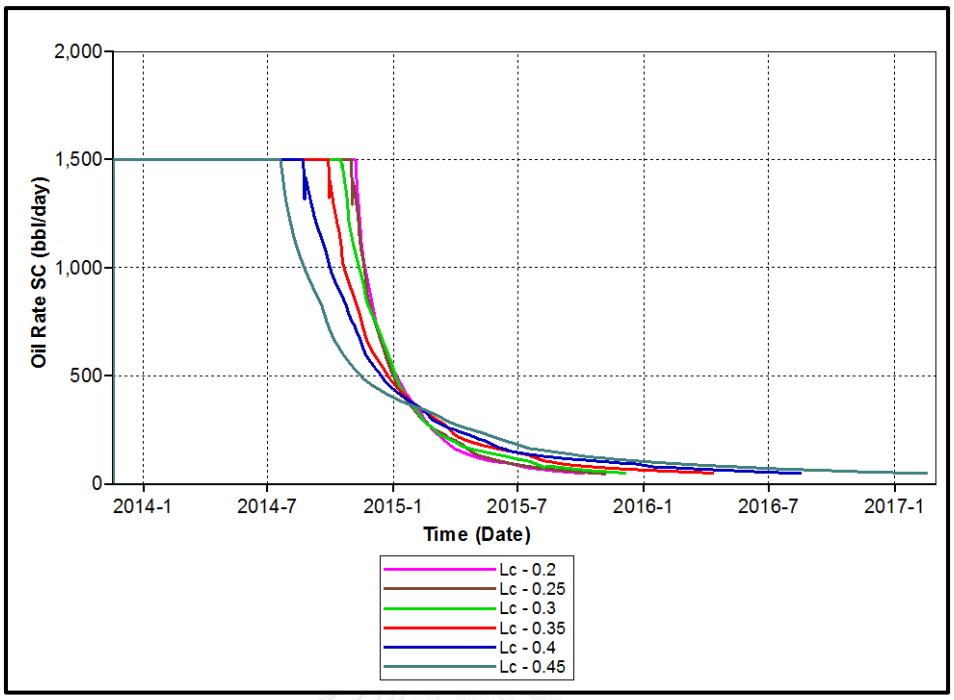

Figure 5.53 Oil production rates from different Lorenz coefficients as a function of time

Even through foam can displace oil in lower layers in case of high heterogeneity reservoirs, oil production profile at the end of production still show that abundant of oil saturation is still remained at bottom layers as illustrated in Figure 5.54. Longer production period cannot make foam to overcome low flow resistance in lower zone.

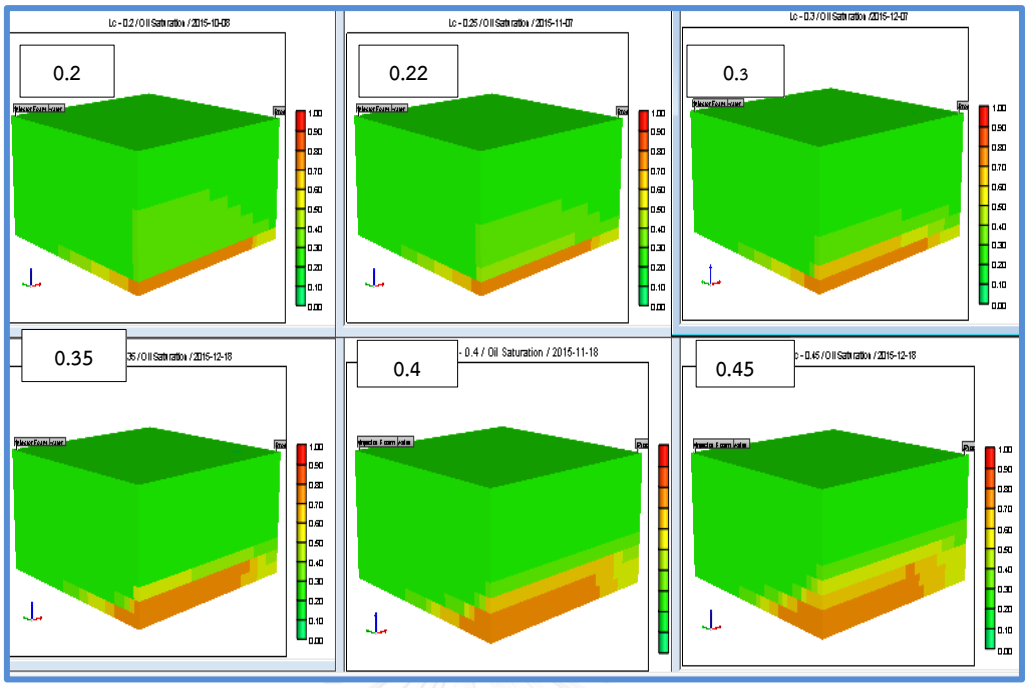

Figure 5.54 Oil saturation profile at the end of production period from different Lorenz coefficients

Evolution of cumulative oil recovery factor is shown in Figure 5.55 for reservoir with various Lorenz coefficients. From this figure, oil recovery factor tends to arrive at maximum value earlier in case of low heterogeneity. This characteristic is found when displacement mechanism is mostly piston-like. As explained previously, after foam breakthrough, most oil is produced and one of the constraints is attained quickly. Differently, oil recovery gradual increases in case of Lorenz coefficient of 0.45 and this takes much longer time to reach one of the constraints. In this study, all cases are terminated due to oil rate

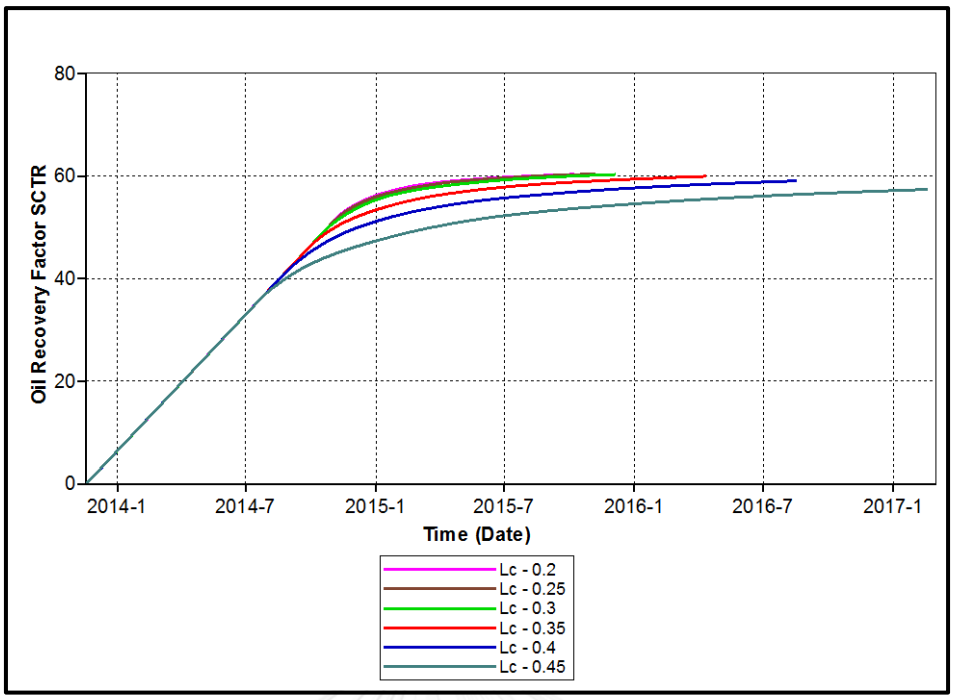

Figure 5.55 Oil recovery factor from various Lorenz coefficients as a function of time

As reservoir heterogeneity is high, early water breakthrough is occurred. Since production constraints can be minimum oil rate or maximum water cut, a mix flow between water from early breakthrough and gradual reduction of oil production rate cause longer time to reach production constraints. As production period increases, high amount of chasing water is produced. Table 5.6 summarizes simulation outcomes for all cases in this study.

Table 5.6 Summary of simulation outcomes from reservoirs with different Lorenz coefficients

Lorenz coefficient	0.20	0.25	0.30	0.35	0.40	0.45
Total production period (days)	689	719	749	876	1,004	1,188
Cumulative oil production (MSTB)	617.60	618.32	617.34	613.65	604.58	587.36
Oil recovery factor (%)	60.35	60.42	60.32	59.96	59.07	57.39
Cumulative gas production (BSCF)	0.362	0.447	0.576	0.906	1.208	1.386
Cumulative water production (MSTB)	120.15	136.82	153.00	235.11	325.67	493.24

Oil recovery factor obtained from Lorenz coefficient value of 0.2 is slightly lower than the case of 0.25. As these values of heterogeneity can maintain stability of flood front, longer production period can recover more oil. Reservoir with Lorenz coefficient of 0.25 where permeability is less uniformly distributed therefore causes an extension of production period. Higher Lorenz coefficient than 0.25 yields reduction of oil recovery with an increment of production period. Even though production period is increased, vertical sweep efficiency is decreased with an increase of Lorenz coefficient. It is agreed that foam is more suitable for heterogeneous reservoir but range of heterogeneity is still concerned as it may affect to production period as well as amount of water produced.

Figure 5.56 summarizes relationship between oil recovery factor and Lorenz coefficient. From the figure, oil recovery factors are maintained in the same range (approximately 60 %) at Lorenz coefficient values from 0.2 to 0.35. Higher heterogeneity than 0.3 will cause a rapid drop in oil recovery factor.

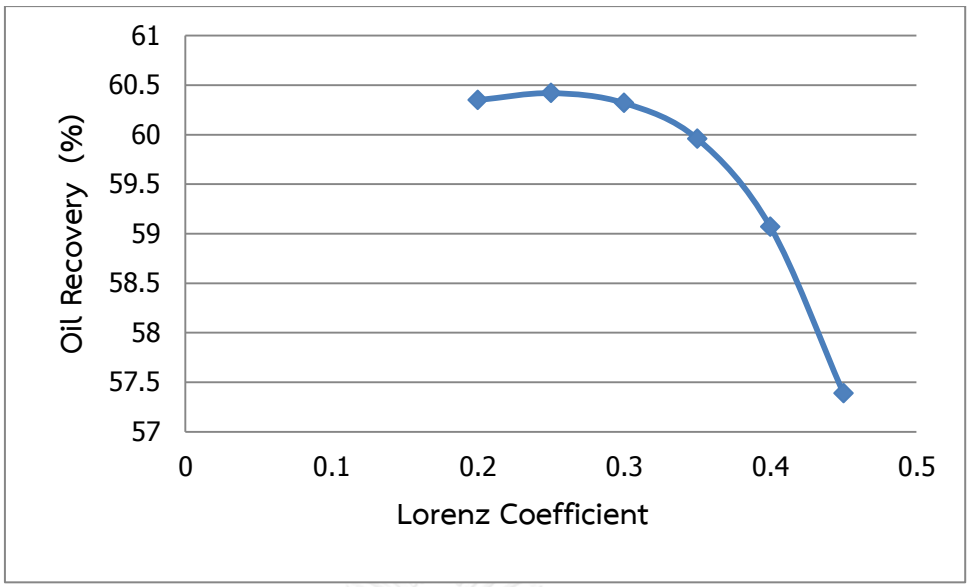

Figure 5.56 Oil recovery factors as a function Lorenz coefficient

From this study, it is still difficult to draw a line of maximum Lorenz coefficient that nitrogen-foam is still applicable. Nevertheless, results show that a rapid drop in oil recovery starts from Lorenz coefficient of 0.35. Longer production period to reach one of the constraints is observed when heterogeneity increases due to gradual reduction of oil production rate and gradual increment of water production rate. Nitrogen-foam flooding efficiently recovery oil in lower heterogeneity values up to value around 0.35. Isolation of high permeability zones is suggested when heterogeneity is too high to prevent early breakthrough of nitrogen-foam and water.

5.2.2 Co-effects of Heterogeneity and Ratio of Vertical to Horizontal permeability

Vertical permeability is an important parameter which controls displacement mechanism especially when mobility ratio is improper. Usually, different grain sizes causes variation in permeability and this might affect any displacement mechanism where big difference of density between displacing and displaced phases exists. This study aims to observe effects of permeability anisotropy (changing flow ability in vertical direction) along with heterogeneity on effectiveness of nitrogen-foam flooding. A study is performed on reservoir model with Lorenz coefficient value of 0.35. Change of vertical permeability to horizontal permeability ratio (k_v/k_h) causes

only a change of vertical permeability. In this study selected ratios are 0.05, 0.1 (base value), 0.2, 0.3, 0.5, and 1.0.

First, observation of lamella slug at the end of 0.25 pv foam injection is made over 2-D and 3-D views and is shown in Figures 5.57a and b. From Figure 5.61a, generation of lamella is almost the same for k_v/k_h from 0.05 to 0.5. But when vertical flow ability is as high as horizontal one, foam starts to displace downward as can be seen from smoother flood front. However, when consider 3-D view, it can be seen that since foam tends to flow downward due to effects of gravity together with high vertical permeability, displacement in top layer is decreasing with increment of vertical permeability. At the end of production, oil and water saturation profiles are pictured and shown in Figures 5.58 and 5.59 respectively.

จุฬาลงกรณ์มหาวิทยาลัย
Chulalongkorn University

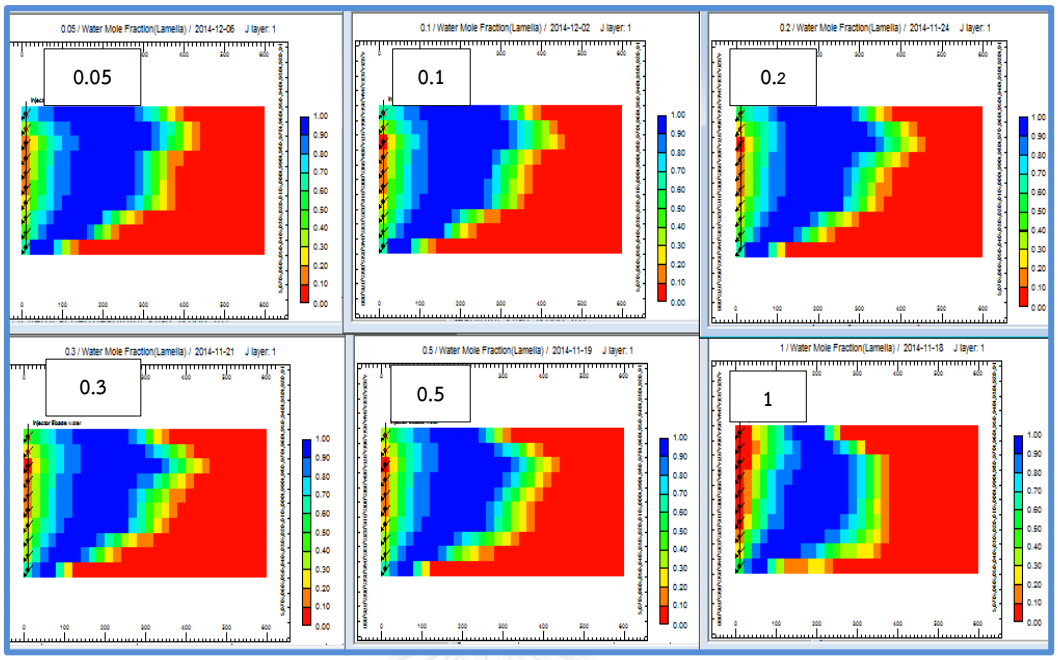

(a)

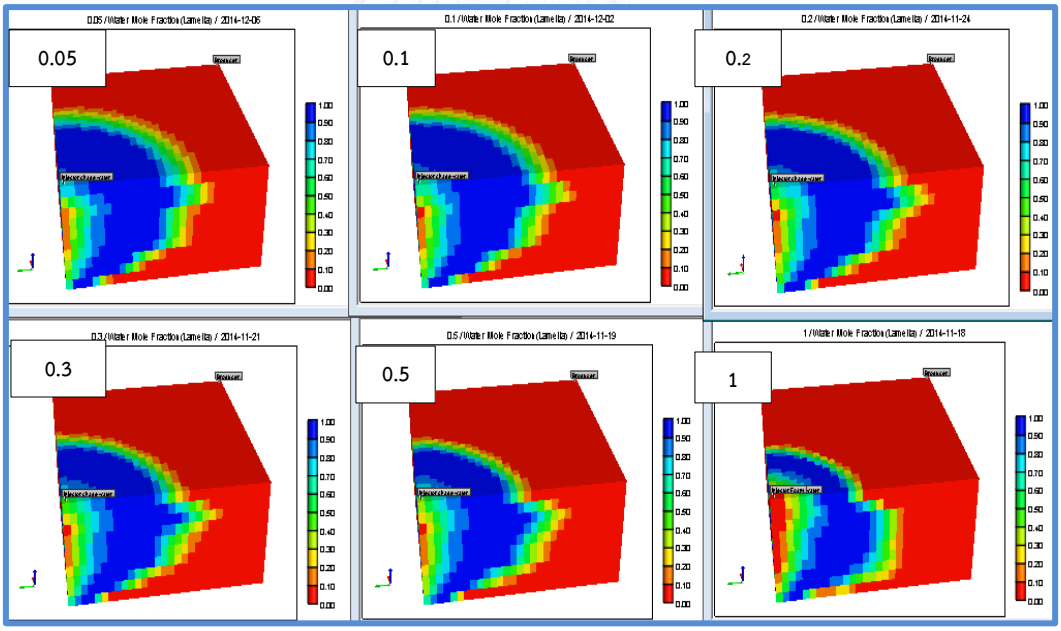

(b)

Figure 5.57 Lamella profiles from different ratios of vertical to horizontal permeability (a) 2-D view (b) 3-D view

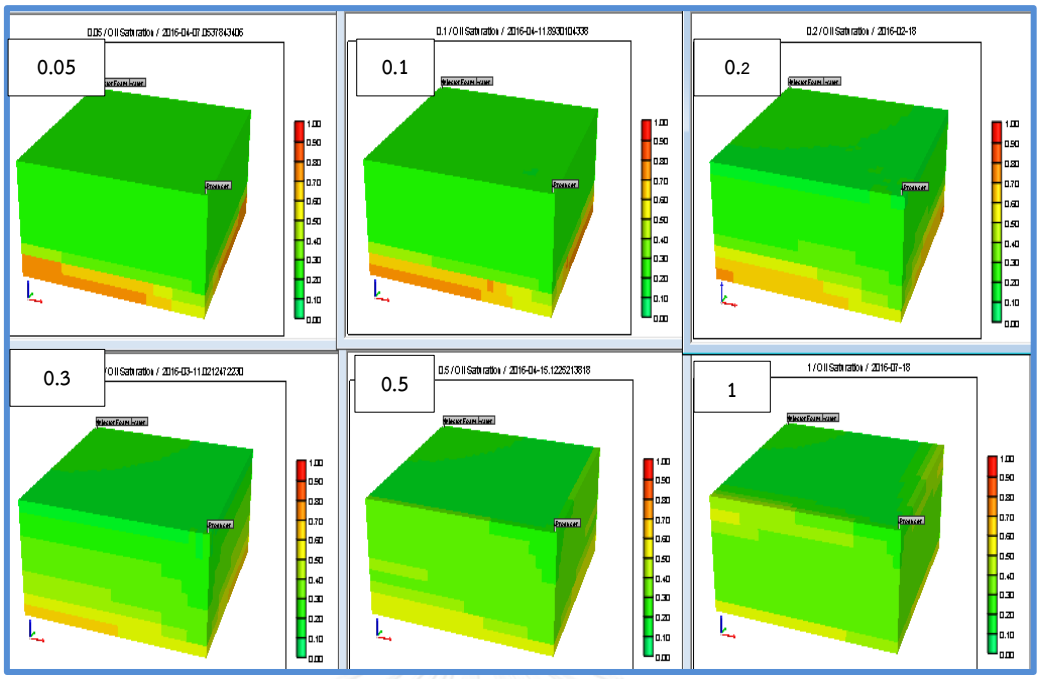

Figure 5.58 Oil saturation profiles from different ratios of vertical to horizontal permeability at the end of production

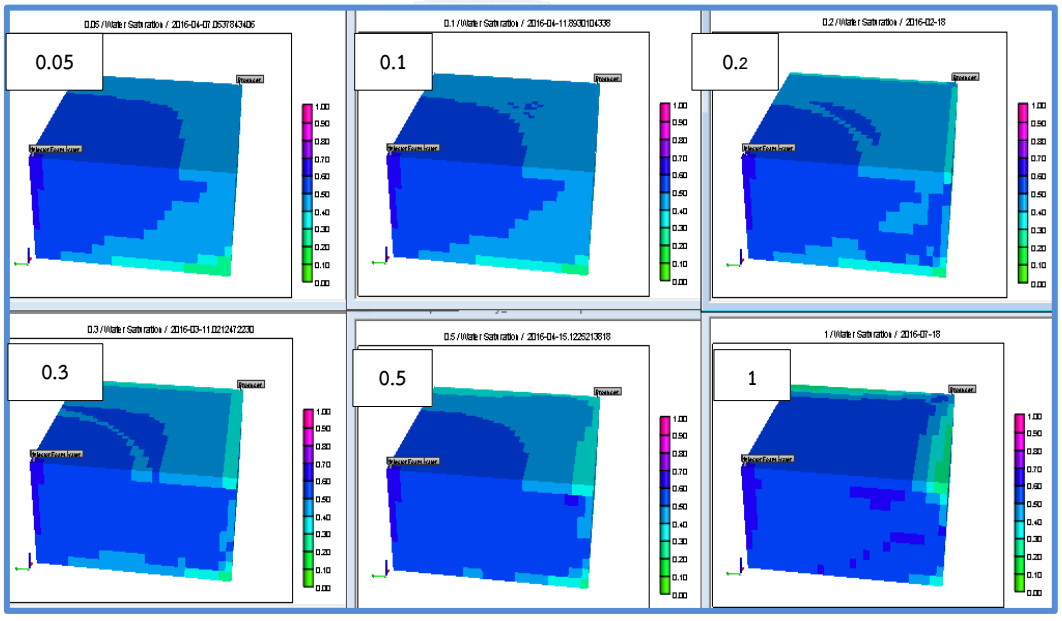

Figure 5.59 Water saturation profiles from different ratios of vertical to horizontal permeability at the end of production

From Figure, 5.58 it can be seen that remaining oil at bottom layers disappears with increment of vertical permeability. However, oil is remained in top layers instead and color profile from model with k_v/k_h ratio of 1.0 shows that higher oil saturation is remained in all layers of reservoir compared to k_v/k_h of 0.05. This could be implies that foam cannot form buffer slug, leaving chasing water to bypass. From Figure 5.59, water saturation profiles at the end of production shows that, chasing water occupies most volume of reservoir in chase of k_v/k_h ratio of 1.0. As foam is bypassed by chasing water, foam cannot work efficiently and oil saturation is remained. This could lead to longer production period to remove remaining oil and hence, high amount of chasing water is injected. In case of k_v/k_h ratios of 0.05 and 1.0, it can be seen that chasing water has not reached yet production well. This is because foam can be maintained and most oil is displaced by foam slug.

Oil production rate plotted as a function of time shown in Figure 5.60. As explained previously by saturation profiles. Total production period is shorter in case of low k_v/k_h ratio. Moreover, oil production rate is maintained for longer time in case of k_v/k_h ratio.

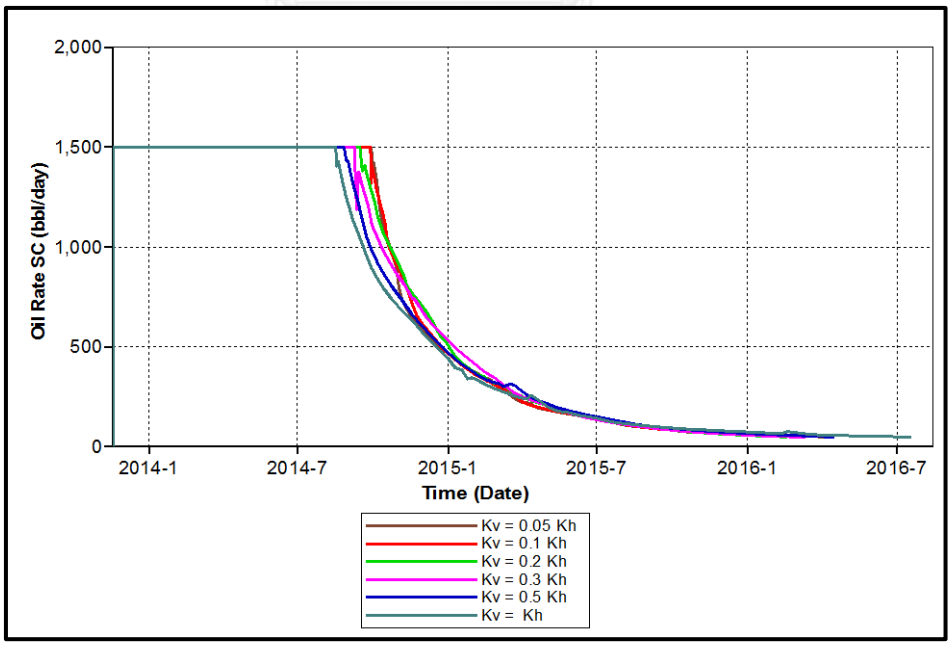

Figure 5.60 Oil production rates from different ratios of vertical to horizontal permeability as a function of time

Together with oil production rates, water and gas production rates are illustrated in Figures 5.61 and 5.62. From Figure 5.64, water breakthrough starts first in case of the lowest vertical permeability. As horizontal flow is favorable surfactant solution reaches production well first in lop layers. Breakthrough time decreases as surfactant solution percolates down to lower layers of reservoir. However, early drop of oil production rate is caused from gas breakthrough as shown in Figure 5.62. It can be obviously seen that, time when oil production rate drops and gas breakthrough is coincident.

When vertical permeability increases, pressure difference to maintain flow rate decreases. This results in average pressure to attain bubble point pressure first in case of high vertical permeability. Average reservoir pressure is illustrated in Figures 5.63 to confirm liberation of gas.

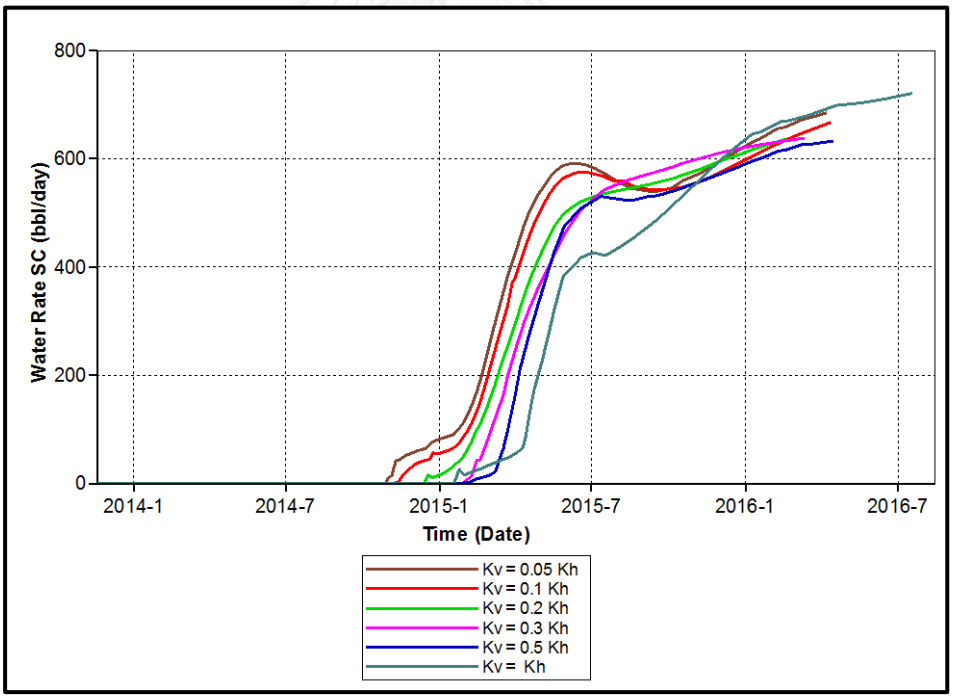

Figure 5.61 Water production rates from different ratios of vertical to horizontal permeability as a function of time

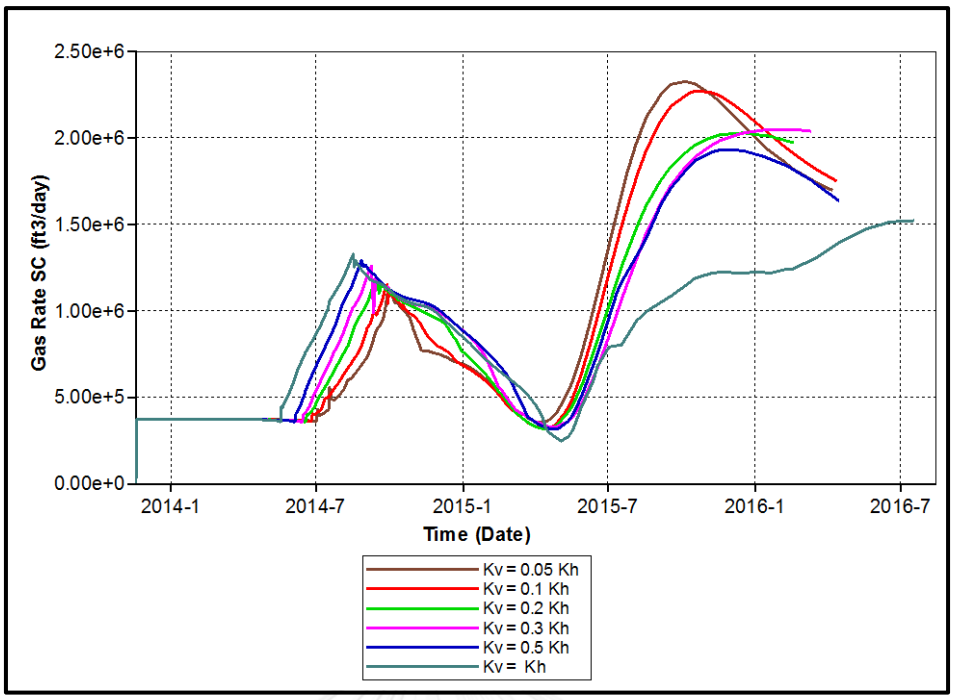

Figure 5.62 Gas production rates from different ratios of vertical to horizontal permeability as a function of time

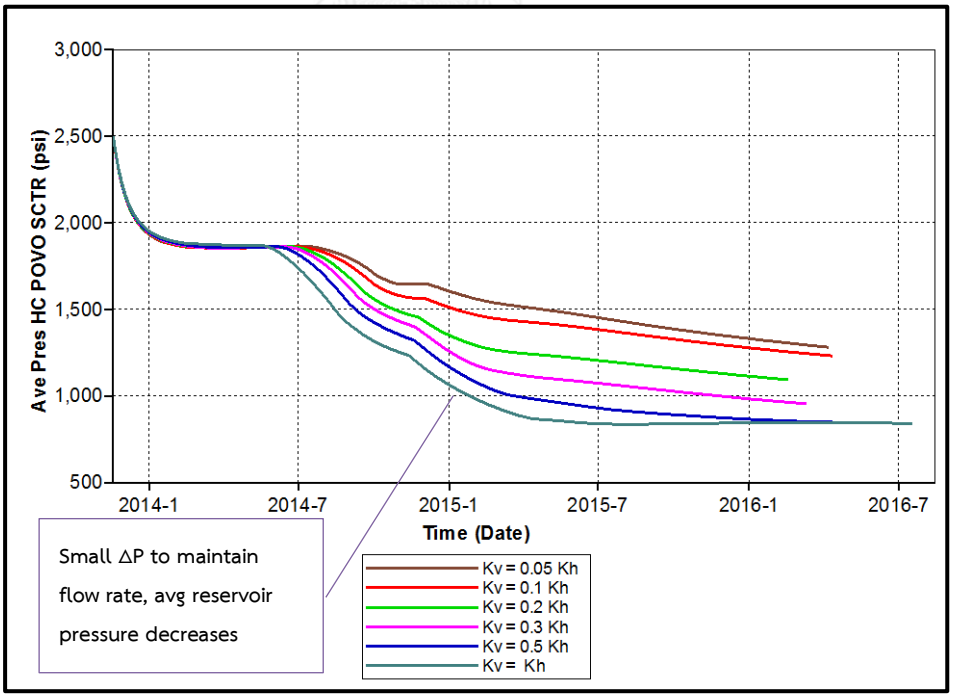

Figure 5.63 Average reservoir pressures from different ratios of vertical to horizontal permeability as a function of time

Nevertheless, it seems not only effect of reservoir pressure and solution gas liberation that affect nitrogen-gas foam flooding. Figures 5.64a and b are captured to compare between lamella profile and water saturation profile at certain time between k_v/k_h = 0.1 and 1.0. It can be seen that as foam slug is still in reservoir, chasing water tends to bypass this slug when k_v/k_h is 1.0. This results in less efficiency of foam and as a consequent, oil saturation remained after foam passes is not as low as case of k_v/k_h is 0.1.

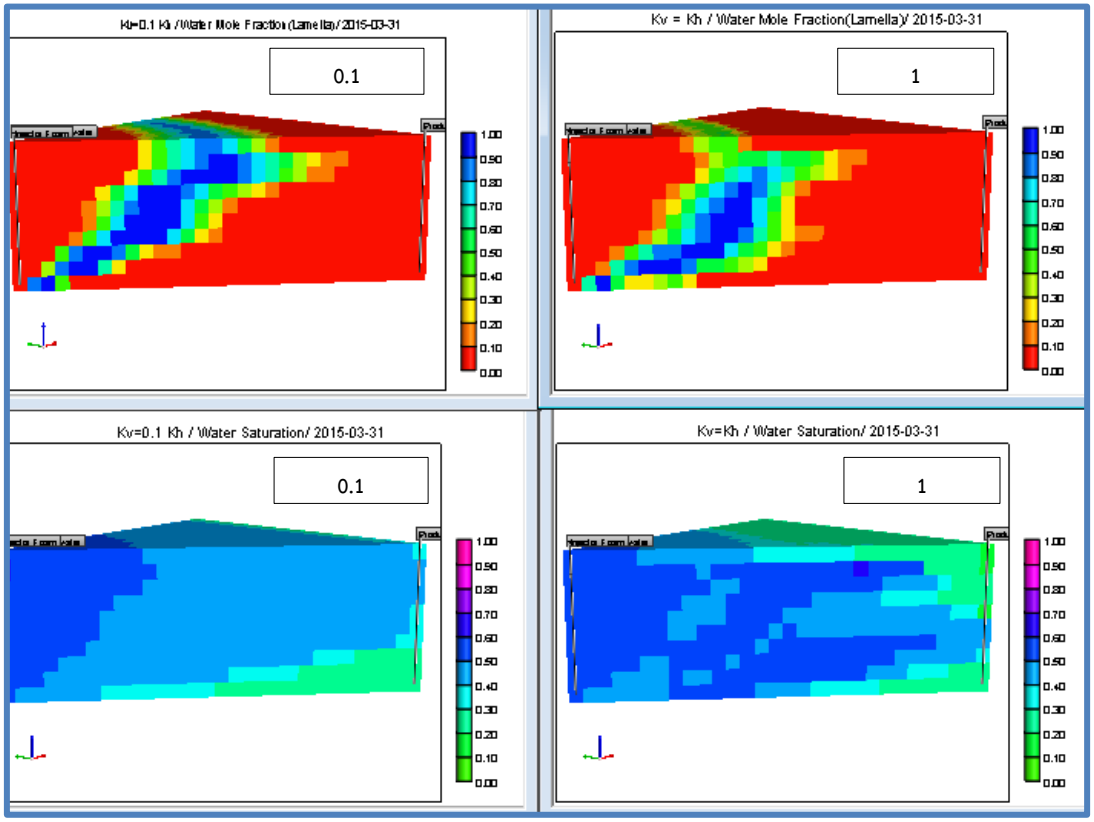

(a) (b)

Figure 5.64 Lamella profile and water saturation profile from different ratio of vertical to horizontal permeability a) 0.1 and b) 1.0

Simulation outcomes are summarized in Table 5.7 and oil recovery factor as a function of time is plotted shown in Figure 5.65.

Table 5.7 Summary of simulation outcomes from different ratios of vertical to horizontal permeability

Ratio of vertical to horizontal permeability	0.05	0.1	0.2	0.3	0.5	1.0
Total production period (days)	882	876	822	844	879	973
Cumulative oil production (MSTB)	610.73	613.65	611.95	607.44	597.41	588.58
Oil recovery factor (%)	59.58	59.96	59.79	59.35	58.37	57.51
Cumulative gas production (BSCF)	0.89	0.91	0.78	0.83	0.89	0.88
Cumulative water production (MSTB)	243.50	235.11	189.68	198.43	206.95	268.81

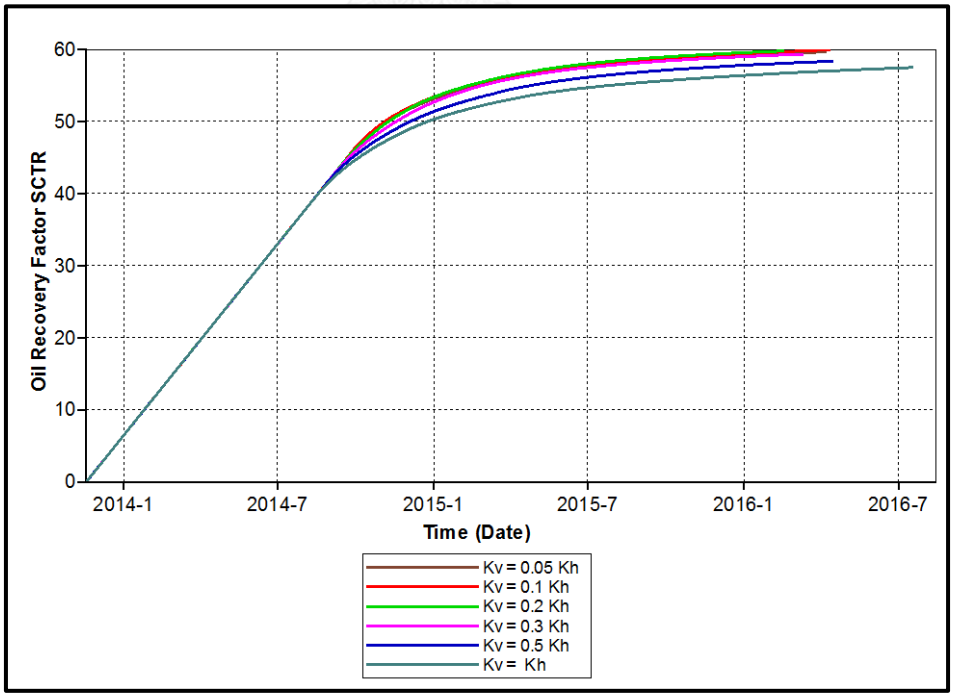

Figure 5.65 Oil recovery factors from different ratios of vertical to horizontal permeability as a function of time

From Figure 5.65, oil recovery factors are different with change of k_v/k_h ratio. It can be obviously seen that, time required to reach the production constraints is the longest in case of k_v/k_h equals to 1.0. As explained earlier, higher vertical permeability does not result in early gas breakthrough, bypassing of chasing water also causes higher of oil remaining behind foam slug. Production period is therefore extended and final oil recovery is obviously lower than other cases. Final oil recoveries regardless production period are plotted together kv/kh ratio and depicted Figure 5.66

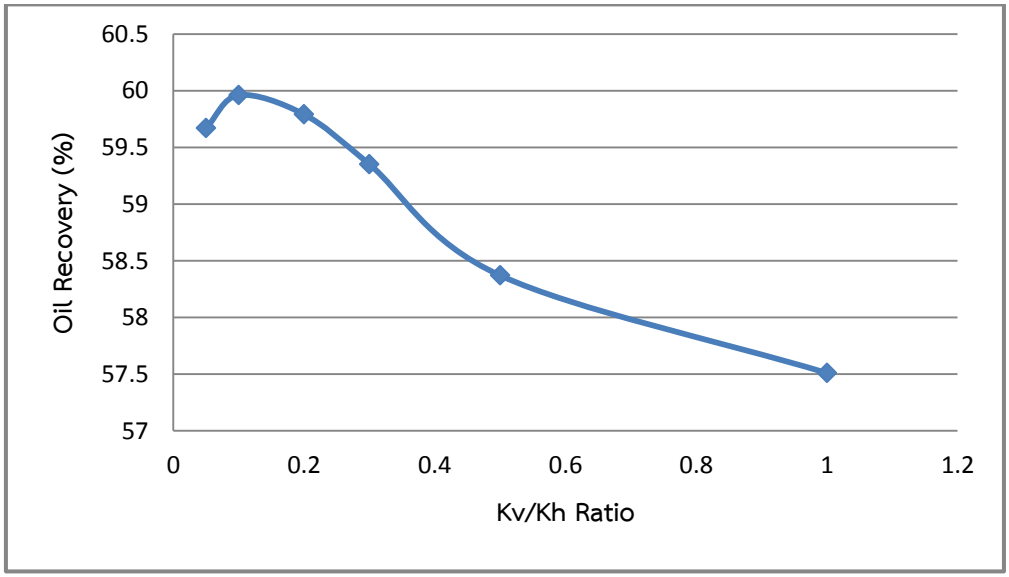

CHULALONGKORN UNIVERSITY

Figure 5.66 Oil recovery factors as a function of ratio of vertical to horizontal permeability

From Figure 5.66, it is obviously shown that vertical permeability tends to reduce oil recovery factor from nitrogen-foam flooding performed in heterogeneous reservoir. Higher vertical permeability obviously causes early liberation of solution gas due to early attainment of bubble point pressure. Even though foam slug tends to adjust vertical flood front profile when whole slug is injected into heterogeneous reservoir, chasing water bypass foam slug to due favorable vertical permeability. This causes low sweep efficiency compared to lower vertical permeability values. However, when vertical permeability is 0.05, it can be observed that oil recovery

factor is slightly lower than the case of 0.1. This might be due to favorability of horizontal flow that over comes vertical permeability and hence effect of heterogeneity is more pronounced.

5.2.3 Co-effect of Heterogeneity and Wettability

Wettability condition is very important point for oil recovery process as it controls interaction between fluid (oil, gas and water) and solid (rock) surfaces. Wetting condition is defined as tendency to oil one fluid to adhere on rock surface in a presence of immiscible phase. There are different types of wetting condition such as water-wet, oil-wet, intermediate wet. It is understood that water-wet is very favourable condition for oil recovery process as water mobility is less, helping to recover more oil.

This study aims to evaluate the effects of wetting conditions when applying nitrogen-foam flooding to enhance oil recovery in heterogeneous reservoir. Previous base case is performed in formation that has characteristics of very strong water-wet condition. This case is labelled as wetting condition no.1. Other 3 wetting conditions are constructed by editing relative permeability. Increasing number is corresponding with decreasing of water-wetting condition or moving toward oil-wet condition. Changing of wetting condition is performed by maintaining difference between irreducible water saturation and residual oil saturation in all cases. This difference is mobile oil by means of physical displacement. Changing wettability toward oil-wet condition is done by decreasing irreducible water saturation, increasing residual oil saturation and increase relative permeability to water at residual oil saturation. Table 5.8 summarizes data involved in construction of different wetting conditions. Constructed relative permeability curves using Corey's correlation for different wetting conditions are consecutively shown in Figure 5.67.

Table 5.8 Summary of parameters involved in construction of different wetting conditions

Wetting condition	Irreducible water saturation (S_{wi})	Residual oil saturation (S_{or})	Mobile oil saturation	k_{rw} at S_{or}
No.1	0.28	0.24	0.48	0.13
No.2	0.235	0.285	0.48	0.19
No.3	0.145	0.375	0.48	0.31
No.4	0.1	0.42	0.48	0.37

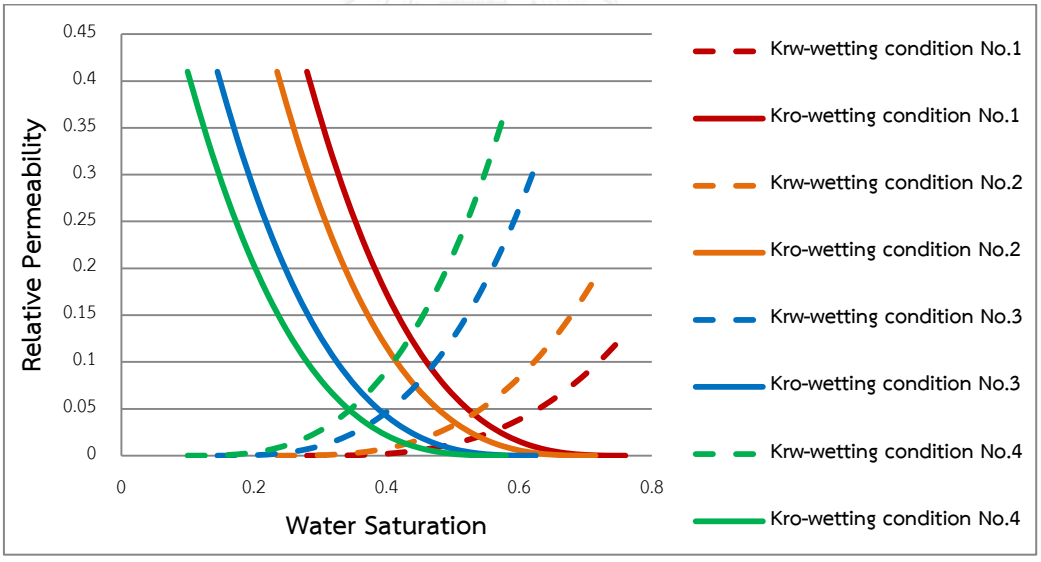

Figure 5.67 Relative permeability curves for different wetting condition

Surfactant solution and nitrogen gas are totally injected at the rate of 1,000rb/day with slug size 0.25 PV. Cumulative amount of fluid injected is exactly same for all cases. Comparison of lamella profiles of wetting condition No.1 and No.4

at day 546 (where foam in wetting condition No.1 reach breakthrough) is illustrated in Figure 5.68

As foam follows relative permeability to water in this study, foam should breakthrough first in more oil-wet condition. However, initial oil saturation is not the same in this study. Even movable oil saturation is kept constant in all cases; presence of surfactant can further reduce residual oil saturation. This increases a gap of displaceable volume in oil-wet case and hence, it requires more time to reach breakthrough.

Oil production rates of different wetting conditions are illustrated in Figure 5.69. From the figure, constant oil production rate is maintained for almost the same period. However, when observe better in detail, it can be seen that oil rate starts to drop first in case of more oil-wet condition. Since fluid saturations are not the same at initial condition, this results in attaining bubble pressure at different time. However, the difference is very small. In case of more water-wet, production period is relatively short as recoverable oil saturation (including effect of surfactant) is less compared to other cases and together with favorable flow of foam, production constraint is reached quickly. For case of wetting condition No.3 and No.4, second peaks of oil production rate appears. As initial oil saturation is high and mobility control of foam is poor due to high water saturation, foam can physically displace only part of oil first. As foam also contains surfactant, high remaining portion of oil can be in contact with surfactant in foam. Reduction of IFT results in forming of second oil bank. However, since flow ability of water is high, this result in longer production period before one of the constraints is reached. Table 5.9 summarizes simulation outcomes in this study.

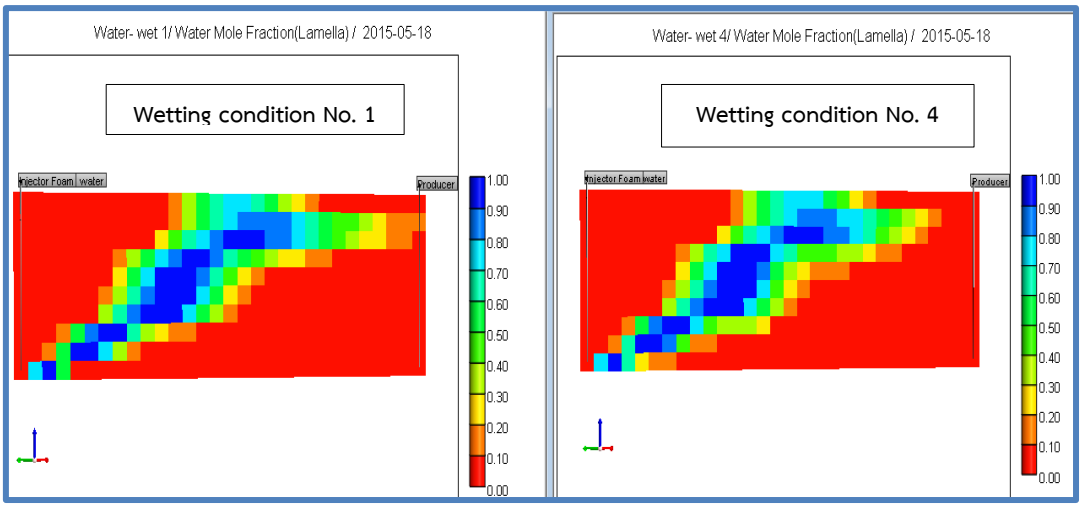

Figure 5.68 Lamella profile of wetting condition No.1 and No.4 at day 546 (where foam in wetting condition No.1 reach breakthrough)

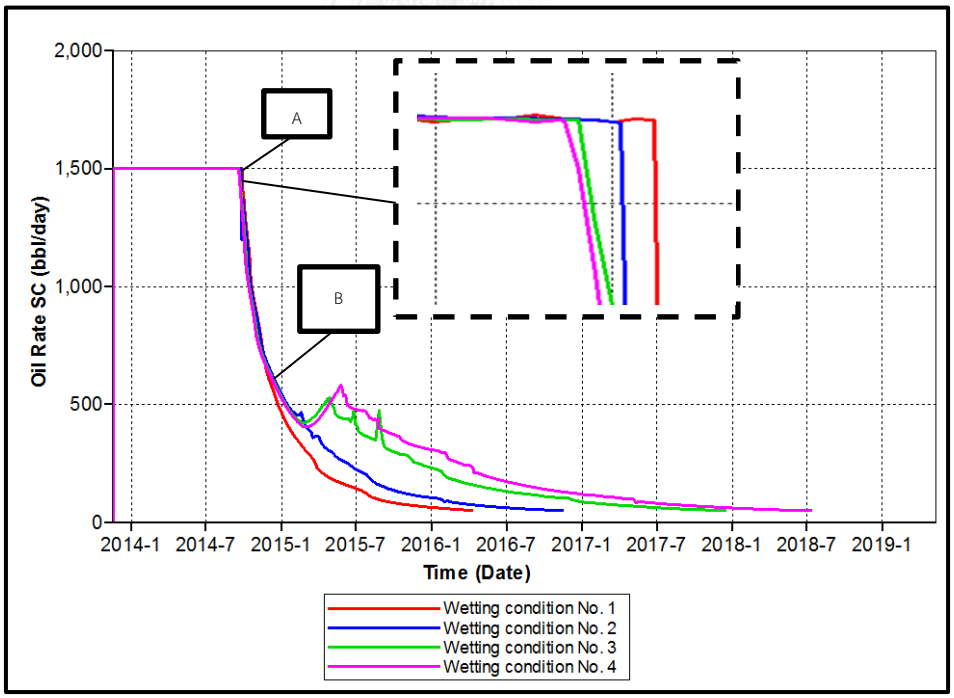

Figure 5.69 Oil production rates from different wetting conditions as a function of time

Table 5.9 Summary of simulation outcomes from different wetting conditions

Wetting conditions	No.1	No.2	No.3	No.4
Total production period (days)	876	1,096	1,491	1,701
Cumulative oil production (MSTB)	613.65	658.80	755.75	805.42
Oil recovery factor (%)	59.96	60.59	62.19	62.96
Cumulative gas production (BSCF)	0.94	1.23	1.52	1.58
Cumulative water production (MSTB)	235.11	244.19	579.52	718.69

From Table 5.9, moving to more oil-wet condition increases more production period. The effect of surfactant can further reduce residual oil saturation. Oil-wet condition therefore obtains this benefit, increasing saturation of recoverable oil. Since pore volume of recoverable oil is increased, higher amount of injectant is required and therefore, production period is substantially longer. Moreover, favorable flow of water also results in gradual change of oil production rate. Longer period also results in higher oil recovery factor in case of more oil–wet condition. Nevertheless, longer injection period also comes together with substantial water production. Figure 5.70 depicts relationship between oil recovery factors from different wetting conditions as a function of time.

From Figure 5.70, it can be obviously seen that, in case of more water-wet condition, total production period is very short. Even oil recovery is lower compared to more oil-wet condition; short production period might cause this case to be more favorable especially if amount of water production is considered. Considering oil recovery at the same day as illustrated in Figure 5.71, it can be seen that higher oil recovery is obtained at the same time in case of more water-wet condition. Only a few percentage of oil recovery is recovered at late production period in oil-wet rock.

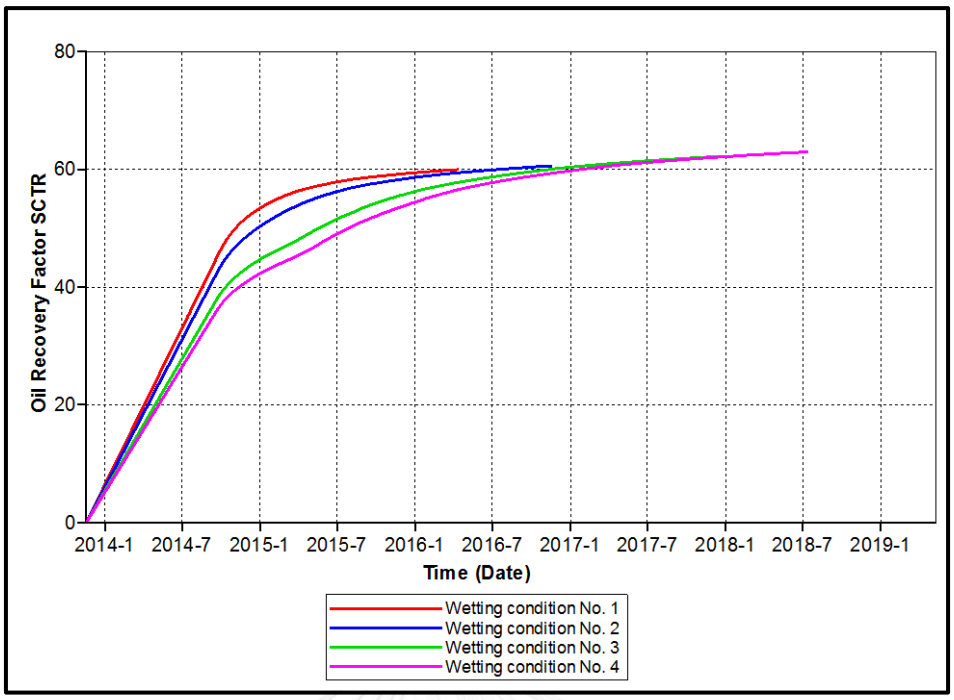

Figure 5.70 Oil recovery factors from different wetting conditions as a function of time

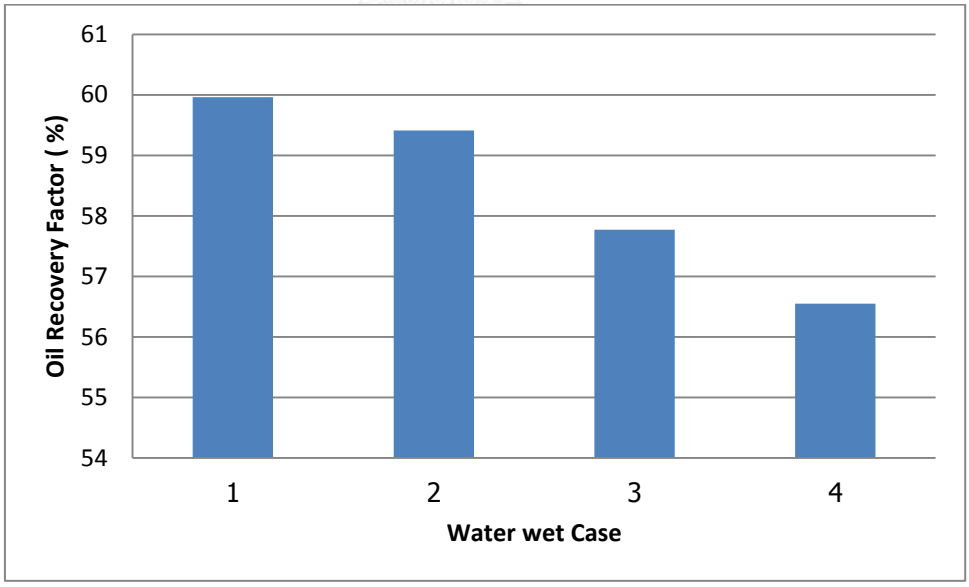

Figure 5.71 Oil recovery factors from different wetting conditions at the same production time

Wetting condition shows some effects on nitrogen-foam flooding. Effect of heterogeneity is not much pronounced compared to relative permeability itself in this study. As foam flow based on relative permeability to water, increasing of relative permeability to water in oil-wet case decreases mobility control of foam. However, more oil-wet condition comes together with lower irreducible water saturation and higher oil saturation. This yields benefit since surfactant can increase a gap of recoverable oil during flooding mechanism. Second oil bank is observed in case of oil-wet conditions. As oil-wet condition results in gradual change of water saturation, flooding mechanism requires more time to reach one of the production constraints. This also comes together with higher water production.

5.2.4 Co-effect of Heterogeneity and Formation Thickness

Specific thickness is important parameter for certain type of flooding process. As thickness increases or decreases, storage capacity of reservoir changes. In flooding of single fluid like water, volume of water at surface is almost same at reservoir conditions and it will never change phase. But if a small amount of surfactant is added to water and co-injected with gas, fluid volume at reservoir condition is not as same as surface. This study aims to observe effects of thickness on foam regeneration and also foam flooding mechanism. As thickness of each grid block increases, formation depth changes as well as oil in place. Only thickness of formation is changed in this section.

Selected formation thicknesses for this study are 100ft (base case), 150 ft and 250 ft. Formation thickness for foam flooding can be as high as to 350 ft [32]. Datum depth of 5,000ft is set constant in all cases at middle layer of formation. Therefore, changing formation thickness requires varying top and bottom depth as shown. Table 5.10 summarizes location of top depth, bottom depth and initial oil in place for different formation thicknesses of 100, 150, and 200ft.

Table 5.10 location of top depth, bottom depth and initial oil in place for different formation thicknesses

Formation thickness	100ft	150ft	250ft
Datum depth (ft)	5,000	5,000	5,000
Top depth (ft)	4,950	4,925	4,875
Bottom depth (ft)	5,050	5,075	5,125
Initial oil in place (MMbbl)	6.48	9.72	16.2

Surfactant solution and nitrogen gas are co-injected at the rate of 130,200 STB/day for 0.25 PV in all cases as shown in Figure 5.72. Main design view is to keep pore volume constant and observe foam generated in reservoir. Fluid injection rate is maintained constant for all the three cases. Cumulative bottomhole fluid is shown in Figure 5.73. Cumulative bottomhole fluid is different in all cases as total pore volume of reservoir is different.

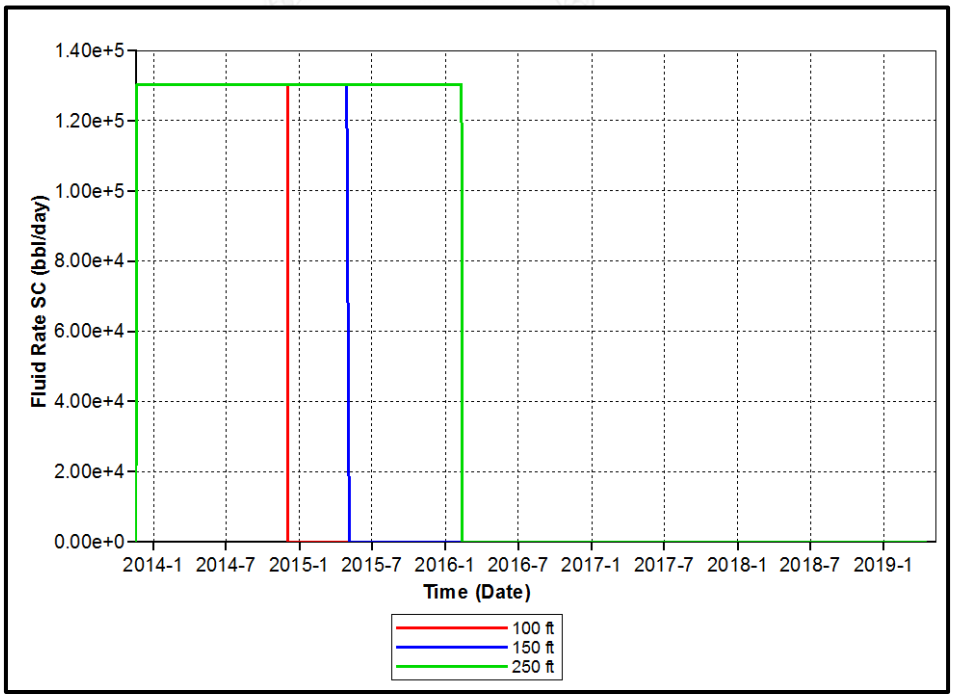

Figure 5.72 Fluid injection rates for different formation thicknesses as a function of time

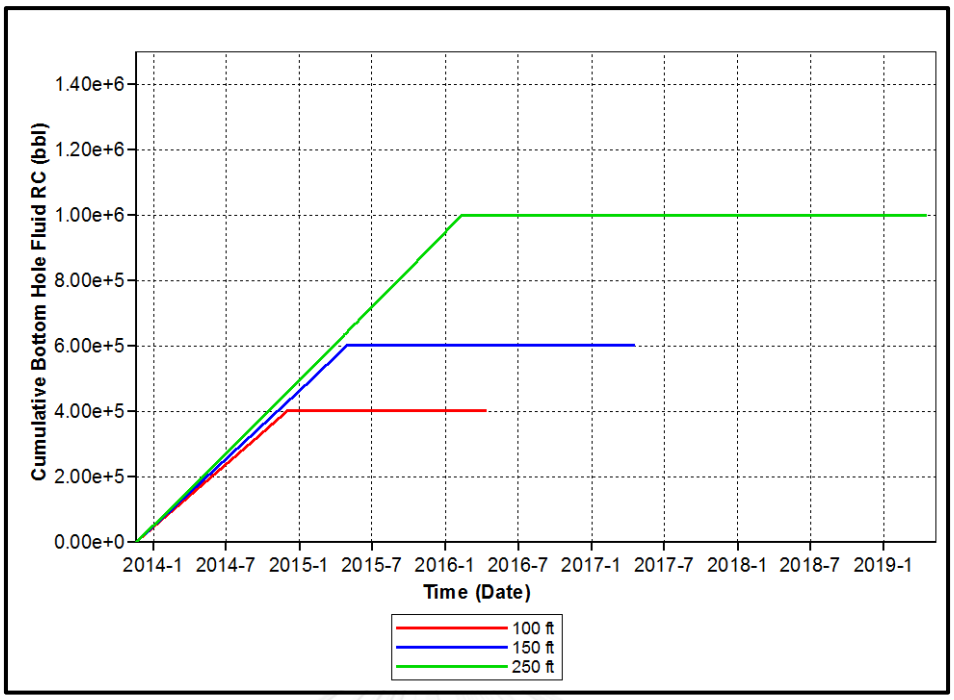

Figure 5.73 Cumulative pore volume of fluid injected for different formation thicknesses as a function of time

Average reservoir pressures of different thicknesses are depicted in Figure 5.74 As thickness increases, upper layers of formation exposes to lower reservoir pressure. This condition favors foam to propagate into these layers where permeabilities are relatively high. Difference does not change much in lower section where permeability is low. From Figure 5.74, average reservoir pressure shows that the highest thickness possesses higher average pressure which indicates that foam generation might be better in higher thickness reservoir. Reservoir simulation outcomes from the study of formation thickness are summarized in Table 5.11.

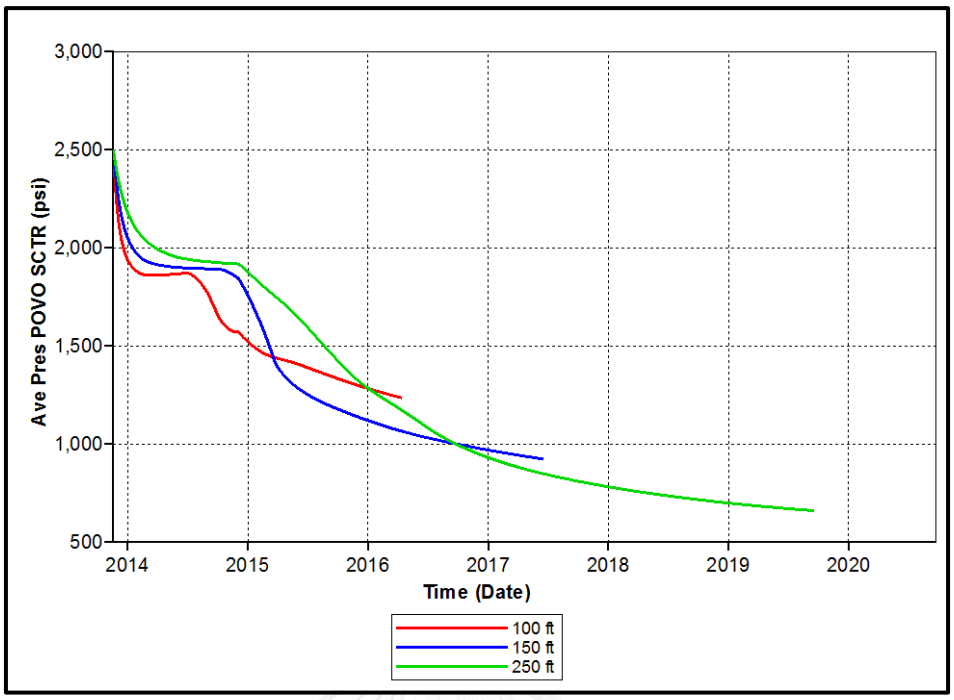

Figure 5.74 Average reservoir pressure of different thicknesses as a function of time

Table 5.11 Summary of simulation outcomes from different formation thicknesses

Formation thickness	100	150	200
Total production period (days)	876	1247	1977
Cumulative oil production (MSTB)	613.65	919.56	1532.87
Oil recovery factor (%)	59.96	59.90	59.91
Cumulative gas production (BSCF)	0.94	1.27	2.00
Cumulative water production (MSTB)	235.11	355.99	602.32

From Table 5.15, it is obviously seen that higher thickness results in longer production period and larger amount of water produce. However, oil recovery is mostly constant. Even though pressure causes different velocity of foam front, mobility control is same since heterogeneity is not varied and hence, volumetric sweep efficiency is mostly constant. Relationship between oil recovery factors and time is illustrated in Figure 5.75.

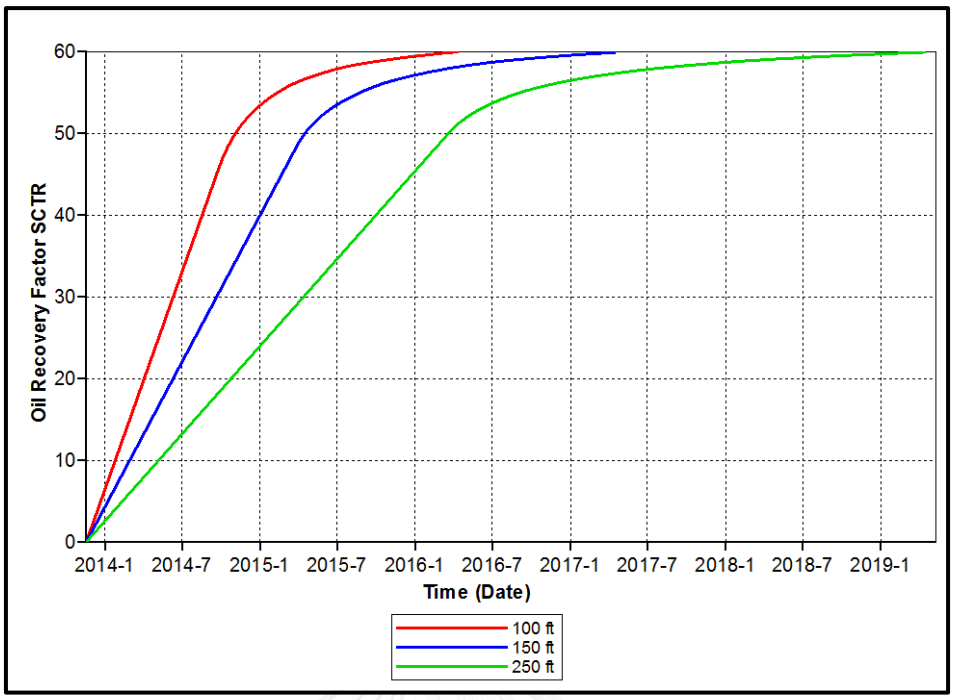

Figure 5.75 Oil recovery factors from different thicknesses as a function of time

Thickness of formation is related to formation depth. When heterogeneity is involved and high permeability layers are located in lower depth formation, this will cause easier foam generation in high permeability zone. Foam advancement is therefore obtained benefit from higher thickness. However, since heterogeneity is the same, changing formation depth might but mobility control of foam will be maintained constant until breakthrough that mostly cause constant oil recovery factors for all cases.

5.2.5 Study of Alternating Foam-Water Flooding

Alternating foam-water is an injection technique where the single slug is divided into smaller slugs and injected at fixed volume followed by chasing water. Single slug may be advantageous over multi-slug, depending on reservoir parameters. This section aims the study effect of multi-slug nitrogen-foam in multi-layered heterogeneous reservoir. Single foam slug obtained from base case is converted to double-slug and triple-slug. Therefore, total pore volume in case of double- and triple-slug will be maintained at 0.25 PV. Since the case of single-slug mode requires

chasing water 0.313, ratio between foam slug and alternate slug is maintained at 0.798.

5.2.5.1 Alternating Foam-Water Flooding with Extended Water Chasing Period

In this section double- and triple-slug are generated by dividing foam in single slug into two and three smaller slugs. In case of double-slug, first foam slug of 0.125 PV followed by chasing water of 0.157 PV to maintain ratio of 0.798. Then second foam slug of 0.125 PV is injected and chased by water until the end of production. Similarly, foam is divided by three and hence each foam slug is 0.083 PV. Chasing water slug is 0.104 to maintain the ratio of 0.798 and after third foam slug is injected, chasing water is injected until the end of production.

Injection time of each slug to operate to different slug mode with extended chasing water period is shown in Table 5.12

Table 5.12 Injection time for foam and chasing water in single-, double- and triple-slug mode with extended water chasing period

Injection mode	Operation	PV	Start (Day)	End (Day)
Single-slug	Foam slug	0.25	1	379
	Chasing water slug	0.313	380	-
Double-slug	1st Foam slug	0.125	1	190
	1st Chasing water slug	0.157	191	440
	2nd Foam slug	0.125	441	621
	2nd Chasing water slug	-	622	-
Triple-slug	1st Foam slug	0.083	1	127
	1st Chasing water slug	0.104	128	293
	2nd Foam slug	0.083	294	413
	2nd Chasing water slug	0.104	414	580
	3rd Foam slug	0.083	581	700
	3rd Chasing water slug	-	701	-

Cumulative volumes of fluid injected and cumulative chasing water injected for single-, double- and triple-slug mode are shown in Figures 5.76, 5.77 and 5.78, respectively. From Figures 5.76 to 5.78 together with Table 5.12 it can be seen that as division number of slug increases number of days required to reach 0.25 PV decreases. After first foam slug is injected, chasing water is injected and this increases injectivity especially in bottom layers where foam hardly propagates.

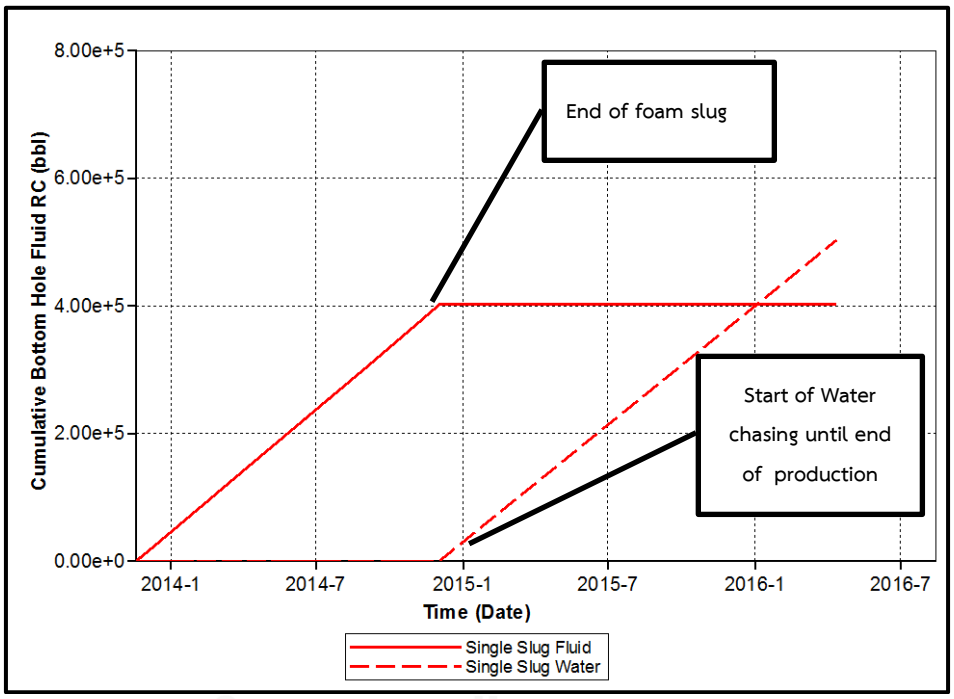

Chulalongkorn University

Figure 5.76 Cumulative volumes of fluid and chasing water for single-slug mode as a function of time

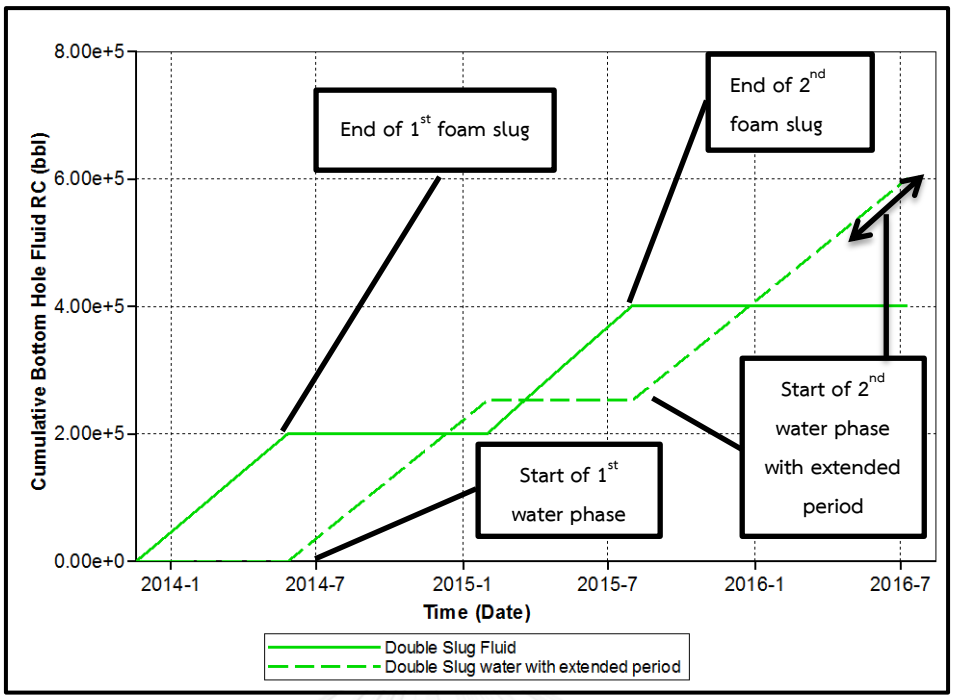

Figure 5.77 Cumulative volumes of fluid and chasing water for double-slug mode as a function of time

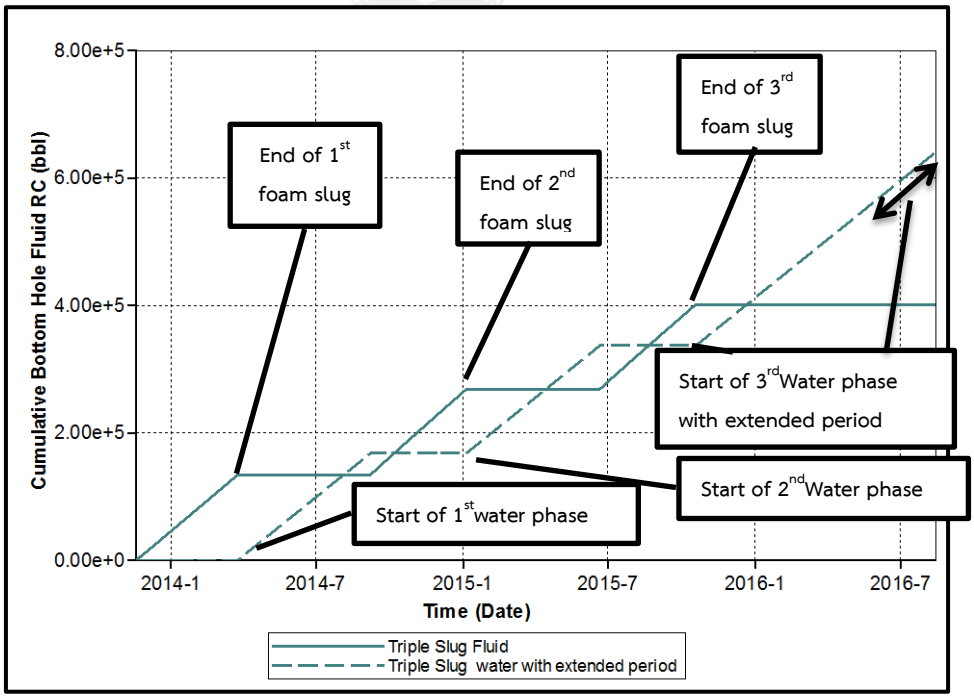

Figure 5.78 Cumulative volumes of fluid and chasing water for triple-slug mode as a function of time

Lamella profiles in 3-D obtained from three different injection modes are illustrated in Figure 5.79a, b and c at time where each foam slug injection is completed. It is clearly seen that as number of slug size increases, foam displaces more in lower layers of formation. However, it can be also seen that intensity of lamella is weaken when foam is performed as multi-slug.

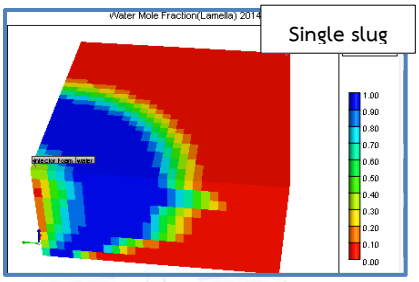

(a)

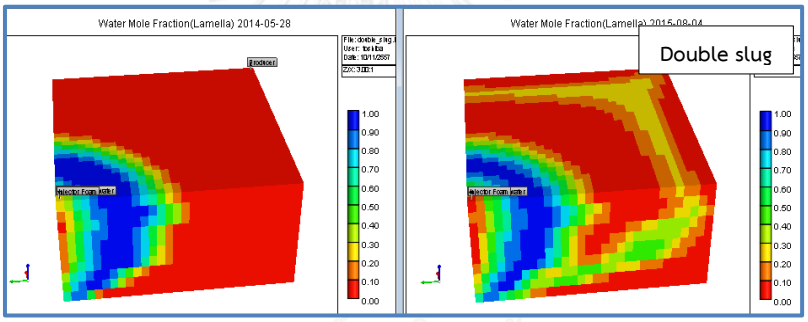

(b)

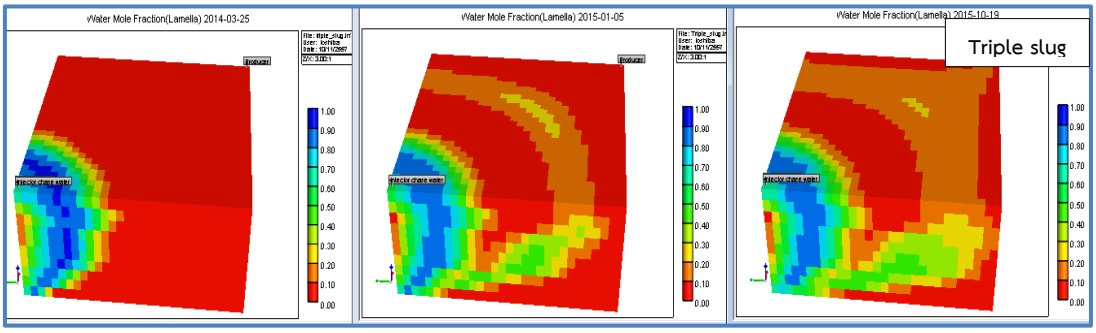

(c)

Figure 5.79 Lamella profiles at different time when each foam slug is injected in (a) single-slug (b) double-slug (c) triple-slug

5.2.5.2 Alternating Foam-Water Flooding with Limited Water Chasing Period

After the last chasing water slug is injected, exact amount of water is injected to keep volume of injectant equal in every case. Therefore, for double- and triple-slug cases, the last day where the last chasing water slugs are injected are 870 and 865 days, respectively. Results obtained from this section are collected at shorter period of production. Comparison of simulation outcomes obtained from multi-slug with and without extended water chasing are summarized in Table 5.13.

Table 5.13 Summary of simulation outcomes from different injection modes compared between extended and limited chasing water

Chasing water period	Extended chasing water			Limited chasing water	
Injection mode	Single	Double	Triple	Double	Triple
Total production period (days)	876	964	1000	870	865
Cumulative oil production (MSTB)	613.65	612.41	613.08	607.40	605.36
Oil recovery factor (%)	59.96	59.84	59.91	59.34	59.15
Cumulative gas production (BSCF)	0.94	0.52	0.76	0.59	0.71
Cumulative water production (MSTB)	235.11	344.44	385.30	280.92	294.54

From Table 5.13, production period is longer when number of slug size increases and chasing water is kept injected until the end of production. However, oil recovery does not change much in all three cases. However, when comparing all three cases with the same volume of fluid and chasing water injected, it can be observed that total fluid can be injected within shorter time. As explained previously, alternating foam slug could result in a slight improvement in injectivity in lower

section as water density is higher than foam. Oil recovery factors obtained from both observations are mostly the same, meaning no significant oil obtained additional during extended period.

Oil and water production rates from five cases are shown in Figures 5.80 and 5.81, respectively. From Figures 5.80 and 5.81, it is obviously seen that even oil recovery factor of these three cases are mostly the same, dynamicity is not. Oil production rate starts to drop earlier in triple-slug followed by double-slug. But these reductions are coincident with water production. This can be explained that when foam slug is not big enough, by passing of chasing water could occur. Nevertheless, reduction of oil production rate in case of triple-slug changes the trend after first chasing water breakthrough. A small higher oil production rate could be cause by displacement of water in lower layer occurring during alternation between foam and water.

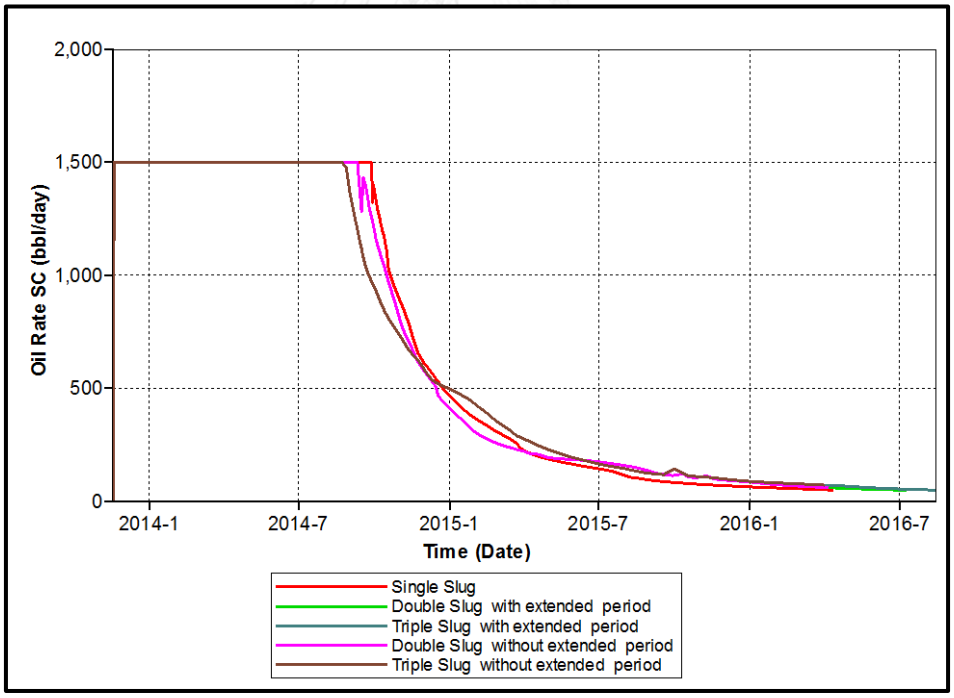

Figure 5.80 Oil production rates from different injection modes as a function of time

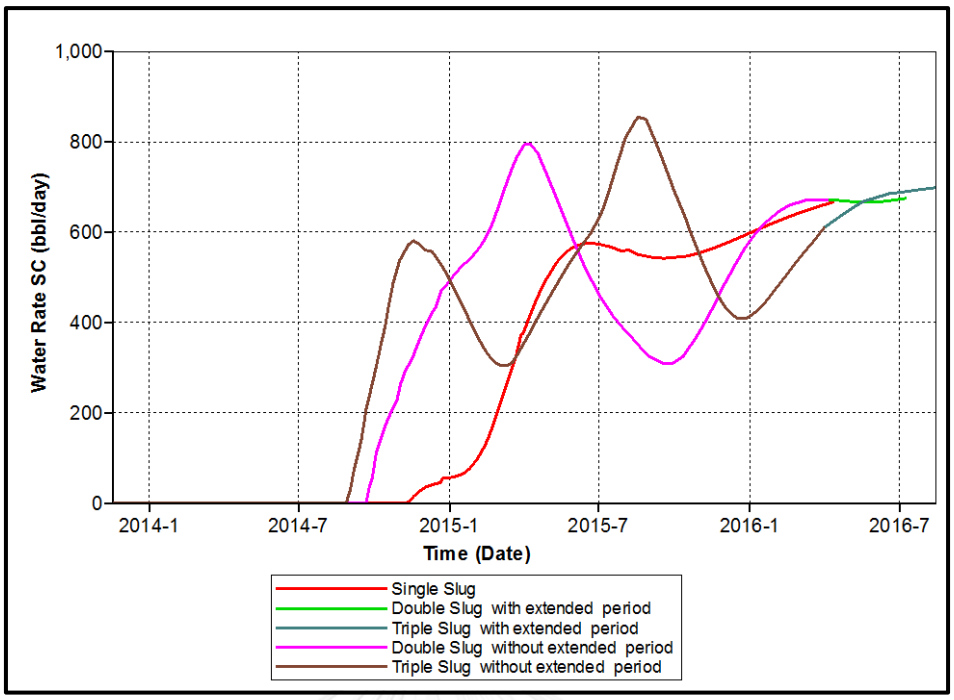

Figure 5.81 Water production rates from different injection modes as a function of time

Oil recovery factors as a function of time of all cases are plotted in Figure 5.82. Single slug yields the highest oil recovery. Alternating foam in many slugs can weaken foam buffer and this may cause bypassing of chasing water especially when heterogeneity is involved. Total water production is therefore high in these cases. Increasing amount of chasing water until the end of production does not improve further oil recovery because remaining oil is bypassed, located in bottom layers of formation.

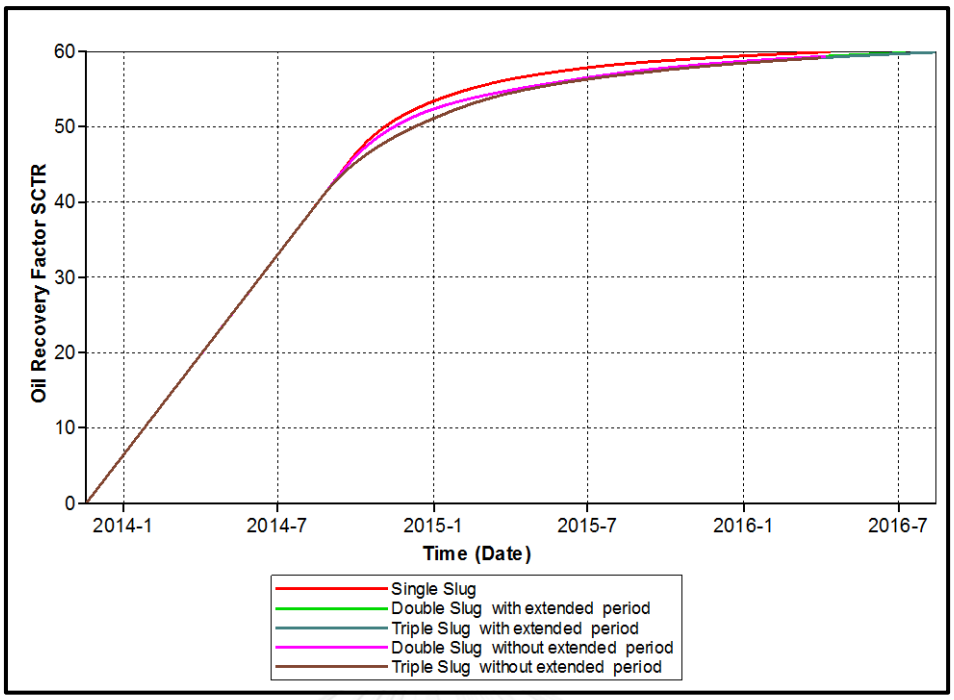

Figure 5.82 Oil recovery factors from different injection modes as a function of time

Alternating of foam-water flooding does not show much different compared to single slug injection. Since foam slug is smaller, water can bypass easily, causing early water breakthrough. Nevertheless, oil recovery factor obtained from injecting multi-slug is just slightly lower than single-slug since multi-slug mode obtains benefit from improvement in vertical sweep efficiency since chasing water is early injected. Since early chasing of water is performed in multi- slug, the water production is higher compared to single slug.

CHAPTER VI
CONCLUSION AND RECOMMENDATION

Discussion of nitrogen-foam flooding in multi-layered heterogeneous reservoir is performed in previous Chapter based on selection of operational parameters and studies of interest parameters. In this chapter, conclusions are made. Recommendations for further study are stated at the end.

6.1 Conclusion

1. Injection rate affects foam generation process. Too low injection rate might cause weak foams, resulting in poor sweep efficiency and also longer production period is required. Lower permeability areas are not accessed and high amount of residual oil is left in reservoir. High fluid injection rate yields also drawback by increasing water production due to higher rate of chasing water. .Selected fluid injection rate in this study is 1,000rb/day. Injection foam with this rate in moderate heterogeneity reservoir yields high oil recovery within short period with moderate water production.
2. The main purpose of adjusting production - injection ratio is to maintain well bottomhole pressure of injection well since foam injection is performed in virgin reservoir. Increasing of production rate helps to partially deplete high reservoir pressure, increasing injectivity of both nitrogen-gas and surfactant solution. Too low production - injection ratio fails to deplete reservoir pressure and too high production - injection ratio increases total production rate. In this study, P-I ratio of 1.5 shows good results in partial depletion of reservoir pressure and improving fluid injectivity along with reasonable real implementation of total production rate.
3. Gas-liquid ratio plays an important role for injection quality as well as oil production. Oil recovery factor increases with amount of surfactant solution or reduction of gas-liquid ratio. However, too high amount of surfactant solution leads to less oil recovery because nitrogen-gas volume is too small

and too much surfactant solution causes higher water production. Too high gas-liquid ratio also causes weak foam as amount of surfactant is not adequate. Selected best gas-liquid ratio in this study is 2.0 as it yields the highest oil recovery.

4. Proper slug size must be determined as it controls production period as well as amount of surfactant required to recover oil. High amount of surfactant with small increment in oil is not feasible. Smaller slug size than 0.25 PV leads to less oil recovery as chasing water can penetrate through, causing high water production. Slug size bigger than 0.25 PV leads to small increment in oil recovery, sacrificing large amount of surfactant. Foam slug size of 0.25 PV in this study as it can form buffer slug to maintain mobility and oil recovery per surfactant required is the smallest.

5. Based on selected operational parameters foam flooding is efficient in heterogeneous reservoir, improving sweep efficiency. However, results show that a rapid drop in oil recovery occurs from Lorenz coefficient of 0.35. Longer production period to reach one of the constraints is observed when heterogeneity increases, causing gradual reduction of oil production rate and slight increment of water production rate. In this study, nitrogen-foam flooding efficiently recovers oil in lower heterogeneity values up to value around 0.35. Isolation of high permeability zones is suggested when heterogeneity is too high to prevent early breakthrough of nitrogen-foam and water.
6. Vertical permeability tends to reduce oil recovery factor from nitrogen-foam flooding performed in heterogeneous reservoir. High vertical permeability causes early liberation of solution gas due to early attainment of bubble point pressure. Sweep efficiency is lower in high vertical. Very low vertical heterogeneity also shows an effect on nitrogen-foam flooding performance. Horizontal flow is dominated and hence effect of heterogeneity is more pronounced.

7. Formation with more oil-wet condition comes together with lower irreducible water saturation and higher oil saturation. This yields benefit to nitrogen-foam flooding since surfactant can increase a gap of recoverable oil during flooding mechanism. However, oil-wet condition requires more time to reach production constraint and hence the water production is higher compared to rock with water-wet condition.
8. Different formation thickness leads to different original oil in place. Foam advancement obtains benefit from higher thickness due to smaller reservoir pressure at the top layers representing effect of heterogeneity. Oil recovery factor for all cases is mostly constant as mobility control by foam is maintained constant until breakthrough.
9. Alternating of foam-water flooding in double- and triple-slug does not show much different oil recovery compared to single slug injection. Nevertheless, foam slug is smaller and chasing water can bypass easily, causing early water breakthrough. Oil recovery factor obtained from injecting multi-slug is just slightly lower than single-slug since multi-slug mode obtains benefit from improvement in vertical sweep efficiency from chasing water that is early injected. Water production anyway is higher in case of multi-slug compared to single slug.

จุฬาลงกรณ์มหาวิทยาลัย
Chulalongkorn University

6.2 Recommendations

The following useful recommendations are suggested for future study of foam flooding.

1. Laboratory data or study is required to duplicate actual reservoir conditions and to evaluate actual effects of nitrogen-foam flooding in heterogeneous reservoir.
2. Study of SAG (surfactant alternating gas) or pre-foamed injection method can be performed to generate foam and evaluate its effects on heterogeneous reservoir.

จุฬาลงกรณ์มหาวิทยาลัย
Chulalongkorn University

REFERENCES

1. Kvæstad, A.H., *CO2-foaming agent retention in fractured chalk models: Experiments and simulations.* 2011.
2. Boud, D.C. and O.C. Holbrook, *Gas drive oil recovery process*. 1958, Google Patents.
3. Farajzadeh, R., A. Andrianov, and P. Zitha, *Investigation of immiscible and miscible foam for enhancing oil recovery.* Industrial & Engineering Chemistry Research, 2009. **49**(4): p. 1910-1919.
4. Kovscek, A., T. Patzek, and C. Radke, *Simulation of foam transport in porous media.* paper SPE **26402** , 1993.
5. Vikingstad, A.K., *Static and dynamic studies of foam and foam-oil interactions.* ISSN **8230802580**, 2006.
6. Al-Mossawy, M.I., B. Demiral, and D.A. Raja, *FOAM DYNAMICS IN POROUS MEDIA AND ITS APPLICATIONS IN ENHANCED OIL RECOVERY: REVIEW, Journal article.*
7. Dong, X., et al., *Air-Foam-Injection Process: An Improved-Oil-Recovery Technique for Waterflooded Light-Oil Reservoirs SPE-163044, 2012.*
8. Yu, H., et al., *Air Foam Injection for IOR: from Laboratory to Field Implementation in Zhongyuan Oilfield China*. Society of Petroleum Engineers, SPE-113913, 2008.
9. Bo-jun, W., et al., *Foam Assisted Air Injection (FAAI) for IOR at Hailaer Oilfield: Prospects and Challenges*. International Petroleum Technology Conference, IPTC-16416, 2013.
10. Liu, R., et al. *The reservoir suitability studies of nitrogen foam flooding in Shengli Oilfield*. in *SPE Asia Pacific Oil and Gas Conference and Exhibition*. SPE-114800, 2008.
11. Xu, H.X., C.S. Pu, and D.H. Shi, *Research and Application of Air Foam Flooding in Longdong Jurassic Reservoir.* Advanced Materials Research, 2012. **347**: p. 1615-1620.

12. Kuehne, D.L., et al., *Design and evaluation of a nitrogen-foam field trial.* Journal of Petroleum Technology, 1990. **42**(04): p. 504-512.
13. Hou, Q., et al. *Recent Progress and Effects Analysis of Foam Flooding Field Tests in China*. in *SPE Enhanced Oil Recovery Conference*. SPE 165211, 2013.
14. Skoreyko, F.A., et al., *Development of a New Foam EOR Model From Laboratory and Field Data of the Naturally Fractured Cantarell Field*. SPE 145718, 2011.
15. Sheng, J., *Enhanced oil recovery field case studies*. 2013: Gulf Professional Publishing.
16. Schramm, L.L., *Foams: fundamentals and applications in the petroleum industry*. Vol. 242. 1994: American Chemical Society Washington, DC.
17. Tiab, D. and E.C. Donaldson, *Petrophysics: theory and practice of measuring reservoir rock and fluid transport properties*. 2011: Gulf professional publishing.
18. LongBear , L., *Foam Terminology, Compressed Air Foam, Available at www.LongBear.com*
19. Eric Tyrode, A.P., and Orlando J. Rojas, *Foamability and foam stability at high pressures and temperatures. I. Instrument validation. .* May 2003. **Volume 74**.
20. Substech, *Substech Substrance and Technology, Available from www.substech.com*.
21. Evans, D.F. and H. Wennerström, *The Colloidal Domain: Physics, Chemistry, Biology and Technology Meeting.* 1999.
22. Skoreyko, F.A., et al. *Development of a new foam EOR model from laboratory and field data of the naturally fractured Cantarell field*. in *SPE Reservoir Characterisation and Simulation Conference and Exhibition*. 2011. SPE 145718, 2011 .
23. Tiab, D. and E.C. Donaldson, *Petrophysics* 1996.
24. F.Craig.Jr, F., *The Reservoir Engineering Aspect of Water flooding.* SPE of AIME, 1973.
25. 4share, *Waterflooding Theory and Practical Considerations ,Available from 4share.com.* p. page 1-8. .

Chulalongkorn University

26. Heubeck, P.C., *Earth history class at free university Berlin, Department of geological science.*
27. SPE, *ReservoirTemperatureandPressure , Available from: http://petrowiki.org_Reservoir_pressure_and_temperature.* August 2013.
28. Rider, M.H. and M. Kennedy, *The Geological Interpretation of Well Logs*. 2011: Rider-French.
29. Eaton, B.A., *Fracture Gradient Prediction and Its Application in Oilfield Operations.*
30. Mansour, E.M., et al., *Modification proposed for SRK equation of state.* 2012.
31. McCain, W.D., *The properties of petroleum fluids. .*
32. Vikingstad, A.K., *Gravity segregation of foam using different injection methods.* 2005.

จุฬาลงกรณ์มหาวิทยาลัย
Chulalongkorn University

APPENDIX

จุฬาลงกรณ์มหาวิทยาลัย
Chulalongkorn University

CONSTRUCTION OF RESERVOIR MODEL

Purpose of this appendix is to provide brief knowledge of constructing a reservoir model and foam model .Models is constructed with the aid of STARS simulator. STARS simulator is thermal compositional simulator commercialized by Computer Modelling Group (CMG). Six different sections are required to fill the information like properties of reservoir, pressure-volume-temperature, rock-fluid and well and recurrent.

Setting of builder reservoir simulator

Simulator	STARS
Working units	FIELD
Porosity	Single porosity
Simulation start date	18/11/2013

1. Reservoir section

   Reservoir-Grid initialization

Type of Grid	Cartesian
K Direction	Down
Number of blocks (i × j × k)	30 × 30 × 10
Block widths in I direction	20x30
Block widths in J direction	20x30

Reservoir- Array properties

	Grid Top	Grid Thickness	Porosity	Perm-I	Perm-J	Perm-K	water mole fraction
whole		10					1
Layer 1	4950		0.25	300	300	30	
Layer 2			0.25	280	280	28	
Layer 3			0.25	240	240	24	
Layer 4			0.25	160	160	16	
Layer 5			0.25	150	150	15	
Layer 6			0.25	140	140	14	
Layer 7			0.25	120	120	12	
Layer 8			0.25	60	60	6	
Layer 9			0.25	40	40	4	
Layer 10			0.25	10	10	1	

Completion of this step helps simulator to display the reservoir model in three dimensionally or two dimensionally

1.2 Components section

Black oil PVT import wizard will help to generate a new model of fluid for STARS simulator. By using two different methods, black oil PVT data can be input that is can be read from a file or created from analytical correlations using the black oil PVT graphical user interface (GUI) [23]. Even though if the input is read from file, but still one can edit if there is a need to edit.

จุฬาลงกรณ์มหาวิทยาลัย
Chulalongkorn University

Launch the Black oil PVT Graphical User Interface (GUI)	Option
Select units	Fields
Temperature	145 F
Oil density options	use Do

PVT using correlations

Description	Option	Value
Reservoir temperature		145F
Generate data up to max pressure of		3500 psi
Bubble point pressure calculation	value provided	1025 psi
Oil density	Stock tank oil gravity (API)	35
Gas density	gas gravity (Air=1)	0.8
Oil properties correlations	Standing	
Oil compressibility correlation	Glaso	
Dead oil viscosity correlation	Ng and Egbogah	
Live oil viscosity correlation	Beggs and Robinson	
Gas critical properties correlation	Standing	

จุฬาลงกรณ์มหาวิทยาลัย
Chulalongkorn University

Water properties using correlation

General

Description	Value
Reservoir temperature	145F
Reference Pressure	2500 psi
Water Salinity	10000
Undersaturated Co	1.5e-5 1/psi

After filling all the values, plots of all fluid parameters are displayed

1.3 Rock fluid properties

Generate using below table in simulator

Keyword	Description	Value
SWCON	Connate Water	0.28
SWCRIT	Critical Water	0.28
SOIRW	Irreducible Oil for Water-Oil Table	0.24
SORW	Residual Oil for Water-Oil Table	0.24
SOIRG	Irreducible Oil for Gas-Liquid Table	0.05
SORG	Residual Oil for Gas-Liquid Table	0.10
SGCON	Connate Gas	0.00
SGCRIT	Critical Gas	0.15
KROCW	Kro at Connate Water	0.41
KRWIRO	Krw at Irreducible Oil	0.13
KRGCL	Krg at Connate Liquid	0.6
	Exponent for calculating Krw from KRWIRO	3
	Exponent for calculating Krow from KROCW	3
	Exponent for calculating Krog from KROGCG	3
	Exponent for calculating Krg from KRGCL	3

Simulator will generate water oil table and gas liquid table

Water oil table

sw	Krw(Sw)	Kro(Sw)
0.28	0	0.41
0.31	3.17E-05	0.33783
0.34	0.000254	0.274668
0.37	0.000857	0.219915
0.4	0.002031	0.172969
0.43	0.003967	0.13323
0.46	0.006855	0.100098
0.49	0.010886	0.072971
0.52	0.01625	0.05125
0.55	0.023137	0.034334
0.58	0.031738	0.021621
0.61	0.042244	0.012512
0.64	0.054844	0.006406
0.67	0.069729	0.002703
0.7	0.08709	0.000801
0.73	0.107117	0.0001
0.76	0.13	0

จุฬาลงกรณ์มหาวิทยาลัย
Chulalongkorn University

Liquid gas table

Sl	Krg	Krog
0.33	0.6	0
0.355	0.517555	0
0.38	0.443032	0
0.409375	0.365047	4.36E-05
0.43875	0.296797	0.000349
0.468125	0.237632	0.001177
0.4975	0.186904	0.002791
0.526875	0.143964	0.005451
0.55625	0.108162	0.009419
0.585625	0.07885	0.014957
0.615	0.055379	0.022326
0.644375	0.0371	0.031789
0.67375	0.023363	0.043606
0.703125	0.01352	0.058039
0.7325	0.006922	0.075351
0.761875	0.00292	0.095802
0.79125	0.000865	0.119654
0.820625	0.000108	0.147169
0.85	0	0.178609
0.925	0	0.278483
1	0	0.41

After entering the information, simulator will display plots of water –oil relative permeability and liquid gas relative permeability.

1.4 Initialization

Reference pressure - 2500 psi

Reference Depth - 4950 Ft

1.5 Numerical

Keyword Description	**Dataset value**	**Unit**
Time step Control Keywords		
Max Number of time steps (MAXSTEPS)	70,000	
Max Time Step Size (DTMAX)	1.00E+20	day
Min Time Step Size (DTMIN)	0.0000005	day
First time Step Size after Well Change (DTWELL)	1	day
Solution Method Keywords		
Isothermal Option (ISOTHERMAL)	ON	
Model Formulation	ZT	
MAX Newton Iterations (NEWTONCYC)	20	
Linear Solver Iterations	60	
Max Time Step Cuts (NCUTS)	20	

1.6 Well and Recurrent

The Injector well will be injected by water. All 10 layers are perforated.

Well radius 0.28 ft

จุฬาลงกรณ์มหาวิทยาลัย
Chulalongkorn University

Well Definition

Name	Injector water
Type	INJECTOR MOBWEIGHT EXPLICIT
Group	None

Constraint Definition

Constraint	Parameter	Limit/Mode	Value	Action
OPERATE	STW surface water rate	MAX	1000 BBL/Day	CONT
OPERATE	BHP bottom hole pressure	MAX	3500 psi	CONT

This above arrangement is for water flooding

The BHP is set to 3500 psi because the Maximum fracture pressure is 3750 psi and Minimum fracture pressure is 3333 psi calculated using Hubberts and Wills equation.

Injected Fluid- Water

Component	Volume Fraction
Water	1
Surfact	0
Foam gas	0
Lamella	0
Dead Oil	0
Solution gas	0
Total	1

Producer Well Definition

Name	Producer
Type	INJECTOR MOBWEIGHT EXPLICIT
Group	None

Constraint Definition

Constraint	Parameter	Limit/Mode	Value	Action
OPERATE	BHP bottom hole pressure	MIN	200 psi	CONT
OPERATE	STL surface Liquid rate	MAX	1500 STB/day	CONT
OPERATE	STG surface gas rate	MAX	10000000 ft3/day	CONT
MONITOR	WCUT water-cut (fraction)		0.95	STOP
MONITOR	STO surface oil rate	MIN	50 STB/day	STOP

Simulation Dates

18/11/2013	Start
18/11/2033	Stop

จุฬาลงกรณ์มหาวิทยาลัย
Chulalongkorn University

2. **Foam Flood Simulation Model**

Foam model is created by clicking process wizard in above rock and fluid section.

Process Wizard

This wizard will use the available fluid model section for STARS and add necessary data to process the simulation. This wizard should be begun with minimum two or three components that describe the black oil nature of the system.

Choose process

Process : Alkaline, surfactant, foam, and/or polymer model

Choose Model

Model : Foam flood with liquid foam model (add 4 components)

Select options	
Use N2 gas to generate foam	Yes
Weight percent surfactant used to generate the foam	0.5
Number of relative perm sets for interpolation	2
Use adsorption for surfactant	yes
Rock type for conversion of adsorption value	sandstone
Rock density, gm/cm3	2.65

Component selection

Select options	
Add new component for surfactant	Surfactant
Add new component for Foam gas	Foam gas
Add new component for Lamellae	Lamellae
Add new component for N2	yes
Add new component for Trapped lamellae	Yes

Set Rock Fluid Regions

The rock fluid regions are selected to use for capillary number relative permeability interpolation. The two box will be displayed .The first box option is for foam flow and second option box is for IFT reduction.

Rock fluid Region Number 1	
Rock fluid Region Number 2	yes
Rock fluid Region Number 1	yes
Rock fluid Region Number 2	

Interfacial Tension values

Weight% Surfactant	**Interfacial Tension, (dyne/cm)**
0	18.2
0.05	0.5
0.1	0.028
0.2	0.028
0.4	0.0057
0.6	0.00121
0.8	0.00037
1	0.5

Reactions

1.Lamella $\longrightarrow$ Water + Surfactant

2. Foam Gas $\longrightarrow$ Nitrogen

3. Lamella+ Dead oil $\longrightarrow$ Water $_+$ Surfactant +Dead Oil

4. Foam Gas +Dead Oil $\longrightarrow$ Dead Oil+ Nitrogen

5. Water + Surfactant + Nitrogen $\longrightarrow$ Lamella + Nitrogen

6. Water + Surfactant $\longrightarrow$ Lamella

Try to balance the reactions by increasing or decreasing product coefficients and reactant coefficients. If the error is more than simulation result error will be high. Enter proper values of FREQFAC and EACT to reduce simulation errors.

Rock Fluid properties

In this region fist select current rock type to create 2nd rock fluid region.

Foam parameter selection

Foam Parameter	Value
fmmob	76000
fmsurf	0.00001
fmoil	0.2
Epsurf	1
Epoil	1

Fmsurf, fmoil, Epsurf and Epoil is selected from typical values of STARS manual. These values are typically used on average scale. Fmmob is selected from construction of typically used average values graph

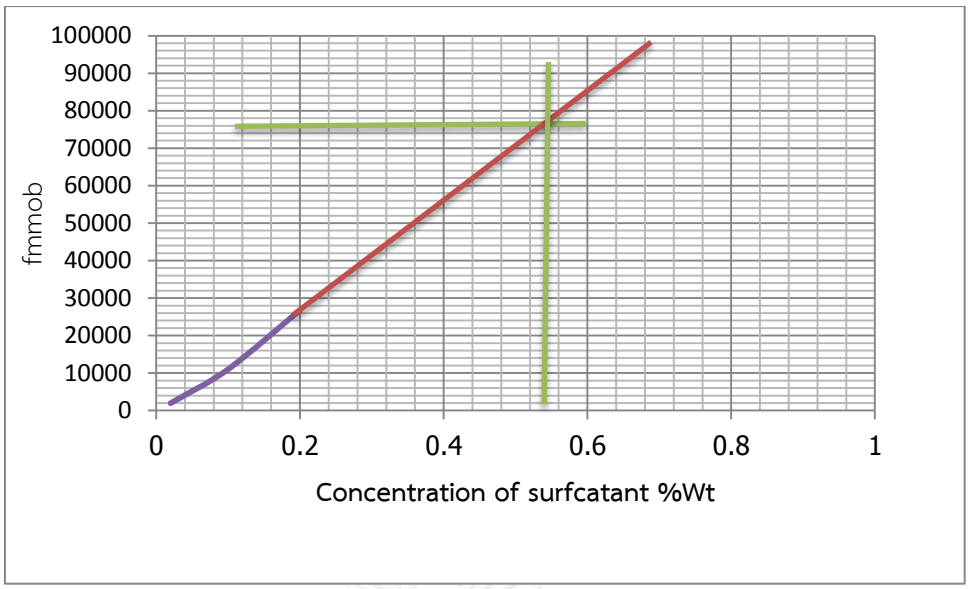

Rock type properties

Rock Fluid Properties	
Rock Wettability	Water Wet
Method for Evaluating 3-phase KRO	Stone's Second Model
Interpolation Components (INTCOMP)	Interpolation enabled
Rock-fluid interpolation will depend on component	Water
Phase for which component's composition will be taken	water (aqueous) mole fraction
Foam Interpolation Parameters	
Critical component mole fraction (FMSURF)	0.00001
Critical oil saturation value(FMOIL)	0.2
Reference foam mobility reduction factor (FMMOB)	76, 000
Exponent for composition contribution (EPSURF)	1
Exponent for oil saturation contribution (EPOIL)	1
Option	Temperature independent
Option	Logarithmic interpolation

Interpolation Set parameters

Wetting Phase (DTRAPW)	-5
Non wetting Phase (DTRAPN)	-5

Well and Recurrent

Injector Foam well

The Injector well will be injected by Liquid and gas. All 10 layers are perforated.

Well radius 0.28 ft

Well Definition

Name	Injector foam
Type	INJECTOR MOBWEIGHT EXPLICIT
Group	None

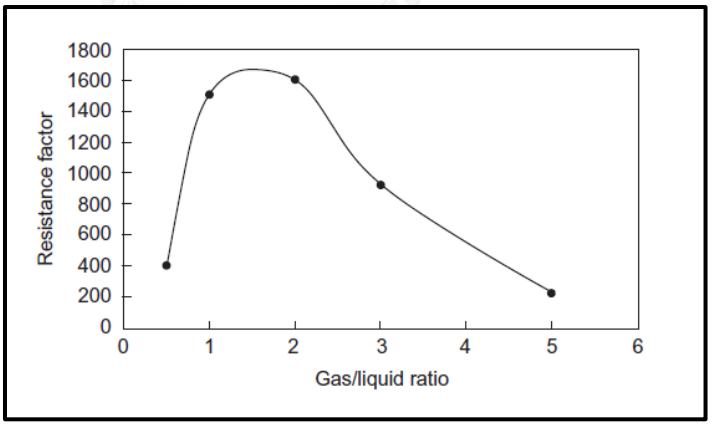

Ref: [15]

Constraint Definition

Constraint	Parameter	Limit/Mode	Value	Action
OPERATE	STF Surface total phase rate	MAX	130200 STB/day	CONT
OPERATE	BHP bottom hole pressure	MAX	3500 psi	CONT

The BHP is set to 3500 psi because the Maximum fracture pressure is 3750 psi and Minimum fracture pressure is 3333 psi calculated using Hubberts and Wills equation.

Injected Fluid

Injected fluid: Water- Gas

Component	Volume Fraction
Water	0.001528418
Surfact	7.68049E-06
Foam gas	0
Lamella	0
Dead Oil	0
Solution gas	0
N2	0.998463902
Total	1

จุฬาลงกรณ์มหาวิทยาลัย
Chulalongkorn University

Volume fraction calculation

Component	Phase rate(P) (STB/day)	Fraction(F)	Comp. rate (C) = P* F	Volume Fraction = C/T
water	200	0.995	199	1.53×10^{-3}
surfactant		0.005	1	7.68×10^{-6}
nitrogen	130,000	1	130,000	0.998
total	130,200	-	130,200	1.00

INJECTOR Chase water well

Constraint	**Parameter**	**Limit/Mode**	**Value**	**Action**
OPERATE	STW Surface total water rate	MAX	1000 STB/Day	CONT
OPERATE	BHP bottom hole pressure	MAX	3500 psi	CONT

Injected fluid: Water

Component	**Volume Fraction**
Water	1
Surfact	0
Foam gas	0
Lamella	0
Dead Oil	0
Solution gas	0
Total	1

VITA

Seema Tarannum Shaikh was born on Febrauary 9th, 1983 in Bhatkal, Karnataka, India. She received her Bachelor degree in Electrical and Electronics Engineering from University Visvesvaraya College of Engineering in 2005. She worked as guest lecturer in University Visvesvaraya College of Engineering for six months and continued working as a lecturer in G.S.S Institute of Technology for three years. She continued her study in the Master's Degree Program in Petroleum Engineering at the Department of Mining and Petroleum Engineering, Chulalongkorn University since the academic year 2012.

จุฬาลงกรณ์มหาวิทยาลัย
Chulalongkorn University